



Calhoun: The NPS Institutional Archive

DSpace Repository

Theses and Dissertations

1. Thesis and Dissertation Collection, all items

1993-03

A water mass analysis of the 1991-1992 El Niño signal in the Farallon Islands region.

Hays, Kevin Austin Samuel; Ramp, Steven R.

Monterey, California. Naval Postgraduate School

<http://hdl.handle.net/10945/24249>

Downloaded from NPS Archive: Calhoun



<http://www.nps.edu/library>

Calhoun is the Naval Postgraduate School's public access digital repository for research materials and institutional publications created by the NPS community.

Calhoun is named for Professor of Mathematics Guy K. Calhoun, NPS's first appointed -- and published -- scholarly author.

Dudley Knox Library / Naval Postgraduate School
411 Dyer Road / 1 University Circle
Monterey, California USA 93943



DUDLEY KNOX LIBRARY
NAVAL POSTGRADUATE SCHOOL
MONTEREY CA 93943-5101

REPORT DOCUMENTATION PAGE

1. REPORT SECURITY CLASSIFICATION UNCLASSIFIED		1b. RESTRICTIVE MARKINGS	
2. SECURITY CLASSIFICATION AUTHORITY		3. DISTRIBUTION/AVAILABILITY OF REPORT Approved for public release; distribution is unlimited	
4. DECLASSIFICATION/DOWNGRADING SCHEDULE			
5. PERFORMING ORGANIZATION REPORT NUMBER(S)		6. MONITORING ORGANIZATION REPORT NUMBER(S)	
7. NAME OF PERFORMING ORGANIZATION Naval Postgraduate School		8b. OFFICE SYMBOL (if applicable) OC	
9. ADDRESS (City, State, and ZIP Code) Monterey, CA 93943-5000		10. NAME OF MONITORING ORGANIZATION Naval Postgraduate School	
11. NAME OF FUNDING/SPONSORING ORGANIZATION		12. ADDRESS (City, State, and ZIP Code)	
		13. PROCUREMENT INSTRUMENT IDENTIFICATION NUMBER	
		14. SOURCE OF FUNDING NUMBERS	
		PROGRAM ELEMENT NO.	PROJECT NO.
		TASK NO.	WORK UNIT ACCESSION NO.
15. TITLE (Include Security Classification) WATER MASS ANALYSIS OF THE 1991-1992 EL NIÑO SIGNAL IN THE FARALLON ISLANDS REGION (U)			
16. PERSONAL AUTHOR(S) Hays, Kevin Austin Samuel			
17a. TYPE OF REPORT Master's Thesis		17b. TIME COVERED FROM TO	17c. DATE OF REPORT (Year, Month, Day) March 1993
17d. SUPPLEMENTARY NOTATION The views expressed in this thesis are those of the author and do not reflect the official policy or position of the Department of Defense or the United States Government.			
18. SUBJECT TERMS (Continue on reverse if necessary and identify by block number)		19. COSATI CODES	
FIELD	GROUP	SUB-GROUP	El Niño, Water Mass Analysis, Temperature-Salinity Relationships, Spiciness, Atmospheric Teleconnection, California Current System
20. ABSTRACT (Continue on reverse if necessary and identify by block number)			
Five hydrographic (CTD) and acoustic Doppler current profiler (ADCP) cruises were conducted in February, May, August and late October/early November, 1991 and February, 1992 near the Farallon Islands off of central California in order to determine the seasonal variation of the circulation in the region. The timing of the study was such that the onset of the 1991-1992 El Niño/Southern Oscillation was directly observed in the data obtained. A detailed hydrographic analysis of the data showed single station temperature anomalies as great as 4.48 standard deviations warmer than the historical 40 year CalCOFI mean, and salinity anomalies 5.58 standard deviations fresher during February, 1992. The maximum anomalies for both temperature and salinity were between 100 - 150 m depth and within one Rossby radius (20 km) of the continental shelf break. A T-S analysis suggested that there were no large intrusions of different water mass types, and that the anomalies resulted primarily from altered mixing processes			
21. DISTRIBUTION/AVAILABILITY OF ABSTRACT <input checked="" type="checkbox"/> UNCLASSIFIED/UNLIMITED <input type="checkbox"/> SAME AS RPT. <input type="checkbox"/> DTIC USERS		22. ABSTRACT SECURITY CLASSIFICATION UNCLASSIFIED	
23. NAME OF RESPONSIBLE INDIVIDUAL Steven R. Ramp		24. TELEPHONE (Include Area Code) (408) 656-3162	25. OFFICE SYMBOL OC/Ra

due to thermocline/halocline depression. Strong positive sea level anomalies for the west coast of North and South America occurred simultaneously at the Equator and the far north (Gulf of Alaska) then spread from both directions towards central California. The broadening and strengthening of the Aleutian low caused onshore transport and downwelling at the Farallones site. Oceanic processes propagating northward may have occurred but could not be rigorously identified with this data set.

Approved for public release; distribution is unlimited.

**A Water Mass Analysis of the 1991-1992 El Niño Signal in the Farallon Islands
Region**

by

**Kevin Austin Samuel Hays
Lieutenant, United States Navy
Bachelor of Science in Political Science, U.S. Naval Academy, 1984**

Submitted in partial fulfillment of the
requirements for the degree of

**MASTER OF SCIENCE IN PHYSICAL
OCEANOGRAPHY**

from the

ABSTRACT

Five hydrographic (CTD) and acoustic Doppler current profiler (ADCP) cruises were conducted in February, May, August and late October/early November, 1991 and February, 1992 near the Farallon Islands off of central California in order to determine the seasonal variation of the circulation in the region. The timing of the study was such that the onset of the 1991-1992 El Niño/Southern Oscillation was directly observed in the data obtained. A detailed hydrographic analysis of the data showed single station temperature anomalies as great as 4.48 standard deviations warmer than the historical 40 year CalCOFI mean, and salinity anomalies 5.58 standard deviations fresher during February, 1992. The maximum anomalies for both temperature and salinity were between 100 - 150 m depth and within one Rossby radius (20 km) of the continental shelf break. A T-S analysis suggested that there were no large intrusions of different water mass types, and that the anomalies resulted primarily from altered mixing processes due to thermocline/halocline depression. Strong positive sea level anomalies for the west coast of North and South America occurred simultaneously at the Equator and the far north (Gulf of Alaska) then spread from both directions towards central California. The broadening and strengthening of the Aleutian low caused onshore transport and downwelling at the Farallones site. Oceanic processes propagating northward may have occurred but could not be rigorously identified with this data set.

TABLE OF CONTENTS

I. INTRODUCTION	1
A. BACKGROUND	2
1. Definitions and Terminology	2
2. The California Current System	3
3. Near-Surface Circulation Patterns	4
B. EL NIÑO THEORY	7
II. DATA COLLECTION AND CALIBRATION	10
A. FARALLON ISLANDS SAMPLING PLAN	10
B. HYDROGRAPHIC DATA (CTD) CALIBRATION	10
1. Calibration Procedures used during 1991 Cruises	10
2. Calibration Procedures used in the February 1992 Cruise	12
C. HISTORICAL CalCOFI DATA COLLECTION	13
D. SEA LEVEL DATA COLLECTION	15
E. MOORED DATA	15
F. SATELLITE AVHRR DATA	15
III. RESULTS	18
A. WATER MASS ANALYSIS	18
1. Anomaly plots	18
a. Single Station Anomalies	19
b. Vertical Sections	28
2. Temperature-Salinity analysis	41
3. Spiciness and depth along density (γ_θ) surfaces	45
a. The 26.4 γ_θ surface	46
b. The 26.8 γ_θ surface	54
B. OTHER SUPPORTING DATA	58
1. Sea Level Analysis	58
2. Atmospheric Teleconnection	60
3. Current Meter Data	62
IV. COMPARISON WITH THE 1982-1983 EL NIÑO EVENT	68
V. CONCLUSIONS AND RECOMMENDATIONS	71
A. THE EL NIÑO MECHANISMS SUPPORTED BY THIS DATA	71
B. RECOMMENDATIONS	72
REFERENCES	75
INITIAL DISTRIBUTION LIST	85

LIST OF TABLES

TABLE 1. WATER MASS SUMMARY IN THE CCS	6
TABLE 2. CTD CALIBRATION REGRESSION COEFFICIENTS	13
TABLE 3. CALCOFI SUMMARY.....	14
TABLE 4. DATA TYPE AND AVAILABILITY FOR FARALLON ISLANDS MOORINGS B AND F	16
TABLE 5. FARALLON ISLANDS STATIONS GROUPED RELATIVE TO HISTORICAL STATIONS	19
TABLE 6. SUMMARY OF MAXIMUM STATION ANOMALIES	29

LIST OF FIGURES

Figure 1.	Thirty Year Summertime Mean for Temperature and Salinity in the CCS (from Lynn et al., 1982).....	5
Figure 2.	Basic Sampling Plan for the Farallon Islands Study.	11
Figure 3.	Single Stations Anomalies for February, 1991.....	20
Figure 4.	Wind stress from NOAA buoys during 1991.....	21
Figure 5.	Single Station Anomalies for May, 1991.	23
Figure 6.	Single Station Anomalies for August, 1991.	24
Figure 7.	Single Station Anomalies for October/November, 1991.	26
Figure 8.	Single Station Anomalies for February, 1992.	27
Figure 9.	Vertical Sections of Anomalies for February, 1991.	32
Figure 10.	Vertical Section of Anomalies for May, 1991.....	33
Figure 11.	Satellite Imagery from 15 May, 1991.	34
Figure 12.	Vertical Sections of Anomalies for August, 1991.	35
Figure 13.	Vertical Sections of Anomalies for October/November, 1991....	37
Figure 14.	Vertical Sections of Anomalies for February, 1992.	39
Figure 15.	Satellite Imagery from 4 February, 1992.	40
Figure 16.	T-S Relationships.	42
Figure 17.	T-S Relationship for Station 15.....	45
Figure 18.	Spiciness Conversion Chart.	47
Figure 19.	The 24.6 γ_0 Surface for February, 1991.	48
Figure 20.	The 26.4 γ_0 Surface for May, 1991.	49
Figure 21.	The 26.4 γ_0 Surface for August, 1991.	50
Figure 22.	The 26.4 γ_0 Surface for October/November, 1991.	52
Figure 23.	The 26.4 γ_0 Surface for February, 1992.	53
Figure 24.a	Depth of 26.8 γ_0 Surface.....	55

Figure 24.b Depth of 26.7 γ_0 and 26.8 γ_0 Surfaces.....	56
Figure 25. Spiciness along the 26.8 γ_0 Surface.	57
Figure 26. IGOSS Monthly Mean Sea Level Anomalies, 1991-1992.	59
Figure 27. Primary Sea Level Pressure Patterns for the North Pacific. (excerpted from <i>Emery and Hamilton, 1985</i>).	61
Figure 28. Sea Level Pressure, October-December, 1991.	63
Figure 29. Sea Level Pressure, January-February 1992.	64
Figure 30. Time series of temperature from Farallones moorings B and F.	66
Figure 31. Time Series of Salinity from Farallones Mooring F.	67

ACKNOWLEDGMENTS

The data collected for this project was part of a study funded by the U.S. Environmental Protection Agency (EPA), Region 9, San Francisco, CA, and the Western Division, Naval Facilities Engineering Command (WESTDIV), San Bruno, CA. The technical expertise in computer programing, raw data manipulation and research assistance was provided by Mr. Paul F. Jessen. I was given tidbits of information along the way by a number of invaluable sources: Dr. Curtis A. Collins, Dr. N. Toby Garfield, Dr. Leslie Rosenfeld, Dr. Tom Murphree, Dr. Marlene Noble, Mr. Norm Hall, Ms. Shikiko Nakahara, Mr. Steve Gill, Mr. Patrick Caldwell, Mr. Dennis Laws, QM1 Ben Martin, Ms. Shirley Isakari and Mr. Pedro Tsai.

Obviously the most valuable asset, however, was Dr. Steven R. Ramp. His many hours, late nights and quick and thorough response to my endless bombardment of questions was critical to the completion of this work. God speed.

More important, however, than the pages you see before you is the fabric that was woven by my family. My wife, Laurie, whose endless support, encouragement and strength has been the seam that has held us together through good times and hard times. Metropolitan Opera company, look out! To my three daughters, Meghan, Brenna and Kelly; I've missed you. It's tickle time!

To our family at St. Mary's By-the-Sea Episcopal Church in Pacific Grove. Laurie, the girls and I have received from you "70 times 70 fold" the love which we have given. Peace be with you.

Finally to the youth at St. Mary's. We love you. Study hard. Love each other. Group hugs. Keep the Faith!

I. INTRODUCTION

Five research cruises were conducted over the continental shelf and slope in the vicinity of the Farallon Islands, CA in February, May, August, late October/early November 1991, and February 1992. The goal of the cruises was to determine the general circulation in the region throughout the year, particularly as it would affect the dispersal of dredged material dumped in the area. The study collected hydrographic, current meter, meteorological, marine biological, and Acoustic Doppler Current Profiler (ADCP) data, however this paper will analyze only the hydrographic data from Conductivity-Temperature-Depth (CTD) casts and the moored temperature, salinity and pressure data obtained during the program (*Ramp et al., 1992*).

The timing of the study allowed us the opportunity to observe the 1991-1992 El Niño event in the collected data. With this data, we were able to examine the mechanisms by which the propagation of El Niño-associated anomalies occurred in the coastal region of the central California Current System (CCS). This is by no means a complete resolution of the El Niño event; simply, it is an analysis of the oceanic response to this complex, teleconnected oceanic-atmospheric phenomenon.

A brief introduction to El Niño, the El Niño/Southern Oscillation (ENSO) cycle, the CCS and a generally accepted El Niño-manifestation theory completes this section. After describing the data collection and calibration procedures in section II, section III will present a detailed analysis of water masses, coastal sea level, current meter data and atmospheric teleconnections. A comparison with the 1982-1983 El Niño event and conclusions are covered in sections IV and V.

A. BACKGROUND

Since the 1976-1977 El Niño event, public and scientific interest in this phenomenon has soared. Its often devastating economic and ecological impact is well-documented (e.g., *Cane*, 1986; *Philander*, 1990; *Rómulo*, 1991), and it is chaotic in that no two events are precisely alike (*Enfield*, 1989). The study of El Niño has evolved into essentially its own science, whose "...aficionados have been known to compare different events in a manner reminiscent of oenologists discussing vintage years (*Cane*, 1983)". And while much effort has been put forth in previous works to define the "canonical El Niño", recent studies have revealed that the events can evolve in all manner of variety (e.g., *Cane and Zebiak*, 1987; *Cannon, et al.*, 1985; *Clarke and VanGorder*, 1992; *Enfield et al.*, 1987; *Philander*, 1990; *Barnett et al.*, 1992), and can even occur without here-to-for thought to be required phases (*Cane*, 1983).

1. Definitions and Terminology

Although historical usage prompts a definition of El Niño in terms of conditions off the South American coast, these changes are connected to changes throughout the world's atmosphere and oceans (*Cane*, 1983). The expanse of the study of El Niño has caused a convolution of the original definitions of the terms used to chronicle these events (*Aceituno*, 1992). This study will use the following definitions: "Southern Oscillation," from *Walker and Bliss* (1932), is a term used to identify an atmospheric phenomenon characterized by a shift in the pressure field across the tropical Pacific. "El Niño" will refer to a "major" El Niño, as defined by the Scientific Committee on Oceanic Research (SCOR, working group 55) as occurring when sea surface temperature from at least three of five stations between Talara (5°S) and Callao (12°S) exceeds 1 standard

deviation for four or more consecutive months (*Cane, 1983*). “La Niña” refers to that period of time when the SO is in its normal or relaxed phase (*Philander, 1990*) (i.e. the compliment to El Niño). Some authors choose to use “ENSO” to refer to single El Niño events (e.g., *Hirst, 1986*), but it is more often used to reference the entire coupled ocean-atmosphere cycle (*Hirst, 1988; Graham and White, 1988; Philander, 1983; Rasmusson and Wallace, 1983*), which is how it will be used here.

One of the most effective means by which the oceanic-atmospheric condition is determined is through use of the Southern Oscillation Index (SOI), which is the anomaly of pressure difference between Papeete, Tahiti, and Darwin, Australia (e.g., *Enfield, 1989*). When the SOI is positive, there is high pressure in the eastern tropical Pacific, and low pressure in the western tropical Pacific. The opposite occurs if the SOI is negative. El Niño (warm) events are usually characterized by negative SOI, and vice versa.

2. The California Current System

The California Current System is spatially and seasonally varied (*Tisch et al., 1992*). The principal oceanographic features of the region are: 1) wind-driven shelf flow; 2) a north to south positive temperature and salinity gradient; 3) poleward flow extending over the slope to a distance of about 70 km from the coast, which occasionally reaches the surface; 4) a meandering, energetic equatorward-flowing jet in the upper 300 m that separates from the coast, usually somewhere north of Point Reyes, yet generally stays within 100-200 km of the coast; 5) mean southeastward geostrophic flow throughout the year; 6) enhanced upwelling near capes; and 7) offshore transport at all depths on the north side of capes, and onshore transport on the south side of capes (*Reid et al., 1958; Huyer, 1983; Simpson, 1984b; Huyer et al., 1991; Tisch et al., 1991*). The

structure of each of these features is influenced by the shape or the orography of the coastline, or by alongshore changes in bathymetry associated with major promontories (*Bray and Greengrove, 1992*).

The conditions during the summer and winter differ most notably near the coast. Summer equatorward wind conditions cause nearshore upwelling, while an opposite wind flow in winter forces downwelling (*Rienecker and Mooers, 1986*). The water masses present in the CCS are summarized in Table 1.

Horizontal mean summer temperature and salinity profiles (Figure 1, from *Lynn et al., 1982*), show the typical hydrological structure in the summer season. The coastal effects of seasonal upwelling can be seen by the upward-tilting isotherms, especially from the coast to 100 km offshore. The SST increases with distance from the coast, as well as from south to north (not shown) (*Simpson, 1983; Tisch et al., 1992*). The salinity has an inshore maximum that is typically on the order of 33.6 ‰. When upwelling occurs, the surface salinity increases due to the vertical salinity profile. As distance offshore increases, a minimum occurs 300-500 km from the coast, indicating the presence of the Pacific Subarctic waters. Salinity then increases further offshore in the region of the North Pacific Central waters (*Simpson, 1984a*). The difference during the winter season is a downward-tilting isothermal structure (warmer) and corresponding salinity gradient (fresher) (*Huyer, 1984*).

3. Near-Surface Circulation Patterns

Equatorward alongshore winds drive offshore Ekman transport, resulting in a drop in sea level at the coast, as well as a return flow at depth of colder, more saline and nutrient-rich water (*Winant et al., 1977*). The resulting structure and variability of the density field can be used to describe many of the

features of coastal circulation. Relative to a deeper reference level, the upwelling of isopycnals corresponds to equatorward average flow. The resultant cross-shelf

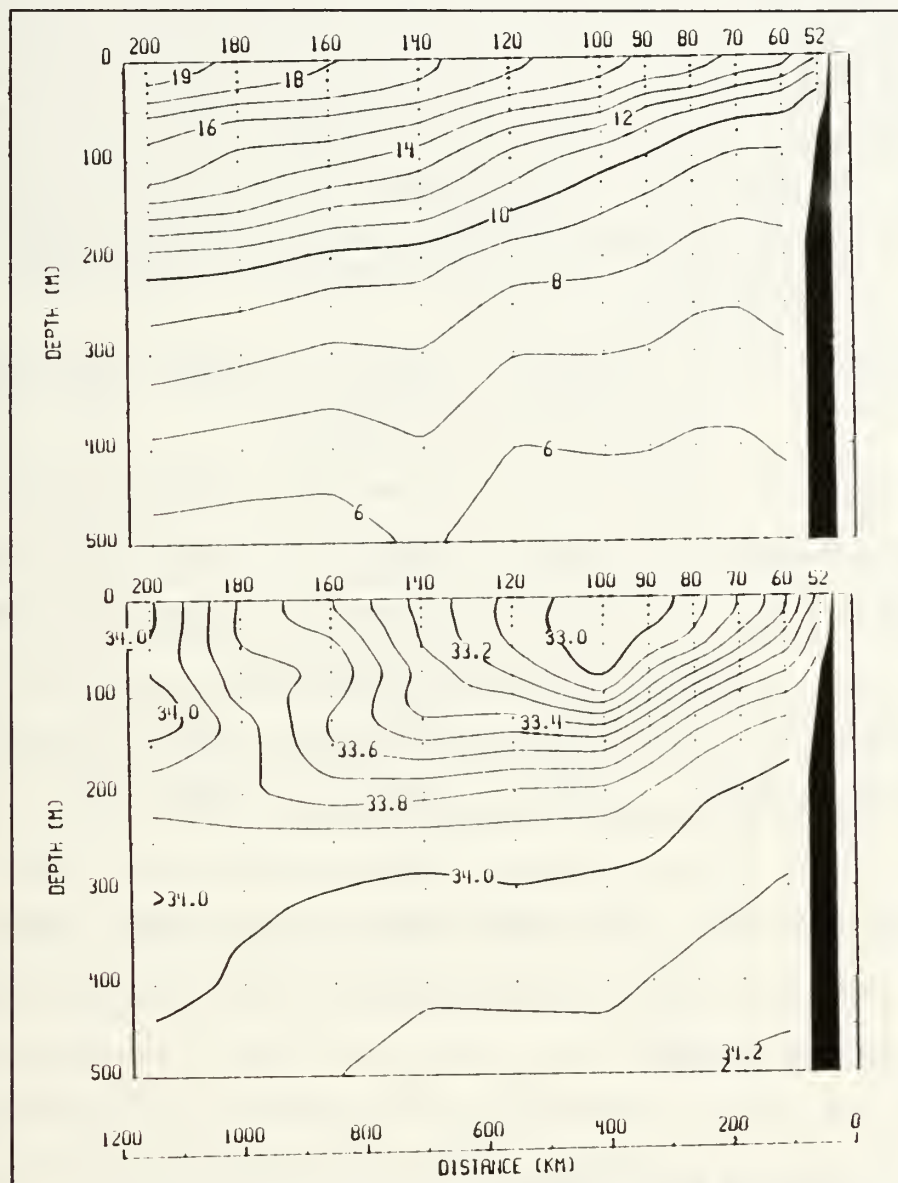


Figure 1. Thirty Year Summertime Mean for Temperature and Salinity in the CCS (from Lynn et al., 1982).

pressure gradient is balanced by geostrophic equatorward shelf flow. Cross-shelf velocity varies on shorter spatial scales: in opposing directions at the surface and

bottom and incoherent between alongshore moorings separated by 25 km or more (*Bray and Greengrove, 1992*).

Huyer (1983) analyzed the large-scale winds from *Nelson (1977)*, and calculated estimates of the resulting vertical velocities. She found maxima in both offshore Ekman transport and vertical velocities in the region from San

TABLE 1. WATER MASS SUMMARY IN THE CCS: The table gives a relative comparison of water masses off the California Current System (from *Simpson, 1984a*, except for NPIW which is from *Pickard and Emery, 1990*).

Water Masses	Temperature	Salinity	Oxygen	Nutrients
Surface Water Masses (0-200 m)				
Pacific Subarctic	Low	Low	High	High
North Pacific Central	High	High	Low	Low
Coastal Upwelled	Low	High	Low	High
Subsurface Water Masses (200-500 m)				
Equatorial Pacific	High	High	Low	High
North Pacific Intermediate	Low	Low	High	

Francisco to Cape Blanco. This spatial variation of wind may contribute to substantial convergences in shelf flow observed in the Gulf of the Farallones region (*Magnell et al., 1991*).

The near-surface characteristics in the region are also influenced by recurring and persistent eddy fields, cool (12.0°-13.5°C), salty (32.7-33.0 psu) filaments, and high mesoscale variability (*Huyer et al., 1991; Kosro et al., 1991; Ramp et al., 1991*). The presence of these features adds to the complexity of the region, necessitating even greater care in determining the source of the anomalies discovered during the Farallones study.

B. EL NIÑO THEORY

Cane (1983) describes El Niño as the result of two-way coupling between the atmosphere and the ocean. The resulting sum of free and forced Rossby and equatorial Kelvin waves imparts an anomalous adiabatic oceanic response on the time scale of a few months. This response causes a rise in sea level in the western Pacific basin at the beginning of the El Niño year. As the year progresses, there is a massive collapse of the trade winds east of the date line causing an across-basin depression of the thermocline and subsequent rise in eastern Pacific coastal sea level.

El Niño conditions are characterized by a large-scale weakening of the Southern Hemisphere trade wind system beyond the normal seasonal weakening at that time, the decrease (or even cessation) of upwelling along the Peruvian and Ecuadorian coasts, the sudden appearance of anomalously warm and low-salinity surface water for nearly a thousand kilometers off the coast, and the southward extension of this water far beyond its usual summer limits (*Hurlburt, et al., 1976*). These wind relaxations generate equatorial Kelvin waves (*Wyrtki, 1975; Cane, 1983*). The equatorial Kelvin waves impinge on the western North American continent and become coastally trapped, spawning westward propagating Rossby waves as the Kelvin waves propagate poleward (*Clarke, 1983*).

There are five basic theories for the mechanism by which warm, fresh anomalies are transmitted by ENSO into the CCS. The first theory ascribes to the northward advection of Equatorial waters. These warmer, saltier southern waters would be forced northward along the coast by an as-yet-poorly-understood mechanism, perhaps as an enhanced undercurrent.

Another theory that is based on oceanic forcing is that of thermocline/halocline depression via a coastally-trapped internal Kelvin wave and subsequent “leaking” offshore via mid-latitude baroclinic planetary Rossby waves. The mechanism by which this occurs is that the downwelling Kelvin wave depresses the main thermocline, such that the normal upwelling processes do not reach the “cold pool” below. The results are positive temperature and negative salinity anomalies. Additionally, a positive sea level anomaly is produced by increasing the warm upper layer thickness.

Thermocline/halocline depression can also be induced by the enhanced onshore transport associated with a basin-scale wind stress. This wind stress forces a strengthening and broadening of the Aleutian low to the east and south of its normal position. The broad low causes southwesterly winds along the central California coast which, via the Ekman forcing, causes onshore transport and subsequent downwelling conditions everywhere. The resulting water mass structure consists of positive temperature and negative salinity anomalies. Additionally, the upper layer thickness is increased and water is “piled up” at the coast, producing a positive sea level anomaly.

The fourth theory is that of an onshore transport of Pacific Subarctic Water (PSAW) by the same mechanism discussed in the previous paragraph (e.g., *Simpson, 1984a*). The onshore transport of this water mass will usually produce positive temperature and negative salinity anomalies, since water offshore is warmer and fresher than onshore in the upper 500 m (see Table 1).

The final theory involves an altered northeast Pacific heat budget. Less upwelling causes a decrease in the amount of coastal fog and low level clouds. This in turn increases the solar insulation and surface heating. The effect is strongest at the surface and generally confined to the upper 100 m. The result is

a positive temperature anomaly, but the effect on salinity is not clear. There may be enhanced evaporation, but this too could be offset by greater rainfall in certain ENSO years.

Each of these theories will be addressed in the context of this study. We will attempt to ascertain the mechanism by which the 1991-1992 El Niño signal was introduced into the Farallones region. Evidence will also be presented to refute those theories that do not apply in this case.

II. DATA COLLECTION AND CALIBRATION

A. FARALLON ISLANDS SAMPLING PLAN

The basic sampling plan consisted of five parallel cross-shelf transections, labeled *a-e*, with 20 km along-shelf separation (Figure 2) and irregularly spaced cross-shelf spacing to better discern cross-slope structures. Coverage during the study was extensive, with the exception of the February 1992 cruise when severe weather prohibited the sampling of line *e* and a number of other individual stations. Additionally, six current meter moorings were deployed along lines *b* and *d* (Figure 2).

The study area encompasses a region from Pigeon Point ($37^{\circ} 11.1' N$, $122^{\circ} 23.2' W$) to Point Reyes ($37^{\circ} 59.9' N$, $123^{\circ} 01.2' W$), extending from the coast to approximately 90 km offshore. This region includes part of the Gulf of the Farallones National Marine Sanctuary. All five surveys were conducted aboard the research vessel *POINT SUR*, home-ported in Moss Landing, CA.

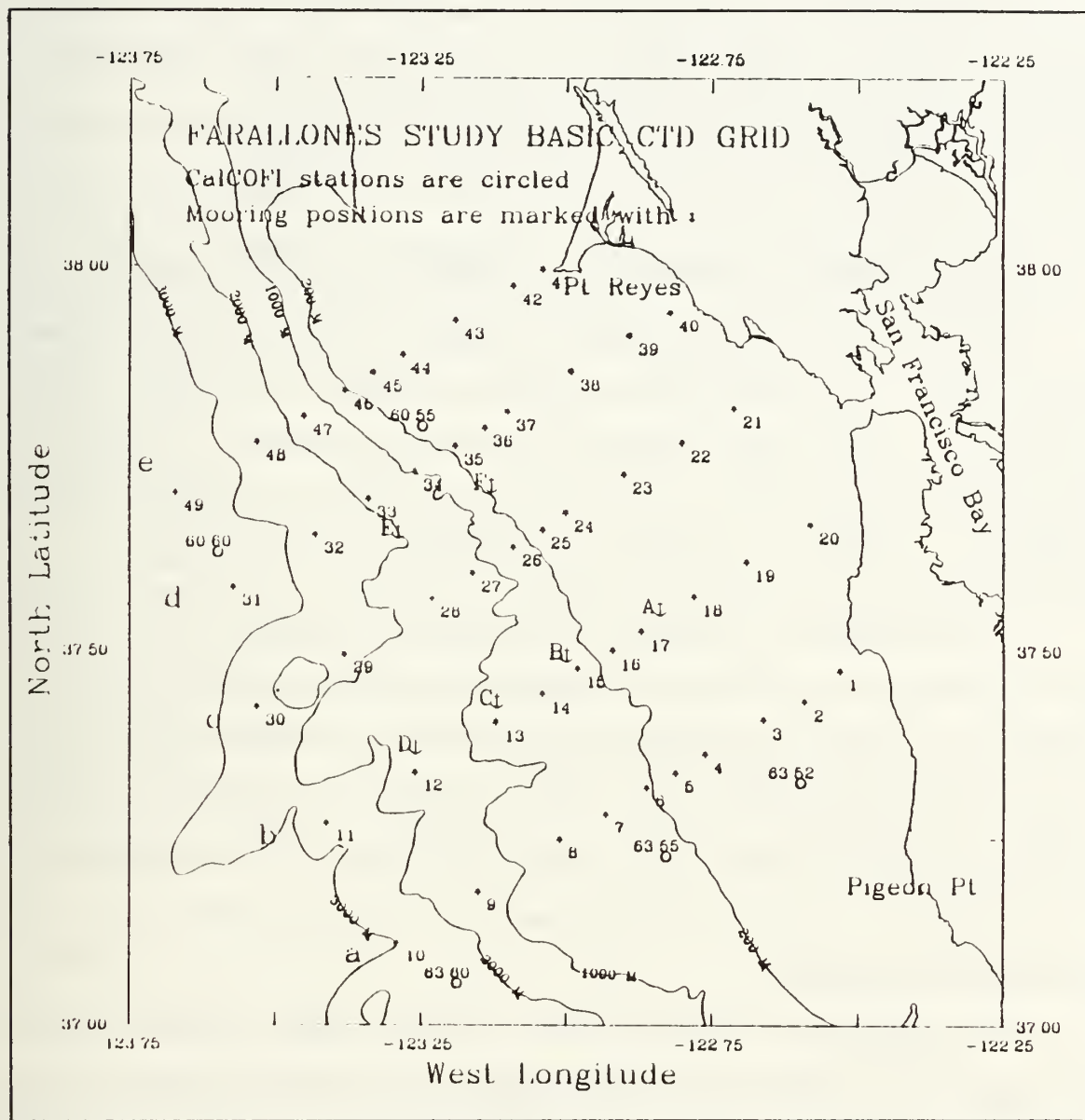
The basic procedure for each cruise of the Farallon Islands study was as described above. An account of the deviations from the basic plan are detailed in *Jessen et al., 1992a, 1992b, 1992c, 1992d*, and *Rago et al., 1992*.

B. HYDROGRAPHIC DATA (CTD) CALIBRATION

1. Calibration Procedures used during 1991 Cruises

Hydrographic data were acquired using a Neil Brown Mark III-B CTD. A General Oceanics Rosette sampler, equipped with twelve 5-liter Niskin bottles for *in situ* water sampling, was attached to the CTD and deployed during each cruise. At the majority of stations, two water samples were taken during the CTD

upcast for salinity calibration; one at the deepest depth of the cast and one near the surface. The CTD sampling rate was 32 Hz, and raw data was collected using



The standard calibration procedures were applied to the data obtained on the four 1991 cruises, and are detailed in various individual cruise summaries (*Jessen et al., 1992a, 1992b, 1992d; and Rago et al., 1992*). A summary of the CTD calibration coefficients is given in Table 2. Due to the uniqueness of the February, 1992 cruise, the procedures used during that study are detailed below.

2. Calibration Procedures used in the February 1992 Cruise

In February, 1992, the hydrographic data was initially acquired using an EG&G Mark V CTD. Following the completion of station 33, the Mark V CTD began showing a large shift in its readings and was replaced by a Neil Brown Mark III-B CTD which was used for the remainder of cruise. The Mark V CTD sampling rate was 16 Hz, while that of the Mark III-B CTD was 32 HZ.

The temperature, conductivity, and pressure sensors on the Mark V CTD were calibrated prior to the cruise. The pressure calibration was conducted at twenty approximately equally-spaced pressures from 0 to 6000 dbar, using a Chandler Engineering deadweight tester as a standard. A regression was then performed fitting the CTD pressures to the standard. The result yielded a linear fit with a slope of 1.00016. The CTD pressure offset at the beginning of each cast was used as the intercept.

The temperature calibration was achieved using a model 162CE Rosemount Platinum Resistance Temperature Standard (PRTS) in conjunction with an EG&G Automatic Temperature Bridge (Model ATB-1250). The standard (PRTS) sensor was calibrated using a triple point cell. The regression procedure is again detailed in the individual cruise reports, and the coefficients are listed in Table 2.

The conductivity calibration was performed using an EG&G Conductivity/Salinity Adapter (model CSA-1250) in conjunction with the

TABLE 2. CTD CALIBRATION REGRESSION COEFFICIENTS:
The slope and intercept calculated through regression analysis done on the calibration of the Mark III-B and Mark V CTDs, as described in sections II.B.1 and II.B.2, are summarized in this table.

CRUISE/ SENSOR	PRESSURE SLOPE	TEMPERATURE SLOPE	TEMPERATURE INTERCEPT	CONDUCTIVITY SLOPE	CONDUCTIVITY INTERCEPT
February 91 Mark III-B	0.99919	0.999441	0.000220	0.9982	0.17707
May 91 Mark III-B	1.00016	0.999898	0.003823	0.9982	0.17707
August 91 Mark III-B	0.999610	0.999818	0.000131	0.9982	0.17707
Oct-Nov 91 Mark III-B	1.000663	0.999818	0.000131	0.9982	0.17707
February 92 Mark III-B	1.000376	0.999738	-0.000673	1.000371	0.116953
February 92 Mark V	0.007354	0.99996189	-3.91438	0.9999265	0.021466

(PRTS) and the ATB-1250. Constant conductivity baths were used to compare the standard and sample sensor conductivities at five different conductivity levels. Regression analysis was used to compare the sample cell conductivities with the standard sensor conductivities.

C. HISTORICAL CalCOFI DATA COLLECTION

Observational physical oceanography of the California Current System (CCS) using hydrographic surveys has its modern origins in the California Cooperative Fisheries (CalCOFI) program, which began in 1937 (*Bray and*

Greengrove, 1992). The CalCOFI data provides a broad overview of circulation along the west coast of the United States. Analyses of CalCOFI data, including the water mass structure of the CCS, were conducted by *Tibby (1941)*, *Sverdrup and Fleming (1941)*, *Reid et al. (1958)*, *Roden (1971)*, *Reid (1972)*, *Churgin and Halmiński (1974)*, *Reid and Arthur (1974)* and *Lynn and Simpson (1987)*.

Individual CalCOFI stations were obtained from Dr. Norman F. Hall, the National Oceanographic Data Center (NODC), Southwest Liaison Officer, in La Jolla, CA, to provide a historical comparison with the Farallones data. The individual stations are actually the compilation of many casts, both part of the CalCOFI program and others collected and archived in the NODC data base. The stations were searched using an algorithm which extracted any cast that was within 4 nm (7.4 km) of the historical position of each CalCOFI station. The stations were selected from Lines 60 (stations 60.55 and 60.60) and 63 (stations 63.52, 63.55 and 63.60) for their spatial coverage within the Farallones study area (Figure 2, Table 3). Due to the nature of the collection procedure, the data set will hereafter be referred to as the “historical” stations or data.

TABLE 3. CALCOFI SUMMARY: This table summarizes the latitude, longitude, record length, and period covered by each CalCOFI station.

CalCOFI Station number	Average Latitude °N	Average Longitude °W	Record Length (# of cruises)	Period covered
60.55	37.784	123.255	50	08/07/51-10/19/84
60.60	37.619	123.612	110	02/15/5010/19/84
63.52	37.315	122.607	75	08/02/51-10/21/84
63.55	37.215	122.835	66	08/02/51-10/21/84
63.60	37.046	123.198	62	07/19/57-10/21/84

D. SEA LEVEL DATA COLLECTION

Sea level anomalies are commonly used to investigate propagating wave and along- and across-shore transport theories (*Cane, 1983; Clarke and VanGorder, 1992; Cornejo-Rodriguez and Enfield, 1987; Hurlburt, 1976; Huyer et al., 1978; Wyrtki, 1975; and Simpson, 1984a, 1984b*). Time series of sea level anomaly were collected along the west coast from Callao, Peru to the Gulf of Alaska to investigate the coastal effects of the 1991-1992 El Niño event. The period covered by the sea level data runs from January 1991 to March 1992 and includes the entire scope of the Farallon Islands study.

E. MOORED DATA

Data obtained from six mooring sites, **A-F**, will be used to describe the temporal changes which occurred between the Farallones cruises. The time series from these sites will provide the means by which we will reconstruct the events associated with the onset of the 1991-1992 El Niño. Moorings **A** through **D** are along line *b*, and **E** and **F** are along line *d*, each containing a variety of sensors stationed at a number of depths (Figure 2). The sensors for moorings **B** and **F** are presented in order to show the spatial depth and type of data available from the moorings (Table 4). The calibration procedure for the moored sensors is detailed in *Noble, et al. (1992)*.

F. SATELLITE AVHRR DATA

Cloud-free satellite Advanced Very High Resolution Radiometer (AVHRR) imagery was available for four of the five surveys. Persistent low clouds and fog precluded obtaining imagery for the August 1991 cruise. The raw AVHRR data was obtained in digital form from Ocean Imaging, San Diego, CA and processed

at the Naval Postgraduate School IDEA Laboratory using the University of Miami DSP software.

TABLE 4. DATA TYPE AND AVAILABILITY FOR FARALLON ISLANDS MOORINGS B AND F: This table is an example of two of the six current meter moorings from the Farallones study. The table shows the mooring designator, the start and stop times of the data, the depth of sensor package, and the sensors at those depths. (C = Current meter, T = Sea Temperature, S = Salinity, P = Pressure)

Site	Start Time (M/D/Y)	Stop Time (M/D/Y)	Sensor Depth	Data Type
B	07/04/91	09/23/91	10	C,T
B	03/09/91	02/08/92	150	C,T
B	03/09/91	02/08/92	260	C,T,S
B	03/09/91	02/08/92	390	C,T,S
F	03/11/91	02/10/92	75	C,T
F	03/12/91	02/13/92	180/223	C,T,S,P
F	03/11/91	02/13/92	280/324	C,T,S,P
F	03/11/91	02/13/92	417/456	C,T,S,P

Data obtained from the AVHRR (or AVHRR/2) instruments carried on the TIROS-N/NOAA series of polar orbiting satellites were used to obtain SST images for the study region. All AVHRR (NOAA 10) instruments measure emitted radiation in four wavelength bands, visible (0.6-0.7 μm), near infrared (0.7-1.1 μm), and thermal infrared (3.5-3.9 μm and 10.5-11.5 μm). The AVHRR/2 (NOAA 11) sensor has an additional thermal infrared band (11.5-12.5 μm) which enables daytime estimation of the sea surface temperature by correcting for atmospheric contamination (*Bernstein 1982; McClain 1985*). Sea surface temperature estimates were done for all the AVHRR/2 data using channels 4 and

5 and the nighttime AVHRR data using channels 3 and 4. AVHRR daytime data were left as black body brightness temperatures from channel 4 and were uncorrected for atmospheric contamination. The satellite data were first calibrated and navigated to Earth coordinates and then temperature was computed pixel by pixel. Each image was then co-registered to an identical coordinate map of the study region. Additional details can be found on the processing in *Cornillon et al. (1989)* and on the data extent in *Tracy (1990)*.

III. RESULTS

A. WATER MASS ANALYSIS

The first operation was to compare the Farallones and historical data to determine the strength and character of the El Niño event. Plots of temperature versus salinity (T-S) at all stations were then constructed in order to determine the water masses present in this region of the CCS at the different stages of the study. From those plots, critical density anomaly (γ_θ) surfaces were discerned, on which depth and spiciness (π) were of interest. The values of γ_θ were calculated using the procedures outlined in *Unesco (1991)*. Spiciness (Munk, 1981; Flament, 1986) is a measure of both temperature and salinity, and is useful for identifying water masses. Spiciness is useful for the description of interleaving at the boundary between different water types on different γ_θ surfaces. Waters which are warm and salty have higher π values, while those which are cool and fresh have lower π values.

1. Anomaly plots

Anomalies of temperature and salinity were calculated using two averaging methods; one to determine the collective anomaly in a particular sub-region, say the southern shelf of the study area, the other to produce vertical sections of anomalies along Farallones lines *a* and *d* (e.g., *Rienecker and Mooers, 1985*, their Figure 6). The first type required the averaging of multiple Farallones CTD stations which were geographically representative of the historical stations. The second involved interpolation of historical data to match a line of CTD stations.

a. Single Station Anomalies

When comparing fine-scale gridded fields, such as the Farallon Islands study to individual historical stations, horizontal averaging of the observational data must be conducted to match the coarse spatial structure of the historical fields. As a first step, data from several Farallones stations near the historical stations were averaged together for comparison (Table 5). The historical stations were 20 year seasonal averages, with each season using data from 3 months around each cruise. Averaging the Farallones stations spatially reduces mesoscale “noise” and increases confidence in the results. In the analysis

TABLE 5. FARALLON ISLANDS STATIONS GROUPED RELATIVE TO HISTORICAL STATIONS: This table summarizes the Farallones stations that were averaged to compare to the historical stations, listed by cruise. (See Figure 2 for spatial orientation.)

Historical Station	February 1991	May 1991	August 1991	October-November 1991	February 1992
60.55	23-26, 35, 37, 38, 43-46	23-26, 35-38, 43-46	23-26, 35-38, 43-46	23-26, 35-38, 43-46	24-26, 35-38
60.60	27-34, 47, 48	27-34, 47, 48	27-34, 47-49	27-34, 47-49	27-29, 32-34
63.52	3-5, 16-19	3-5, 16-19	3-5, 16-19	3-5, 16-19	3-5, 16-19
63.55	6-8, 13-15	6-8, 13-15	6-8, 13-15	6-8, 13-15	6-8, 13-15
63.60	9-12	9-12	9-12	9-12	9, 11, 12

that follows, anomalies are expressed both as magnitudes and as multiples of 1 standard deviation (σ) from the historical mean, calculated at each depth (e.g., “0.7767/1.04 σ ” is interpreted as “0.7767 positive units from the historical mean which is equal to 1.04 standard deviations”).

(1) February 1991. The overall characteristics of this cruise were seasonal surface cooling, a warm signature at 100 m depth off of the shelf, and

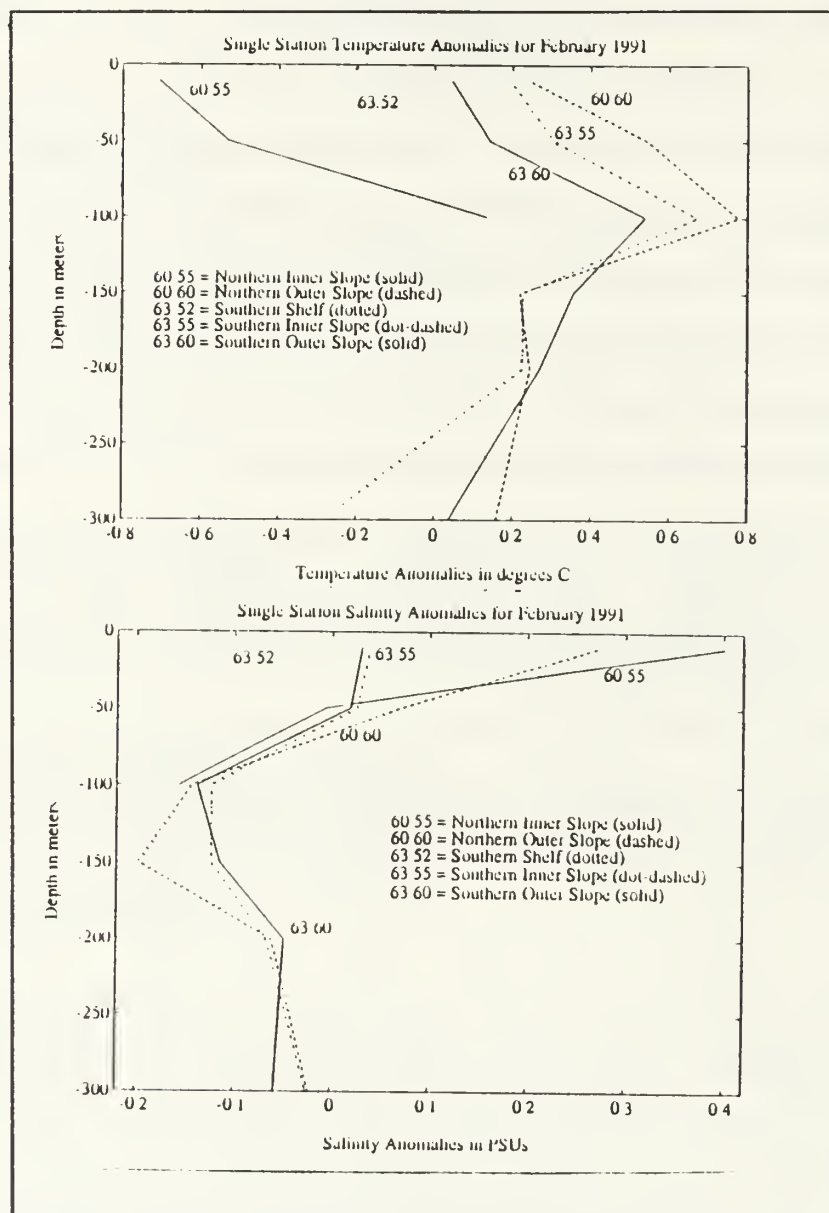


Figure 3. **Single Stations Anomalies for February, 1991.** This is a composite plot of the temperature (top) and salinity anomalies over the northern and southern shelf and slope regions in February, 1991.

high variability in the salinity signature below the mixed layer depth (Figure 3, above). All anomalies which exceeded 1σ were warm and fresh. The winds

during this period were moderately upwelling favorable and consistent with the seasonal average (Figure 4).

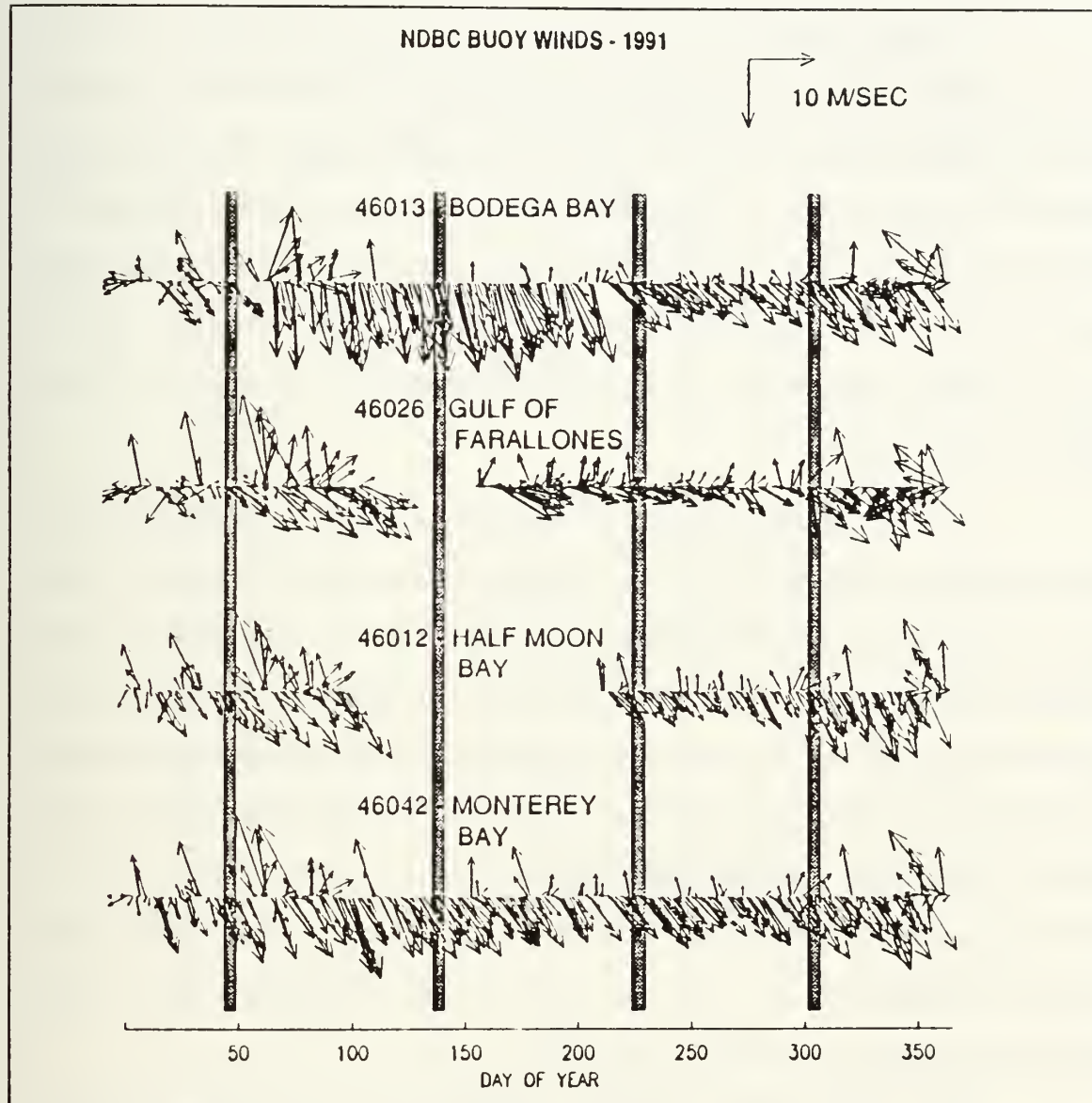


Figure 4. Wind stress from NOAA buoys during 1991. The winds in the vicinity of the Gulf of the Farallones during the four 1991 study cruises (from Ramp et al., 1992).

The few temperature anomalies which exceeded 1σ for this cruise were positive and existed at 100 m or below. Stations over the slope (Figure 2) had positive temperature anomalies which exceeded 1σ at 100 m of 0.7767/

1.04σ , $0.6719/1.3\sigma$, and $0.5392/1.04\sigma$ respectively. Additionally, the southern outer slope was anomalously warm at 150 m ($0.3552/1.36\sigma$).

Greater variability was found in the salinity signature. The southern outer slope had anomalies exceeding 1σ at all depths 100 m and below, with the greatest anomaly at 300 m ($-0.0581/1.53\sigma$). The southern inner slope had large anomalies at 150 m and at 200 m where the maximum anomaly occurred ($-0.0667/1.86\sigma$). The northern outer slope had an anomalous salinity signature from 100-200 m with a maximum anomaly at 150 m ($-0.1977/2.57\sigma$); the data near the northern inner slope had anomalies exceeding 1σ at only the 100 m depth ($-0.1564/2.86\sigma$).

(2) May 1991. Strong upwelling favorable winds dominated this cruise (Figure 4), and nearly all of the temperature anomalies during May 1991 were negative (Figure 5). The southern outer slope was cold at all depths, with a maximum anomaly of $-0.5797/3.05\sigma$ at 100 m. The maximum anomaly at the southern inner slope was at 50 m ($-0.6119/1.18\sigma$), and the station's temperature anomaly also exceeded 1σ at 100 m. The southern shelf and the northern outer and inner slopes had maximum anomalies at 10 m ($-1.6976/1.61\sigma$, $-2.0177/1.59\sigma$ and $-1.6955/1.12\sigma$, respectively). Additionally, the northern outer slope anomalies exceeded 1σ at 50 and 100 m, and the northern inner slope temperature anomaly exceeded 1σ at 100 m.

The only salinity anomalies exceeding 1σ were on the southern outer slope (150 m, $0.0530/1.15\sigma$) and the northern outer slope (10 m, $0.3440/1.08\sigma$). All of the salinity anomalies were weakly positive, indicating that the upwelling observed during this cruise was only slightly stronger than the seasonal climatology.

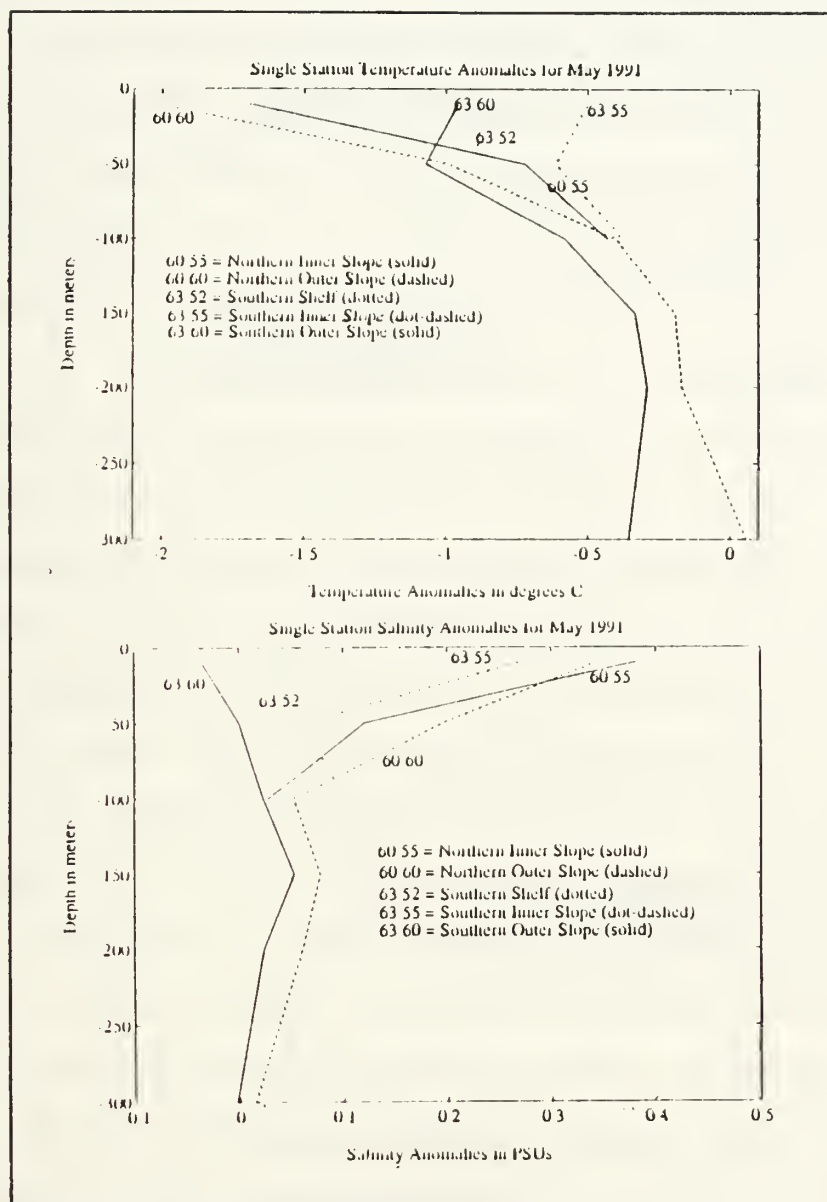


Figure 5. Single Station Anomalies for May, 1991. Same as Figure 3.

(3) August 1991. The calm meteorological conditions during this period (Figure 4) contributed greatly to the near surface warming found in this data set (Figure 6). This cruise was dominated by a warm temperature signature

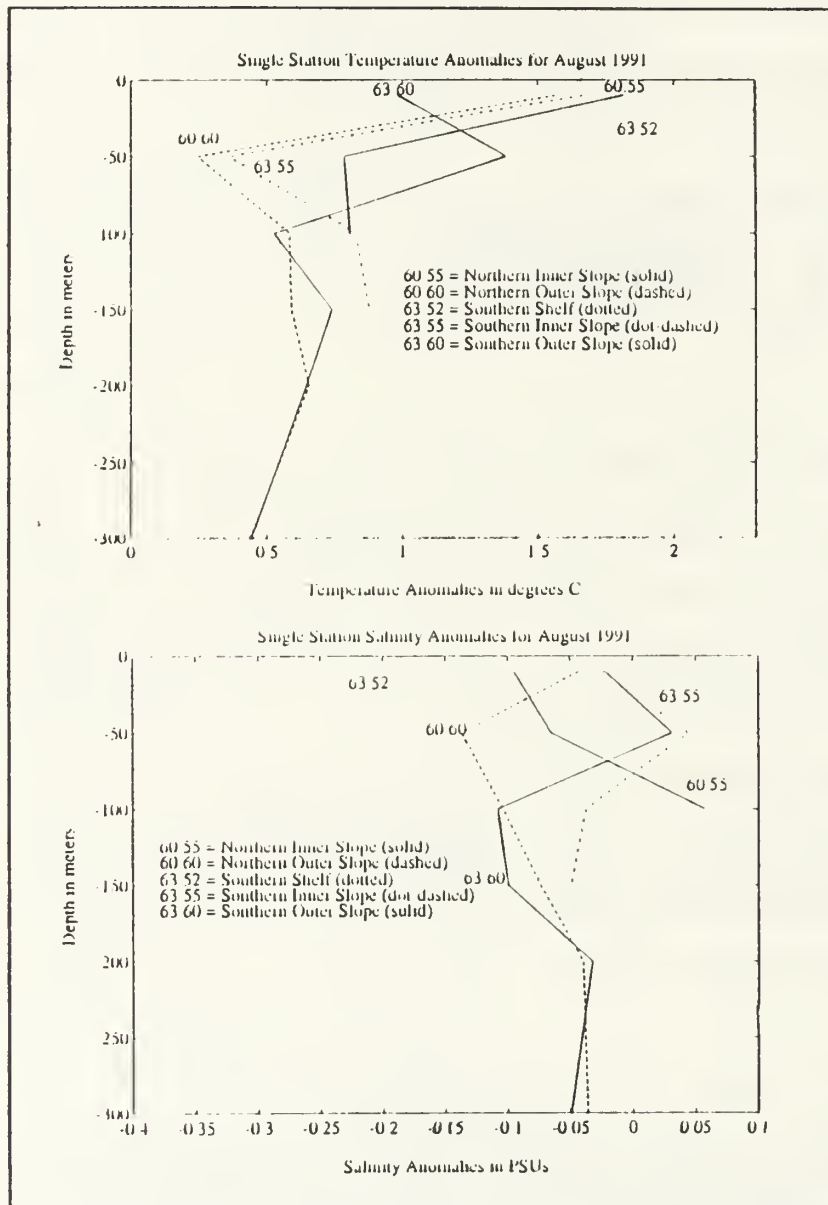


Figure 6. Single Station Anomalies for August, 1991. Same as Figure 3.

throughout the region and at all depths, save the 50 m depth of the southern inner slope. The maximum anomalies for the southern outer and inner slopes and shelf

were 50 m, $1.3843/2.25\sigma$, 150 m, $0.8767/2.58\sigma$ and 50 m, $1.3774/2.03\sigma$, respectively. The northern outer and inner slopes had their maximum anomalies at 150 m ($0.5907/2.42\sigma$) and 100 m ($0.8058/1.53\sigma$), respectively.

The southern outer slope had negative salinity anomalies exceeding 1σ at 100, 150 and 300 m depth with the maximum anomaly at 100 m ($-0.1078/2.17\sigma$). The southern shelf was also anomalously fresh with negative salinity anomalies exceeding 1σ at the 10 and 50 m depths, with 50 m having the maximum anomalous value ($-0.2446/2.03\sigma$).

(4) October/November 1991. The hydrographic anomalies typifying this survey were generally unremarkable, with the exception of the northern outer slope whose temperature characteristics were dominated by an offshore warm eddy (Figure 7). This region was anomalously cool at 10 m ($-1.2629/1.39\sigma$), and conversely warm below, exceeding 1σ at all depths with the maximum temperature anomaly occurring at 150 m ($0.9529/2.82\sigma$). The 10 m mark for the southern outer slope was also exceedingly cold at $-1.0622/1.13\sigma$.

The salinity anomalies had no discernible pattern. The southern outer slope exceeded 1σ at 100 m ($-0.1931/1.40\sigma$), the southern inner slope at 150 m ($-0.0786/1.44\sigma$) and 200 m ($-0.0545/1.43\sigma$) and the northern inner slope at 50 m and 100 m ($-0.1773/1.66\sigma$ and $-0.1123/1.83\sigma$, respectively). Like the February 1991 cruise, there were moderate upwelling favorable winds present at this time (Figure 4). While the Farallones data showed upwelling in the temperature and salinity regimes of the surface layer, the T-S properties were not strongly anomalous and therefore reflect typical seasonal conditions.

(5) February 1992. The warm temperature anomaly exceeded 1σ at all depths at every station, with the exception of the northern inner slope.

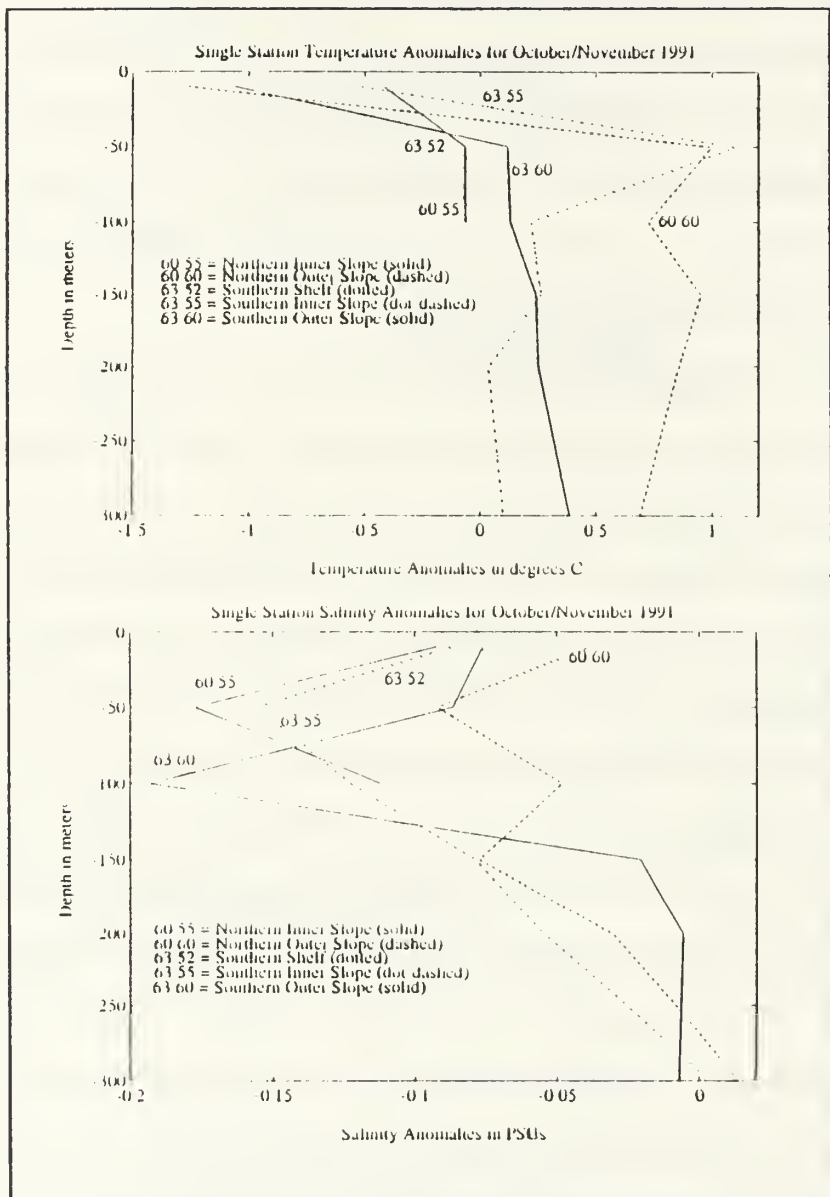


Figure 7. Single Station Anomalies for October/November, 1991. Same as Figure 3.

Similarly, salinity was anomalously fresh, exceeding 1σ at all stations below the mixed layer depth (100 m), with the exception of the 300 m depth of the southern

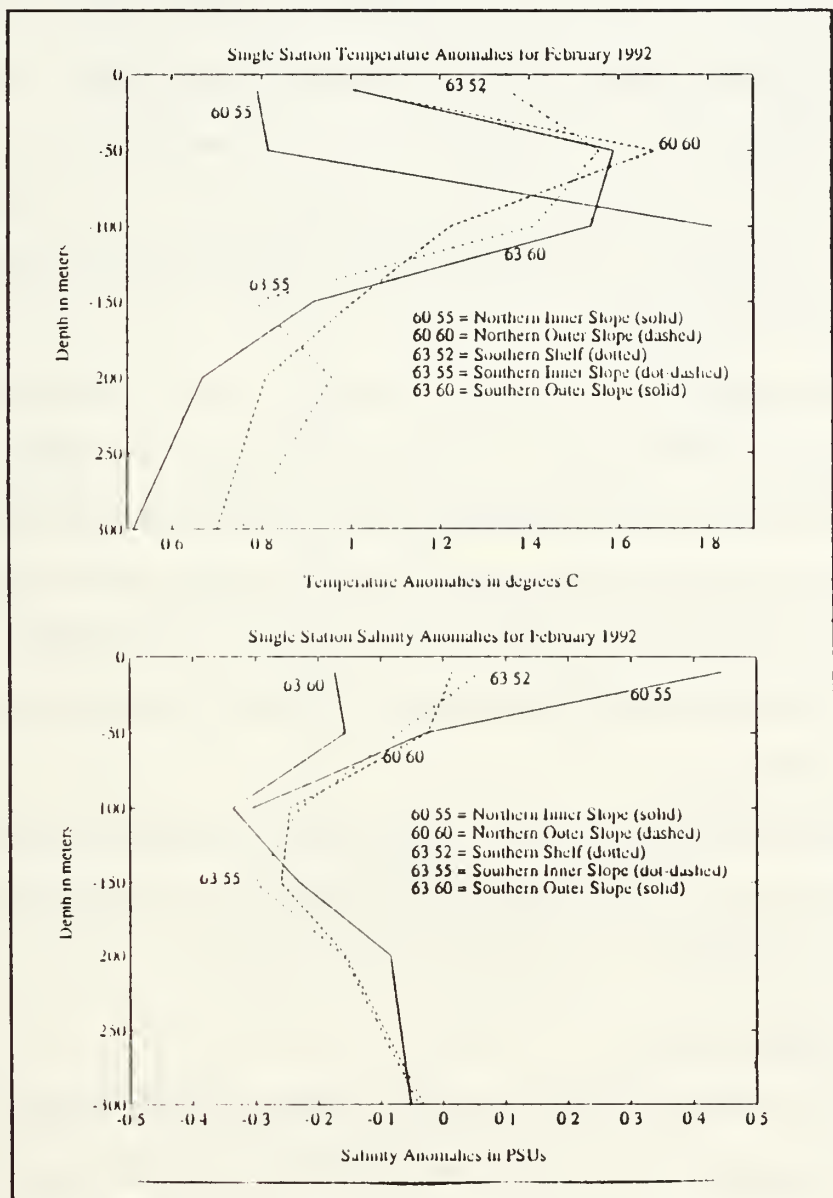


Figure 8. Single Station Anomalies for February, 1992. Same as Figure 3.

inner slope and northern outer slope (Figure 8, above). The southern outer slope had maximum anomalies which exceeded 1σ in temperature and salinity at 150 m depth ($0.9158/3.51\sigma$ and $-0.2302/2.99\sigma$, respectively). The southern inner

slope was most anomalous in temperature at 100 m ($1.4098/2.89\sigma$), and in salinity at 200 m ($-0.1595/4.46\sigma$). The temperature anomaly maximums for the southern shelf were at 10 and 50 m depth ($1.2921/1.48\sigma$ and $1.4012/1.57\sigma$, respectively). The maximum temperature anomaly at the northern outer slope was at 200 m ($0.8085/2.77\sigma$) and the maximum salinity anomaly was at 150 m ($-0.2598/3.38\sigma$). The only anomalies which exceeded 1σ at the northern inner slope for this cruise were at 100 m depth and were $1.8086/4.43\sigma$ for temperature and $-0.3052/5.58\sigma$ for salinity.

We interpret the warm, fresh anomalies which were maximum at mid-depth and persisted throughout the region as the primary signature of the 1991-1992 ENSO event. There were three major synoptic systems consisting of strong southwesterly winds that passed through the region at the time of the observations, causing intense periods of downwelling and onshore transport. However, the anomalies found in the region may also have been caused by oceanic phenomenon.

The maximum anomalies of temperature and salinity and the general features for each cruise are summarized below (Table 6). The dominant processes and their suspected effects will be discussed in detail later.

b. Vertical Sections

Three-month seasonal averages, centered around February, May, August, and November, were extracted from the historical data for comparison with the Farallones cruises. Once the seasonal data files were extracted, the individual historical data were interpolated to discrete depths of 10, 20, 30, 40, 50, 60, 70, 80, 90, 100, 125, 150, 175, 200, 225, 250, 275, and 300 m. This step was required because the historical data is largely comprised of bottle casts

activated at discrete depths; the interpolation was done to correct for the sampling

TABLE 6. SUMMARY OF MAXIMUM STATION ANOMALIES. This table indicates the maximum temperature and salinity anomalies for each depth. The format for the anomaly and its associated standard deviation follow that in the text. The summary and list of features at the bottom of the table applies to the entire cruise, not just the maximum anomalies.

Maximum Temperature Anomalies					
Depth	February 1991	May	August	October/November	February 1992
10 M	-0.7082/0.82	-1.6976/ 1.61	2.1607/1.60	-1.2629/1.39	1.3518/1.64
50 M	0.3072/0.78	-1.0720/ 1.48	1.3843/2.25	0.9988/1.44	1.5552/1.85
100 M	0.6719/1.38	-0.5797/ 3.05	0.5835/1.82	0.7254/1.72	1.8086/4.43
150 M	0.3552/1.36	-0.3323/ 1.45	0.8767/2.58	0.9529/2.82	0.9158/3.51
200 M	0.2695/0.95	-0.2908/ 1.45	0.6540/2.33	0.8576/2.53	0.8085/2.77
300M	0.1587/0.58	-0.3558/ 1.37	0.4355/1.41	0.6892/2.26	0.6992/2.55
Maximum Salinity Anomalies					
10 M	0.4003/0.61	0.3440/1.08	-0.2318/1.52	-0.0759/0.58	0.4453/0.68
50 M	0.0696/0.38	0.1963/0.72	-0.2446/2.03	-0.1773/1.66	-0.1027/0.54
100 M	-0.1564/2.86	0.1013/0.77	-0.1078/2.17	-0.1123/1.83	-0.3052/5.58
150 M	-0.1977/2.57	0.0530/1.15	-0.0994/1.93	-0.0786/1.44	-0.2598/3.38
200 M	-0.0667/1.86	0.0608/0.95	-0.0529/0.80	-0.0545/1.43	-0.1595/4.46
300 M	-0.0581/1.53	0.0146/0.20	-0.0493/1.53	0.0137/0.21	-0.0518/1.36
Summary	Slightly warm, fresh	Strongly warm, salty	Near normal	Near normal	Strongly warm, fresh
Features	No significant features	Sfc trapped cold water	Strong CUC	Warm eddy at north outer slope	Depressed Thermocline

error.

The use of historical data in the vertical cross-section analysis of anomalies necessitated computing the historically-accurate position of each station. Since each historical station is actually the compilation of many casts, the position of each cast was recorded and later averaged. The resulting average latitude and longitude is the central position of the historical station, and is the position used to calculate the vertical cross sections. Historical stations 63.52, 63.55, and 63.60 run parallel to Farallones line *a* with an along-shore separation of 9.67 km, and historical stations 60.55 and 60.60 run along line *d* with an along-shore separation of 5.54 km. (Figure 2). Only those Farallones stations located between the historical stations were used to calculate the sections of anomalies, which were stations 3-10 from line *a* and 31-34 from line *d* for the 1991 cruises. The February, 1992 cruise used stations 3-9 and 32-34 from lines *a* and *d*, respectively. Hereafter, lines *a* and *d* will be referred to as the southern and northern sections, respectively.

Once the historical positions were determined, the relative distance to each Farallones station was computed and the historical values of temperature and salinity were linearly interpolated to the positions of the Farallones CTD casts. These interpolated historical averages were then subtracted from the CTD data to determine the vertical structure of anomalies. The linear interpolation is justified since we assume that the 20 year temporal averaging has smoothed out any mesoscale variability that may have been present. Stations 3, 6, 7, 31, and 34 were close to the historical stations and the anomalies there have high confidence. Stations farther away were compared with the interpolated data and have lower confidence. Overall, the patterns make sense and do not show any trends which might be due to the linear interpolation.

(1) February 1991. Conditions during this cruise were generally warm and fresh, especially below the mixed layer, as can be seen in both the southern and northern sections (Figure 9). There were three prominent features in the southern section: 1) a cold, salty core on the shelf break (station 4) centered around 45 m, whose temperature was highly anomalous (more than 2σ), and whose salinity, while anomalous, was not as large; 2) a cold, fresh tongue intruding from offshore, centered at about 60 m depth; and 3) a much broader warm, fresh feature whose core was on the inner slope (station 8), centered at 110 m depth. The salinity structure below the mixed layer in the southern section was anomalously fresh, exceeding 1σ from about 90 m to 300 m.

In the northern section, there was a fresh core at mid-slope (station 33) centered around 125 m depth that was more than 3σ below the mean seasonal average and was probably an extension of the warm, fresh core observed in the same area in the southern section of this survey. The temperature signature is less well defined, but is still anomalously warm in this northern core.

(2) May 1991. The entire region, with minor exception, was colder and generally saltier than the historical mean, though rarely by more than one standard deviation (Figure 10). There was a weakly negative salinity water mass in the mid-slope region (stations 8 and 9) of the southern section centered around 45 m depth. Additionally, the southern section had a narrow warm wedge in the same mid-slope region, from the surface to 50 m. The two features do not appear to be connected, however.

The northern section was similar in structure within the upper and mixed layers. It did have a highly anomalous (exceeding 2σ) cold, salty surface feature along the mid-slope region (station 32). The surface trapping of this cold, salty mass, in concert with satellite imagery (Figure 11), suggests that the water

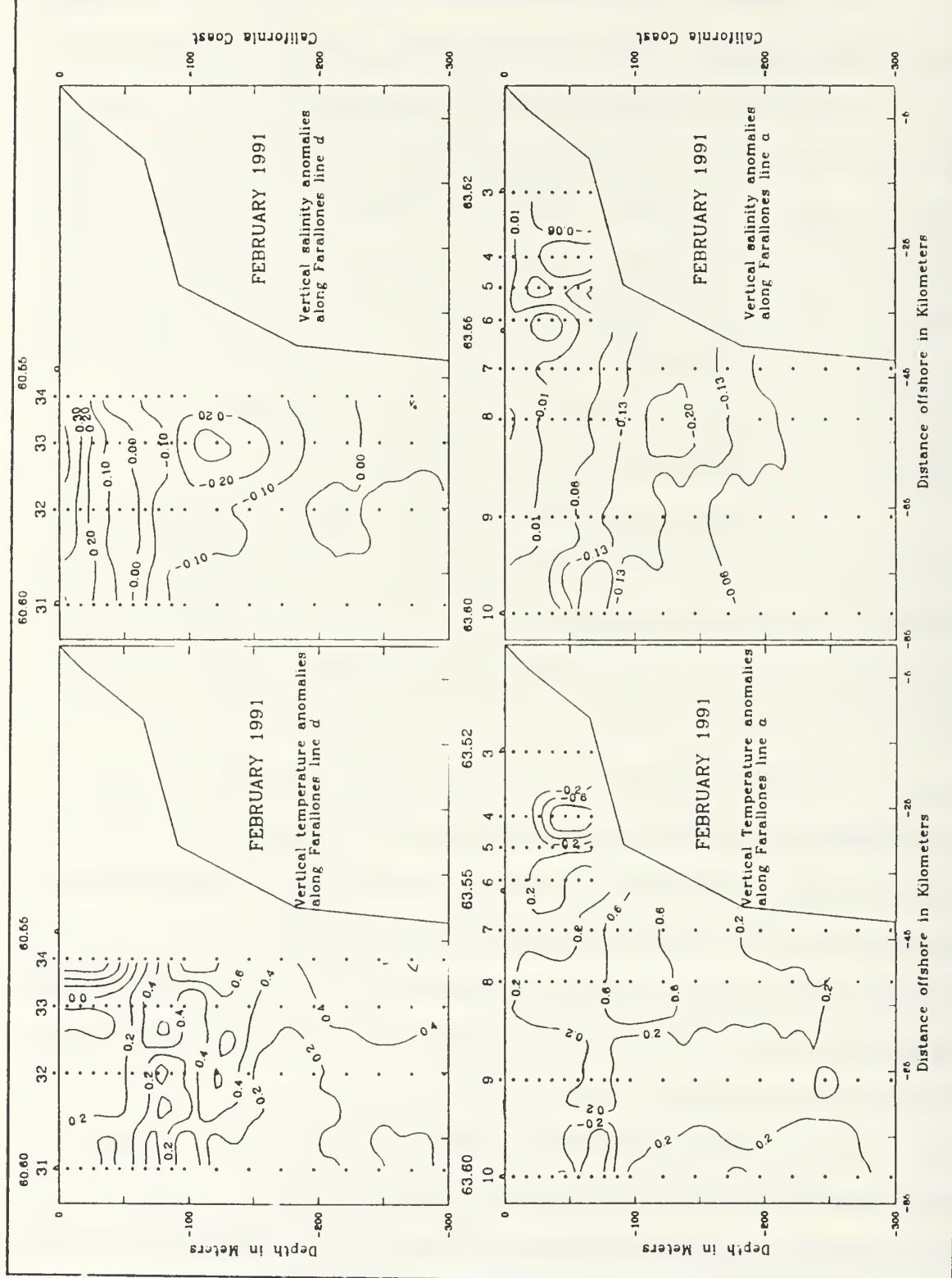


Figure 9. Vertical Sections of Anomalies for February, 1991.

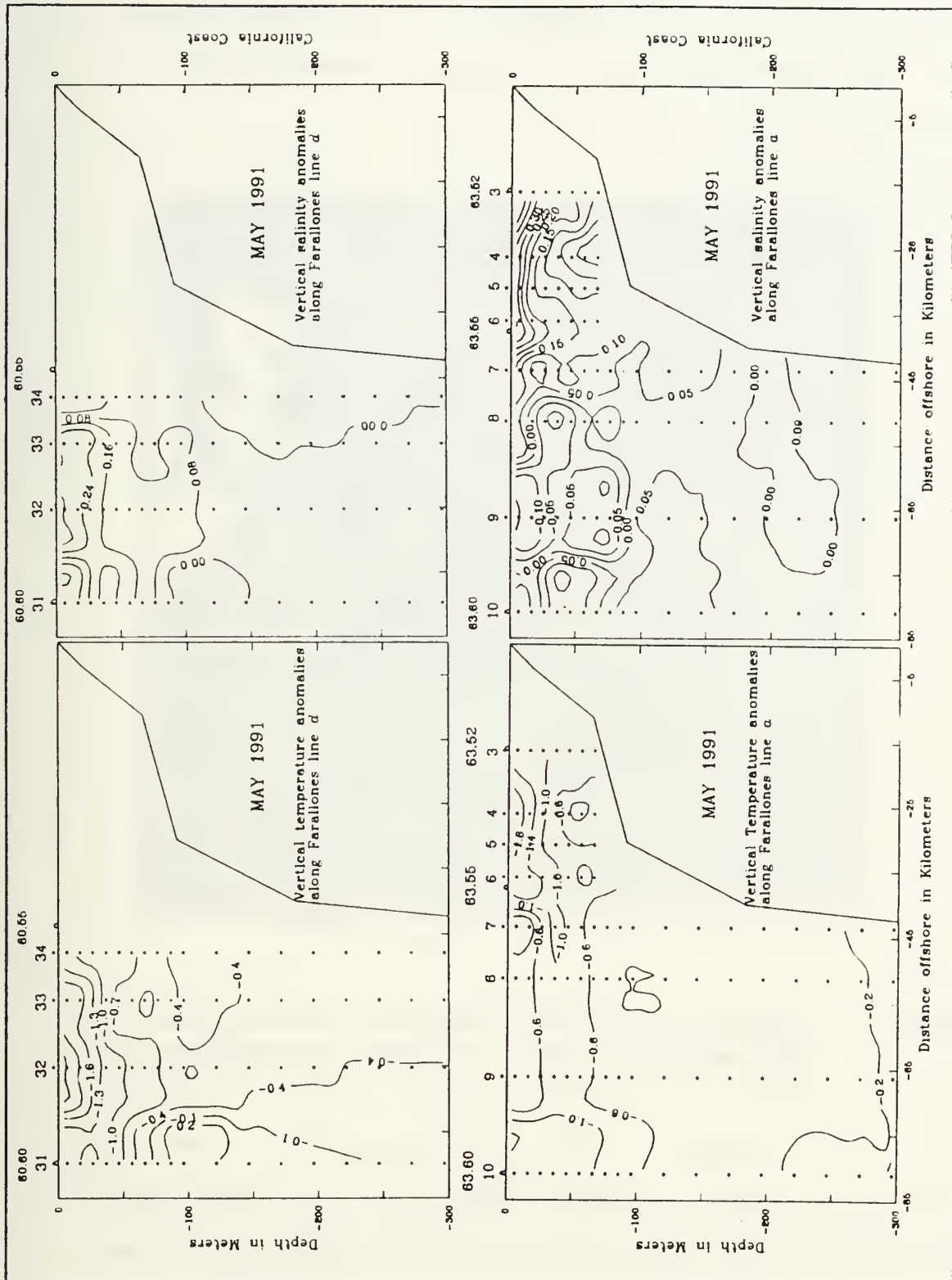


Figure 10. Vertical Section of Anomalies for May, 1991.

is being advected south from an upwelling center to the north of the survey region. Below the mixed layer, this section followed the normal seasonal climatology.

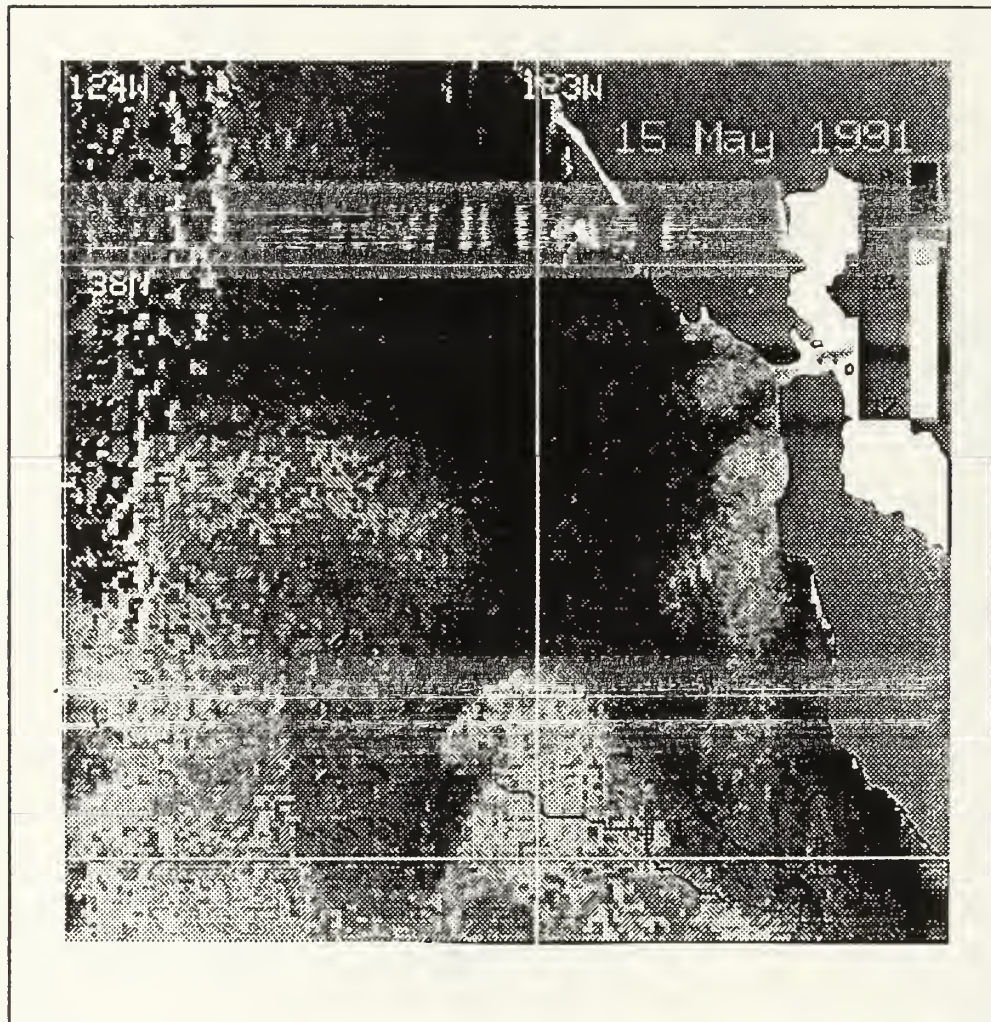


Figure 11. Satellite Imagery from 15 May, 1991. The image shows the cold, salty surface-trapped water mass (dark shading) advected south from the upwelling center to the north of Point Reyes.

(3) August 1991. The vertical sections for this cruise indicate simple surface heating in the absence of any strong vertical mixing (Figure 12). The temperature structure in this section at the shelf break (station 5) centered at 40 m was greater than 4σ , though there was no accompanying salinity anomaly.

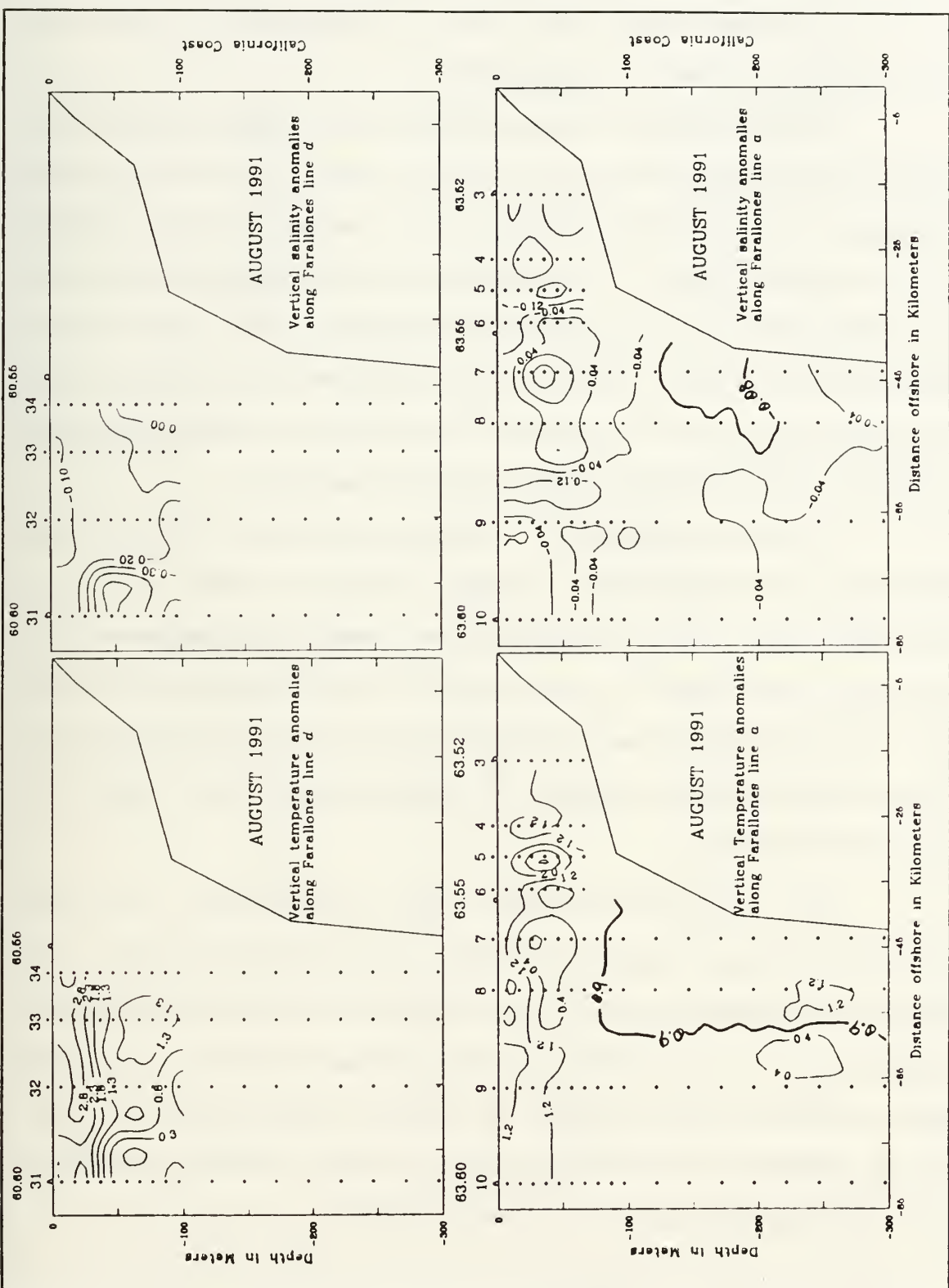


Figure 12. Vertical Sections of Anomalies for August, 1991.

The feature on the inner slope (station 7) had a core structure in temperature and salinity but did not exceed 1σ in either regime.

The 0.9 temperature contour reflects an entire region along the inner and outer southern slopes that were at least 2σ warmer than the mean seasonal climatology. The -0.08 salinity anomaly contour along the inner slope centered at 175 m depth exceeded 1σ . Separate plots of temperature and salinity (not shown) indicated a downward bending of the isopycnals here. There was also enhanced flow of the warm, salty California Undercurrent along the inner slope. The combination of the two mechanisms was sufficient to enhance the warm temperature anomaly and weaken the fresh salinity anomaly.

Surface heating in the northern section can be seen in the horizontal stratification of the temperature anomalies. The entire northern section was anomalously warm. The section also contained a salinity core centered at 50 m on the outer slope (station 31) which was over 2.5σ fresher than the historical mean. Historical data were not available below 100 m for the summer season on the inner slope (historical station 60.55), and therefore precluded evaluation of the lower water column.

(4) October/November 1991. The temperature and salinity anomalies for both the southern and northern sections of this cruise (Figure 13) reflected the normal seasonal variability of the region. There were no anomalies which exceeded 1σ in any domain, however the general trend was for cooler, fresher conditions in the mixed layer. As with the August cruise, historical data were not available for the fall season on the inner slope, precluding evaluation of the water column below 100 m in the northern section.

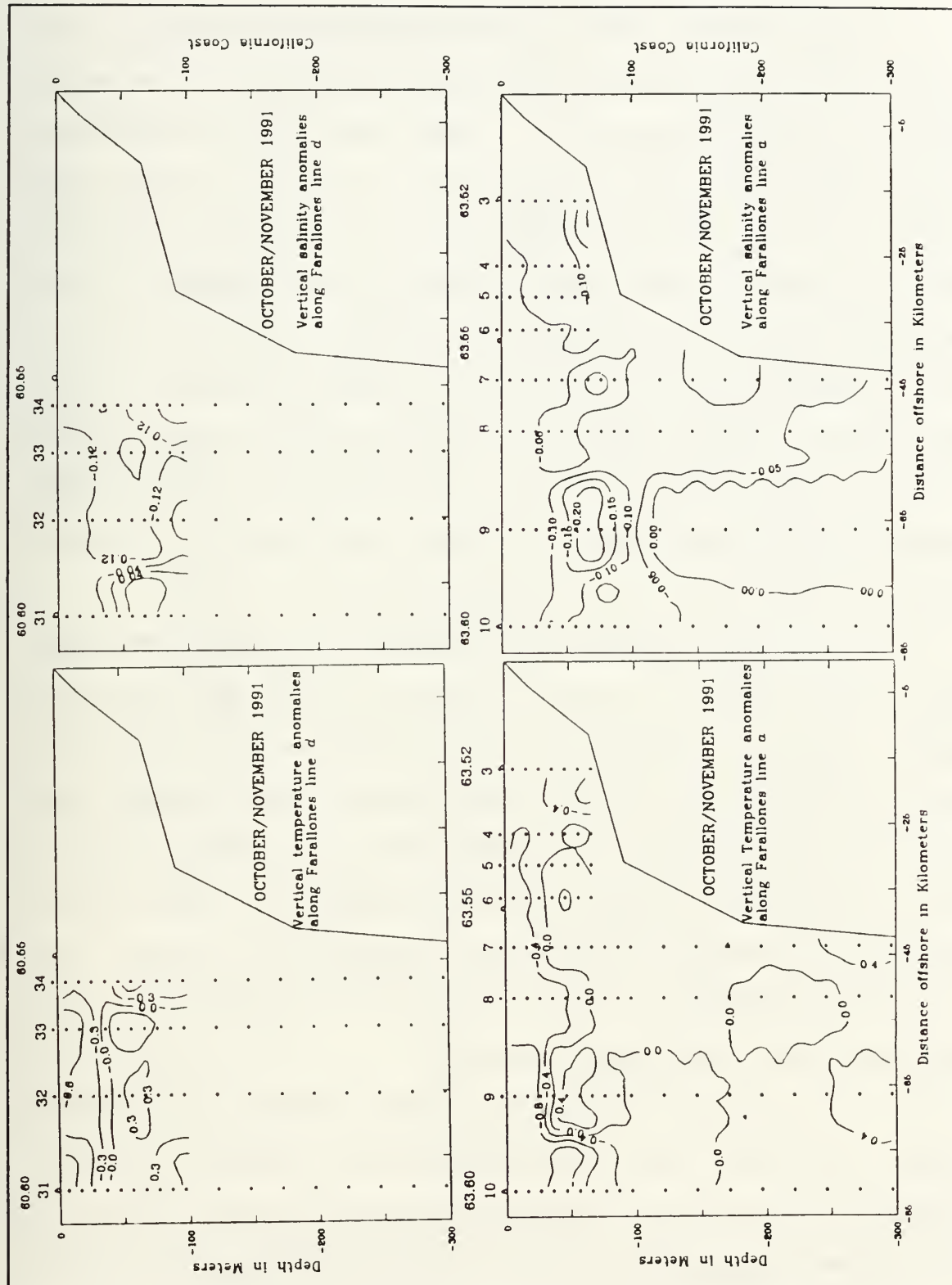


Figure 13. Vertical Sections of Anomalies for October/November, 1991.

(5) **February 1992.** The general characteristics of this survey were a strong warm temperature signature throughout the southern section and most of the northern section, accompanied by an equally strong salinity signature below 60-70 m depth in both sections (Figure 14). The structure on the inner slope (station 7) of the southern section showed a temperature core centered at 70 m that was more than 3σ greater than climatology, as was the thermal core on the outer slope (station 9). The salinity structure was highly stratified in the upper 70 m. The anomalies did not exceed 1 standard deviation until below 60 m on the outer slope and 70 m on the inner slope. The salinity structure centered at 150 m on the inner slope (station 7) was more than 4σ fresher than climatology. The temperature anomaly bounded by the 0.9 contour and the inner slope (175-260 m at station 7) exceeded 2σ above the climatological mean.

The warm anomalies seen throughout the southern section were more closely trapped to the inner slope region in the northern section. The positive temperature signature on the outer slope did not exceed 1σ until 200 m and below. The inner and mid-slope stations however were exceedingly warm from 50 m and 100 m and below, respectively. There was an additional small core of warm, salty water centered at mid-slope around 45 m depth that was remarkable not only due to its positive temperature, but also that it was surrounded by fresh anomalies. This feature may be an extension from a warm, salty front located further offshore (Figure 15).

The structure of the northern section basically agrees with the southern. The salinity core in the northern section at mid-slope (station 32) centered at 100 m was nearly 3σ fresher than climatology. In the lower layer, the mid- and inner slope (stations 33 and 34) temperatures had positive anomalies exceeding 1σ .

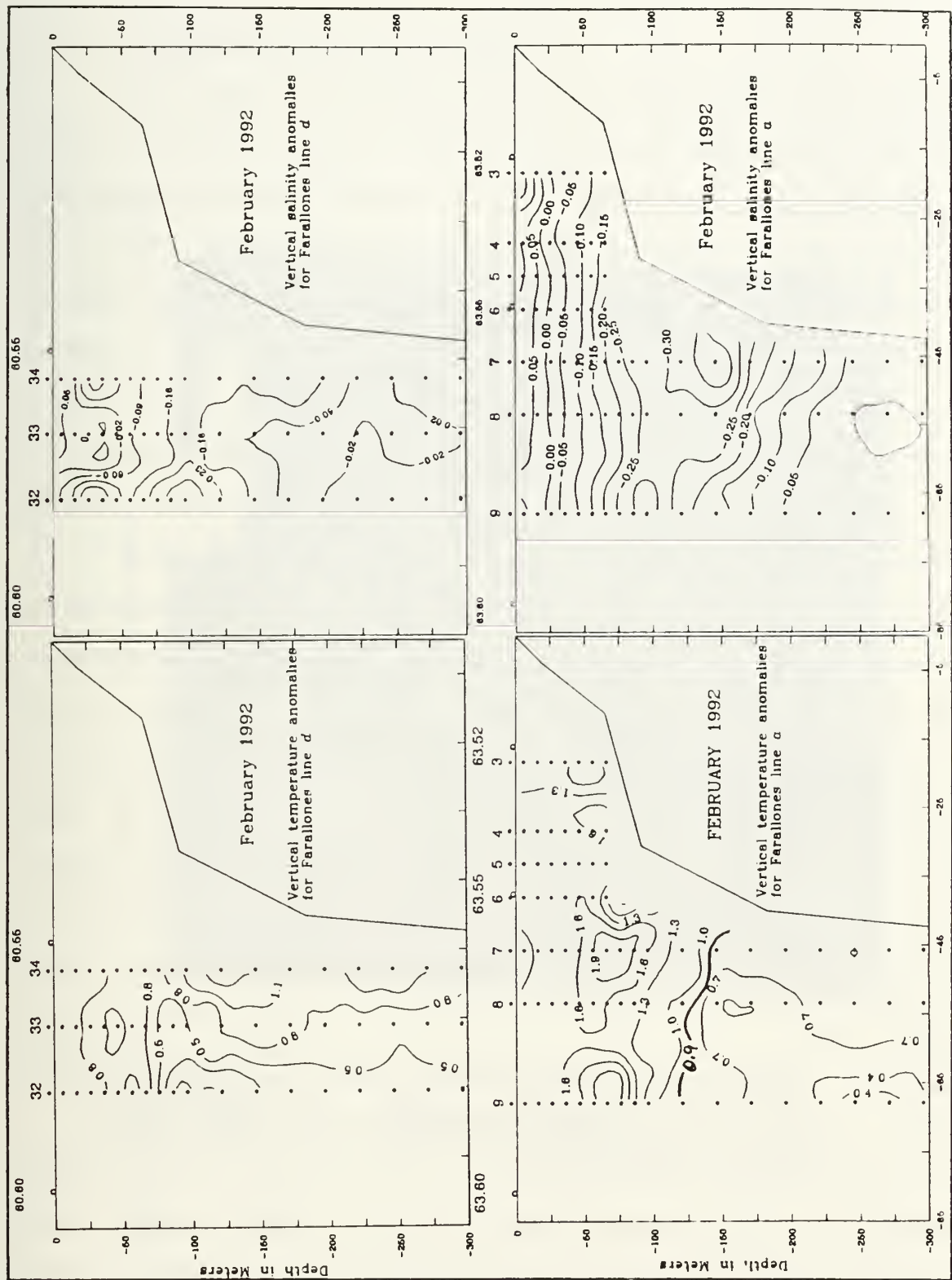


Figure 14. Vertical Sections of Anomalies for February, 1992.

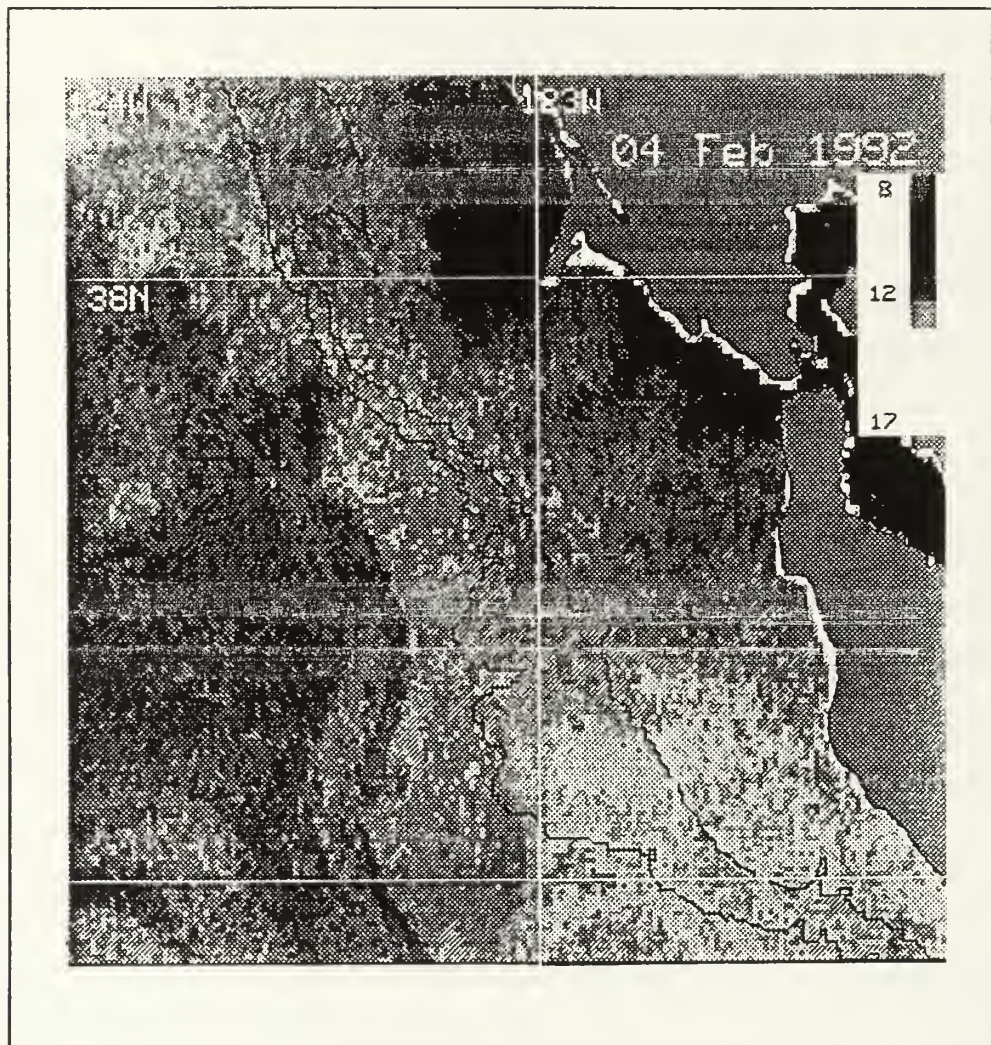


Figure 15. **Satellite Imagery from 4 February, 1992.** The image shows the frontal boundary along the outer slope. A warm, salty meander from this front is thought to cause the structure in the upper layer of section *d* (Figure 14).

2. Temperature-Salinity analysis

Each cruise was examined separately so that unique synoptic features could be identified, and the water mass types determined, using historical Temperature-Salinity (T-S) curves as a guide (*Tibby, 1941; Reid, 1965; Huyer et al., 1991; Tisch et al., 1992*). Farallones line *b* (station 11 on the outer slope to station 20 on the shelf, Figures 2 and 16) was chosen to study the temporal evolution of the T-S relationship because it was representative of each survey period. Most of the major features in the region span this line and coincidentally it was the only complete line for all five cruises. T-S properties below 1000 m were relatively constant, so only the upper water column is shown.

In this region of the Farallones, two surfaces are known to be of interest for the tracing of particular water masses; these are $26.4 \gamma_0$ and $26.8 \gamma_0$. The $26.4 \gamma_0$ surface is below the halocline and is generally accepted as the surface where the core of the California Undercurrent (CUC) lies (*Huyer et al., 1991*). The $26.8 \gamma_0$ surface is near the core of the North Pacific Intermediate water (NPIW) (*Reid, 1965; Huyer et al., 1991*). A typical regional T-S curve will indicate a large warm, salty inflection around the $26.4 \gamma_0$ surface indicating the presence of the CUC (Figure 16). A cold, fresh inflection around the $26.8 \gamma_0$ surface will show the NPIW; there is also the occasional intrusion of Pacific Subarctic water (PSAW) in the upper 200 m which will appear as a cold, fresh “tail” in the upper portion of the T-S curve.

Below the $25.6 \gamma_0$ surface, the February 1991 T-S curve closely approximates those found by others in the region (e.g., *Churkin and Haliminski, 1974; Hickey, 1979*). Above this surface, however, the curve deviates markedly, especially in the salinity field. The cold fresh “tail” is apparent in the February 1991 curve, showing the offshore intrusion of PSAW. The inflection

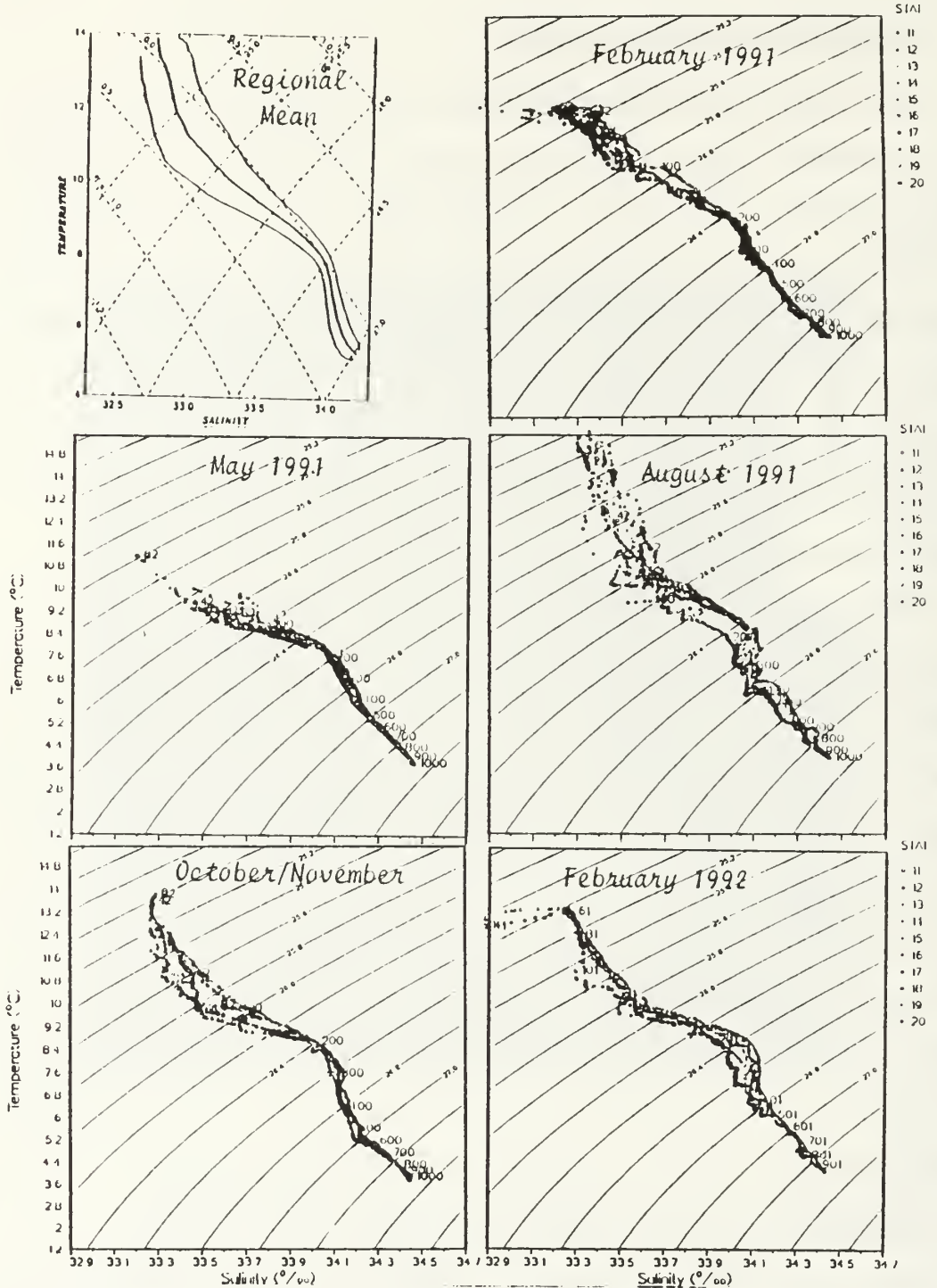


Figure 16. T-S Relationships. These are the T-S plots from Farallones line *b*. The mean curve from July-August 1991 off Point Arena (Huyer et al., 1991) is included for comparison, particularly around the $24.6 \gamma_0$ and above the $25.2 \gamma_0$ surfaces.

around the $26.4 \gamma_\theta$ surface was also less pronounced in this cruise than normal, perhaps indicative of a weak CUC.

The T-S relationship for May shows a general shift toward cool, fresh conditions. The inflection around the $26.4 \gamma_\theta$ surface was again anomalously weak during this period suggesting a still weak undercurrent. The near surface waters show the influence of two different mechanisms: upwelling in the nearshore region (cold, salty) and the intrusion of PSAW (cold, fresh) in the offshore stations (stations 11 and 12).

The August T-S relationship had the same general shape in the mean as the July-August 1991 curve found by Huyer et al., 1991 (Figure 16). The curve indicates slightly warmer temperatures down to about the $26.0 \gamma_\theta$ surface and slightly saltier conditions throughout the upper 800 m: This agrees with the climatological mean gradient which has warmer, saltier water to the south. Of notable exception was the outer-most station (station 11); the cool, fresh structure along the $26.4 \gamma_\theta$ surface indicates a possible front between this and the other stations in the line. The other stations show a strong inflection toward the equatorial side, indicating a strong undercurrent, but station 11 was apparently not in the undercurrent (Huyer et al., 1991; Tibby, 1941). Lines c and d (not shown) contain a cold, fresh “tail” in the near-surface region in the outermost stations suggesting the onshore intrusion of PSAW. The mixed layer reached its seasonal maximum temperature due to surface heating in the absence of any substantial meteorological activity (Figure 4). The interleaving structure around $26.8 \gamma_\theta$ indicates the presence of deep ocean fronts and eddies.

The October/November T-S relationship was very close to the typical curve found in the region, with a few notable exceptions. The inflection at the $26.4 \gamma_\theta$ surface was more pronounced in this curve than those normally observed

(Hickey, 1979; Huyer *et al.*, 1991). Like August, there are also many intrusive features around the 26.7 and 26.8 γ_θ surfaces that will be discussed in the section that follows.

The general shape of the curve during February 1992 was the same as the October/November curve, indicating the absence of any new water masses intruding into the region. The surface layer ($< 25.2 \gamma_\theta$) shows the cold, fresh “tail” in stations 11 and 12 (outermost stations). There was also a cold, fresh inflection in station 11 around the $25.5 \gamma_\theta$ surface (approximately 100 m), both possibly due to a shallow offshore eddy (Figure 15). The structure around the $26.4 \gamma_\theta$ surface was quite varied. Stations 11 and 15 are both cooler and fresher than the stations between, indicating that the warm, salty signature typical of the CUC was contained between 35 and 75 km offshore. There also appears to be a cold, fresh inflection around the $26.8 \gamma_\theta$ surface indicative of a small-scale NPIW intrusion.

The effects of upwelling and downwelling can clearly be seen through the inter-cruise analysis of a single station’s T-S relationship. Here we have chosen station 15, near the shelf break, from each cruise (Figure 17), and have plotted them with the depths labeled. The effects of upwelling were very apparent in May especially when compared to February, 1991. The May curve was shifted roughly orthogonally to the density lines toward larger density values with each corresponding depth shifted in like manner. This indicates upwelling, as deeper, more dense waters are brought toward the surface.

Conversely, downwelling was readily apparent in February 1992. These depths during February 1992 were shifted up and to the left when compared to the October/November plot, indicating that less dense water was being forced deeper into the water column by thermocline depression. Additionally, when

comparing both February plots, the 1992 curve was warmer and fresher throughout and the shift in depths was again indicative of stronger thermocline/halocline depression during February, 1992.

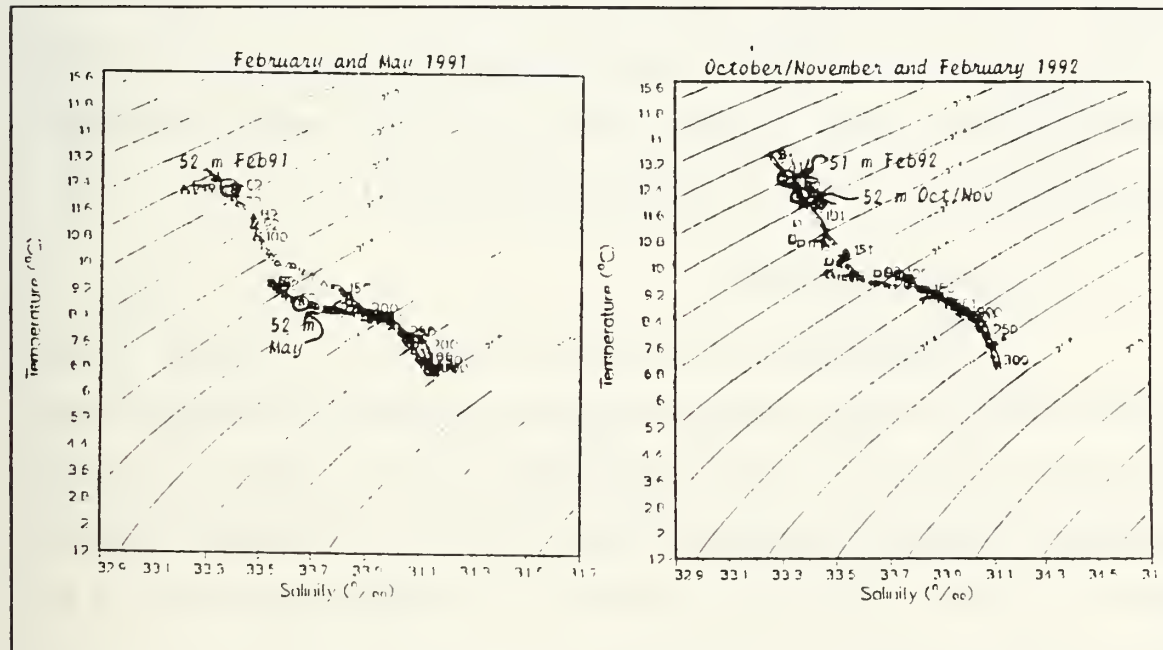


Figure 17. T-S Relationship for Station 15. This is a composite plot of station 15 from four cruises; February and May 1991 are compared in the left panel, November 1991 and February 1992 in the right panel. The migration of the depths of the water particles is indicative of upwelling (May) and downwelling (February 1992).

3. Spiciness and depth along density (γ_0) surfaces

From our T-S analysis it was apparent that the 26.4 and 26.8 γ_0 surfaces were of greatest interest. In the Farallones region, isopycnal surfaces are near the "neutral surfaces" along which particles can move and mix freely (McDougall, 1987). It is for this reason that the depths and water mass intrusions, traced with the spiciness (π), were evaluated along these surfaces. The associated figures show the direction from which the various intrusions advanced along the

isopycnal surfaces. The temperature and salinity values which correspond to referenced spiciness values can be obtained by using Figure 18.

Spiciness values greater than 0.10 on the 26.4 surface clearly show the influence of equatorial (e.g., undercurrent) water with salinities greater than 34.0‰. On this same surface, π values less than 0.02 were influenced by the PSAW. Spiciness values less than -0.04 on the 26.8 surface are strongly influenced by the NPIW with temperatures less than 6.7°C.

a. The 26.4 γ_θ surface

The depth of the 26.4 γ_θ surface in February, 1991 (Figure 19, top) sloped evenly downward onshore throughout the region. The extremes range from 180 m depth on the northern outer slope to a lens 230 m deep on the central inner slope. Similarly, the spiciness (Figure 19, bottom) during this cruise was uniformly moderate (0.05-0.10 π) relative to the other cruises indicating the absence of the warm, salty CUC signal.

The upwelling and southward geostrophic flow was clearly evident in the depth of the 26.4 γ_θ surface for May (Figure 20, top). The depth of this surface on the outer slope was as deep as 158 m and shoals on the shelf to 37 m. This was also a period of low spiciness (-0.01 to 0.05 π), again indicating the absence of the CUC waters (Figure 20, bottom). The low spiciness water mass (0.02 π contour) intruding from offshore was likely PSAW. Equatorward flow and the absence of the CUC permitted this water mass to enter into the region.

During the August cruise, the 26.4 γ_θ surface was depressed in the south and in the northeast corner (Figure 21, top). The position of the northeastern depression suggests that it was tied to Point Reyes in some fashion, perhaps by one of the cold filaments that is recurrent in this area. However, there

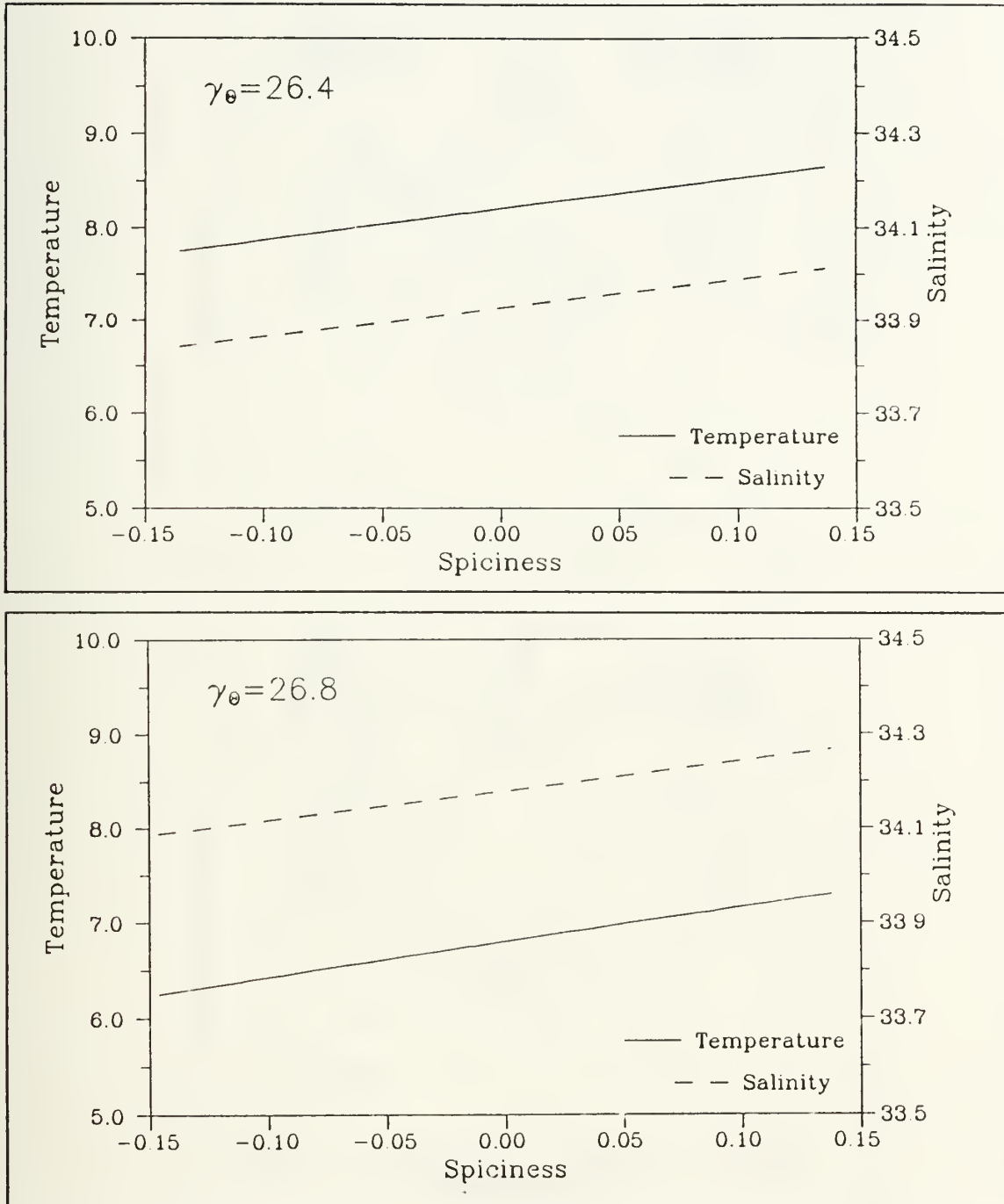


Figure 18. Spiciness Conversion Chart. Temperature and salinity values can be converted into spiciness values for use in evaluating Figures 19-23 and 25. The top chart is for the $26.4 \gamma_\theta$ surface, and the bottom figure is for the $26.8 \gamma_\theta$ surface.

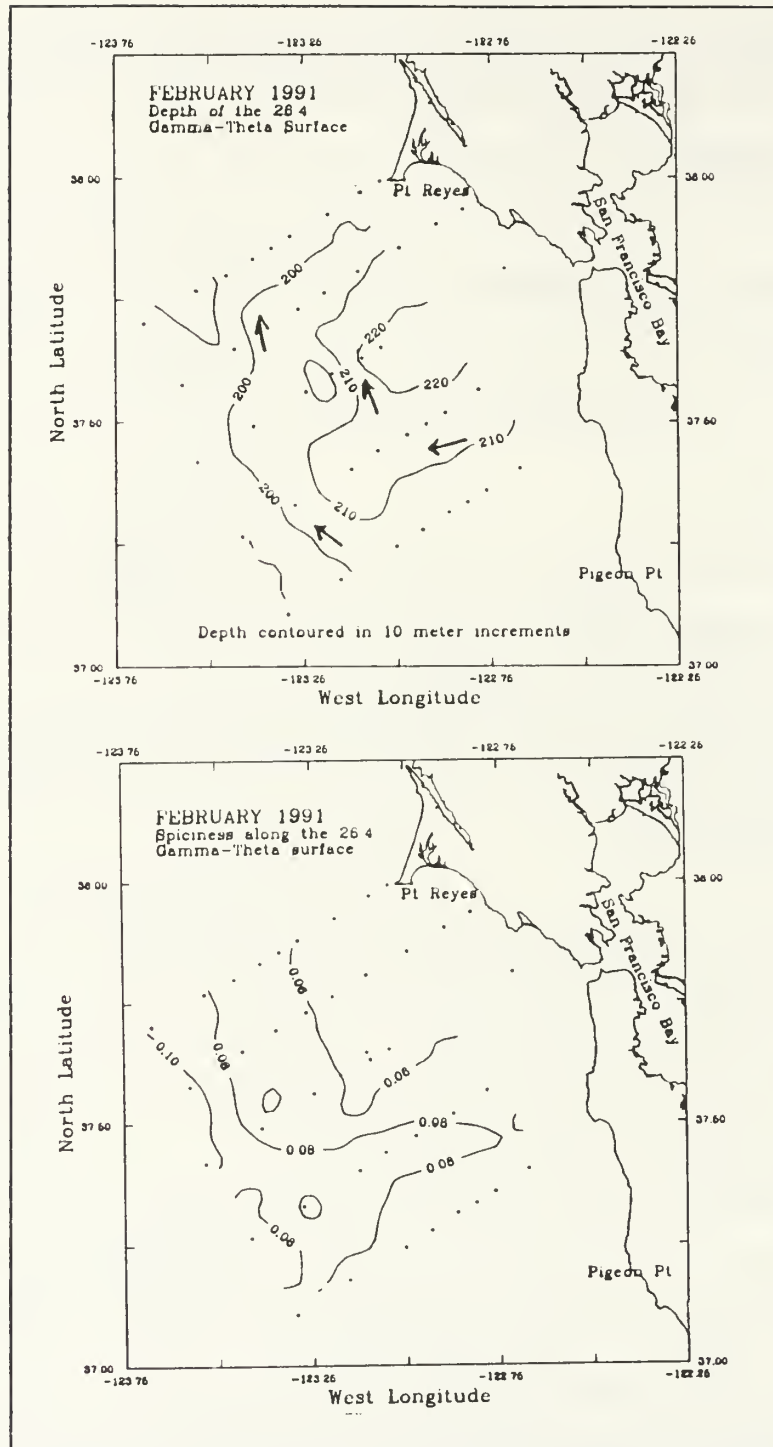


Figure 19.

The $24.6 \gamma_\theta$ Surface for February, 1991. The depth of the $24.6 \gamma_\theta$ surface is shown in the top plot, with spiciness (π) below. The annotated arrows (top) indicate the direction of flow along this surface implied by the geostrophic balance.

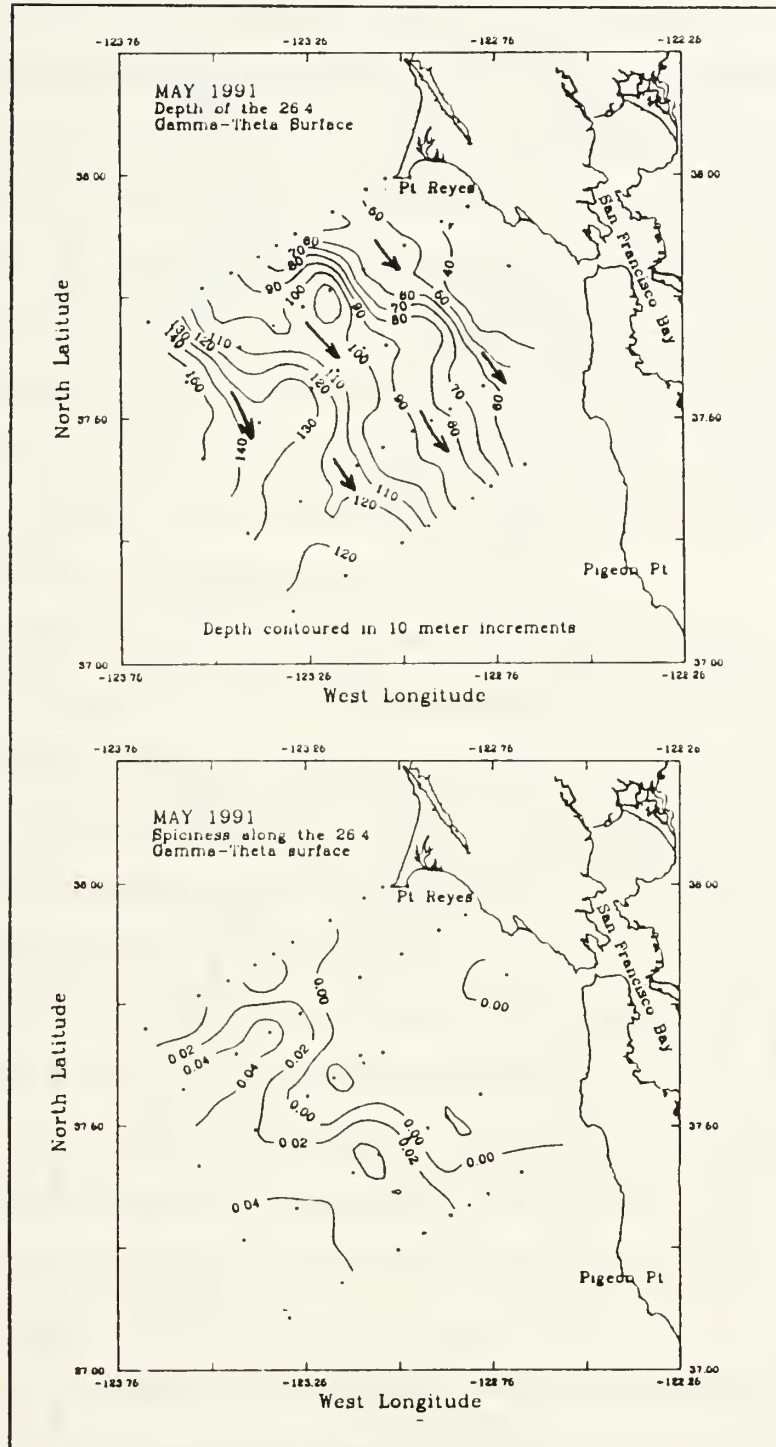


Figure 20.

The $26.4 \gamma_\theta$ Surface for May, 1991. The depth of the $24.6 \gamma_\theta$ surface is shown in the top plot, with spiciness (π) below. The annotated arrows (top) indicate the direction of flow along this surface implied by the geostrophic balance.

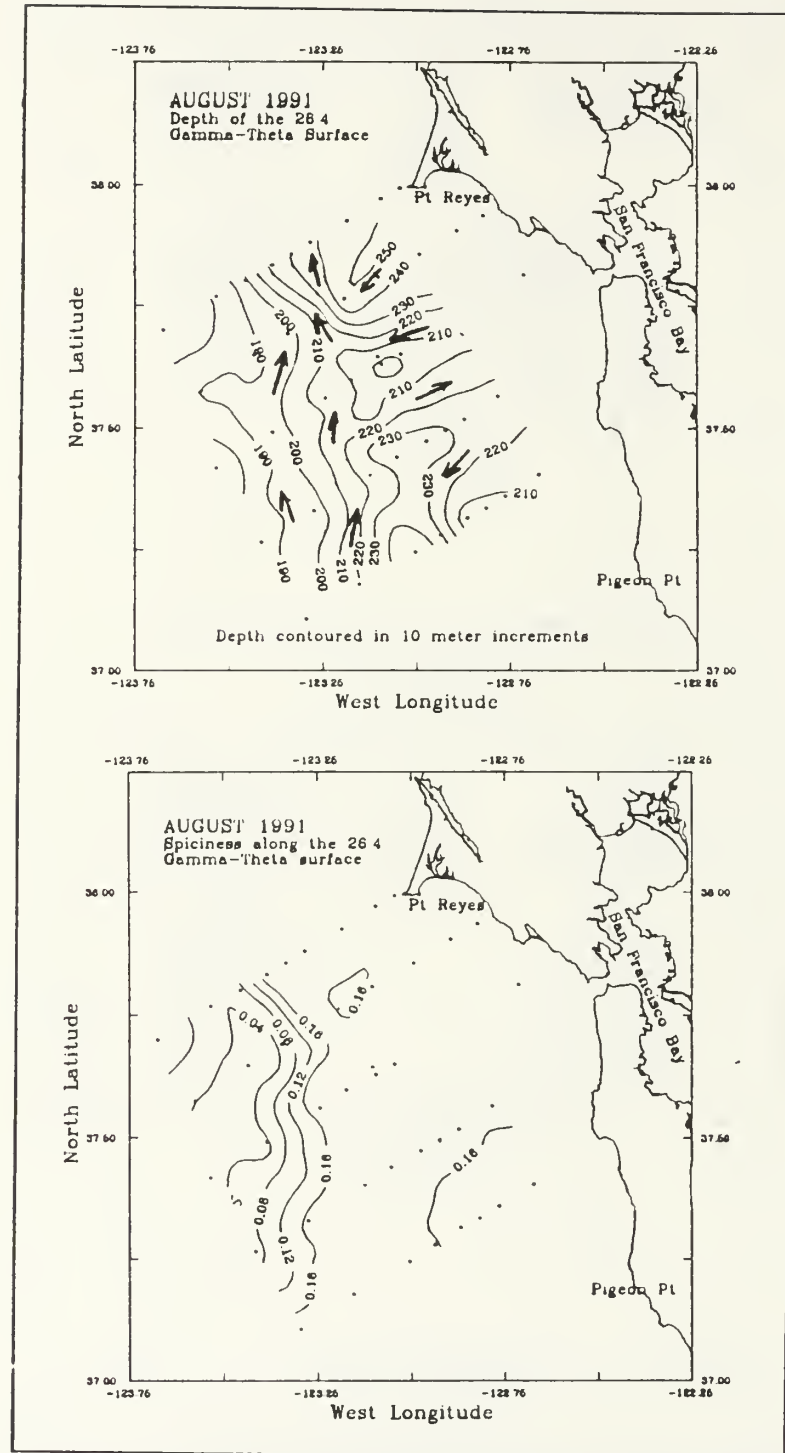


Figure 21.

The $26.4 \gamma_\theta$ Surface for August, 1991. The depth of the $24.6 \gamma_\theta$ surface is the top plot, with spiciness (π) below. The annotated arrows (top) indicate the direction of flow along this surface implied by the geostrophic balance.

was no corresponding spiciness signature or clear satellite imagery to fully support this hypothesis (Figure 21, bottom). A broad high spiciness signature of the CUC core flowing onshore over the slope from the south contrasts with the low spiciness core of the PSAW from the north. As was discussed in the previous section, there was a definite temperature-salinity front during this period, and this figure shows its along-slope orientation as a gradient of π , parallel to isobaths of density anomaly. The May conditions were such that the PSAW signature dominated the entire outer slope region; the movement of this water mass to the northwest in August indicates the dominance of the CUC relative to the PSAW, associated with poleward geostrophic flow.

Equatorial waters were found throughout the survey area in October/November as indicated by the 0.14π contour. The isopycnal surface was correspondingly depressed throughout region, with the exception of some shoaling in the southwest section (Figure 22, top), where there was a low spiciness core intruding from the south (Figure 22, bottom). The geostrophic flow is indicative of the complex nature of the CCS (see arrows annotated on Figure 22, top). The reemergence of the 0.04π contour of the PSAW to the south was probably the result of the meandering of the CUC.

While downwelling and associated poleward geostrophic flow clearly dominated the depth characteristics of the February, 1992 cruise (Figure 23, top), some of the sub-grid scale structure was artificially induced by the non-synoptic method by which this February survey was conducted. The southernmost line was surveyed on February 9th, followed three days later by the northernmost line. A two day gap thus ensued before each of the two lines *b* and *c* (Figure 2). The spiciness structure appears as a “pulse” of the CUC that seems to be developing during this period (Figure 23, bottom). Surveying the northern

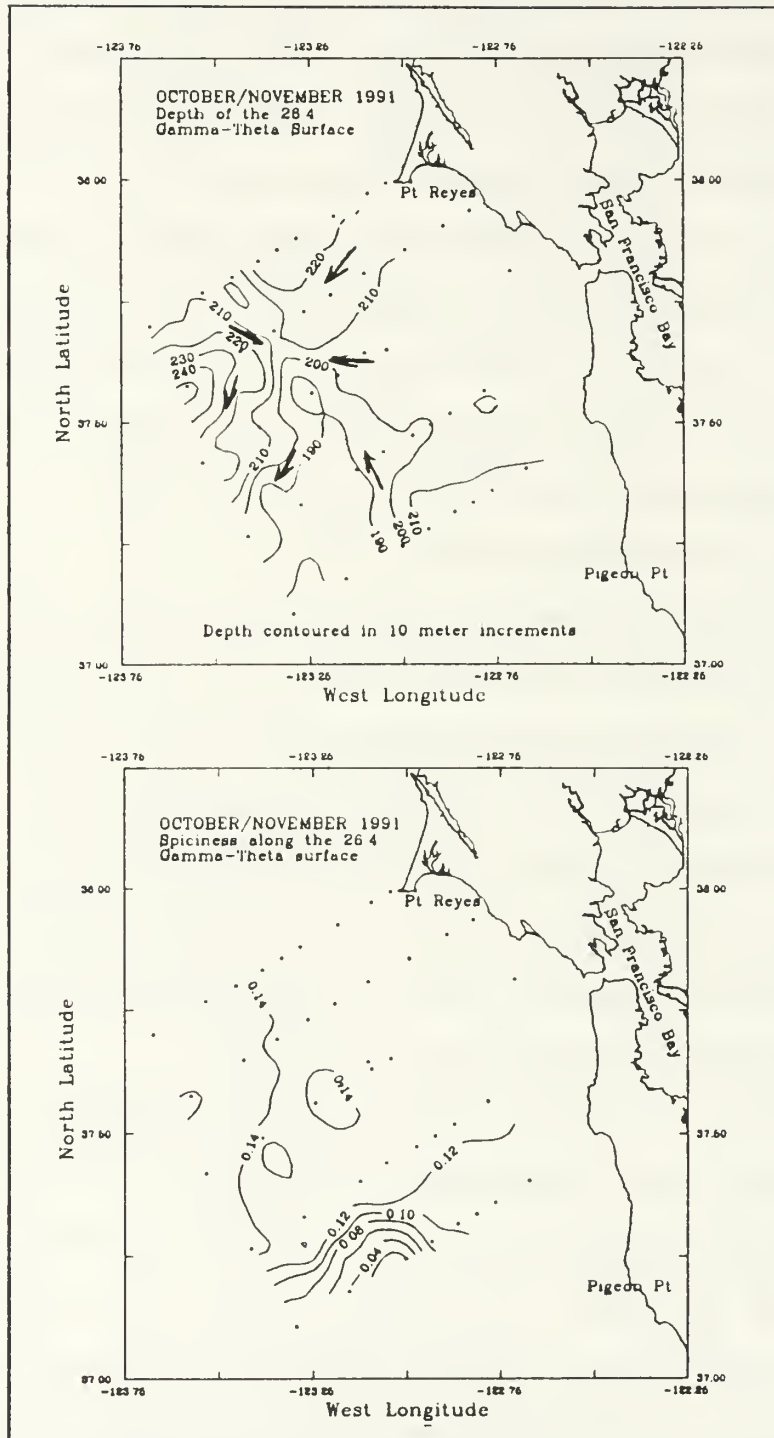


Figure 22.

The 26.4 γ_θ Surface for October/November, 1991. The depth of the 24.6 γ_θ surface is shown in the top plot, with spiciness (π) below. The annotated arrows (top) indicate the direction of flow along this surface implied by the geostrophic balance.

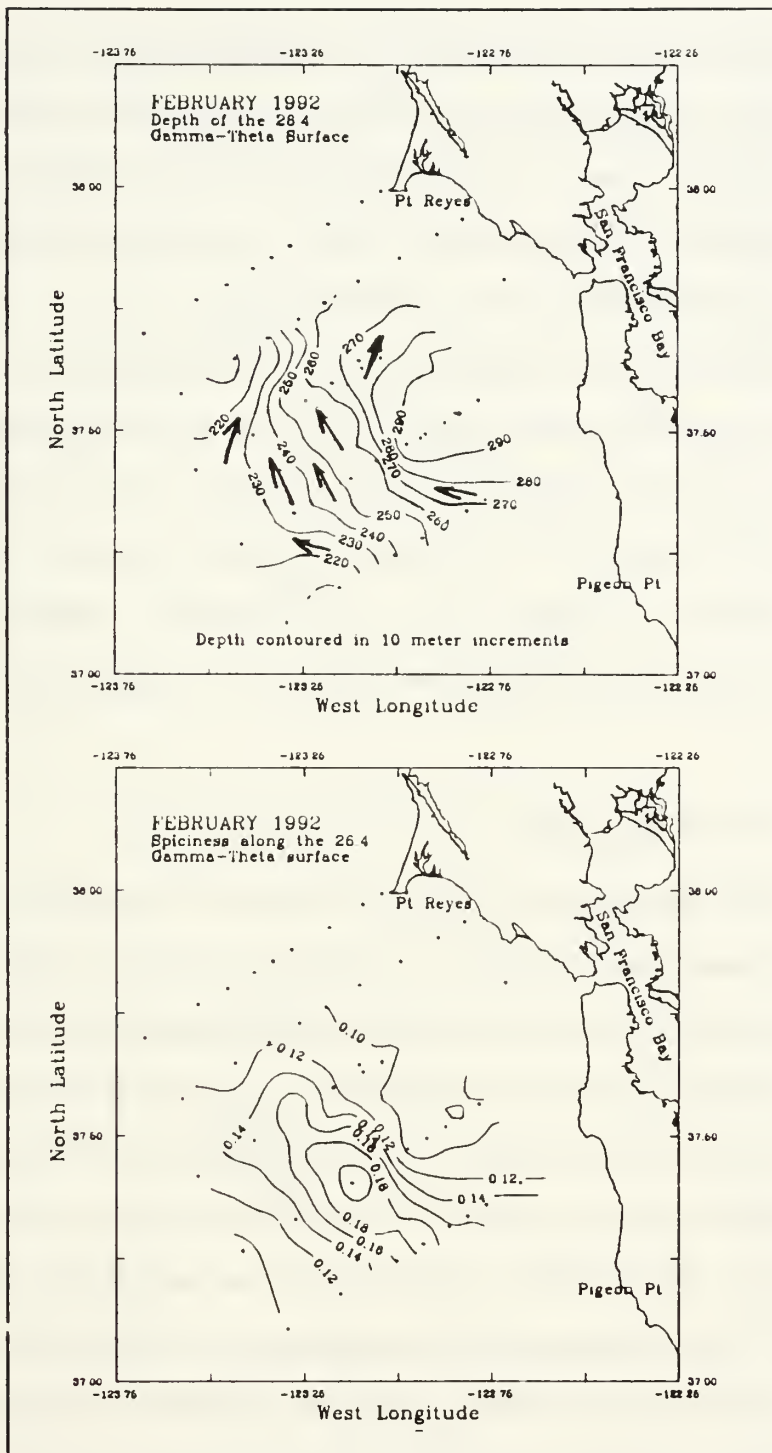


Figure 23. The $26.4 \gamma_\theta$ Surface for February, 1992. The depth of the $24.6 \gamma_\theta$ surface is shown in the top plot, with spiciness (π) below. The annotated arrows (top) indicate the direction of flow along this surface implied by the geostrophic balance

line early in the study may have fortuitously captured the leading boundary of the poleward flowing equatorial water, which later flooded the entire region. The core of the equatorial water, as indicated by the 0.14π contour, was further offshore in February 1992 than in August 1991. In contrast to August, the CUC appeared to be headed offshore during this time.

The interannual comparison between the two February cruises shows different structures in both depth, horizontal pressure gradient and spiciness. The $26.4 \gamma_\theta$ surface was 30 m deeper over the outer slope and 70 m deeper on the inner slope in 1992 than in 1991, the increased slope associated with stronger poleward geostrophic currents. There was uniform moderate spiciness throughout the region in 1991 but higher spiciness (the equatorial water signal) in 1992.

b. The $26.8 \gamma_\theta$ surface

There were several instances of inflections in the T-S curves which prompted our investigation of the $26.8 \gamma_\theta$ surface. The main features of interest were deep ocean eddies found during the last three cruises (Figures 24a and 24b). The $26.7 \gamma_\theta$ surfaces were also investigated in order to verify the persistence of these eddies, where they were found to be equally energetic. While these eddies seem to have little to do with the ENSO signal in the region, their existence was notable. The cold, fresh NPIW intrusions into the area during the May and August cruises were coming from the northwest and southwest, respectively (Figure 25). The remainder of the surveys were generally unremarkable in the spiciness regime.

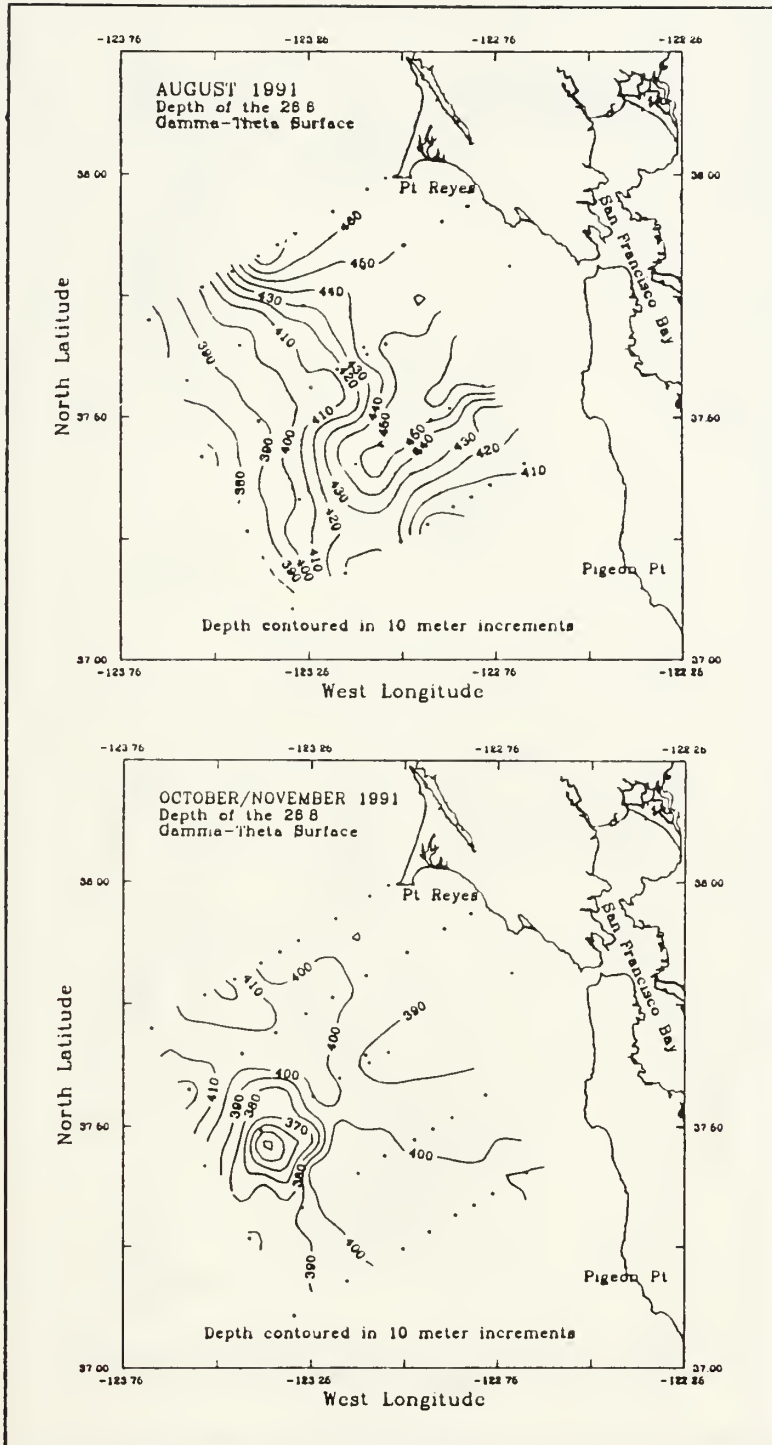


Figure 24.a Depth of $26.8 \gamma_\theta$ Surface. This figure shows the deep ocean eddies along the $26.8 \gamma_\theta$ surface in August and October/November 1991.

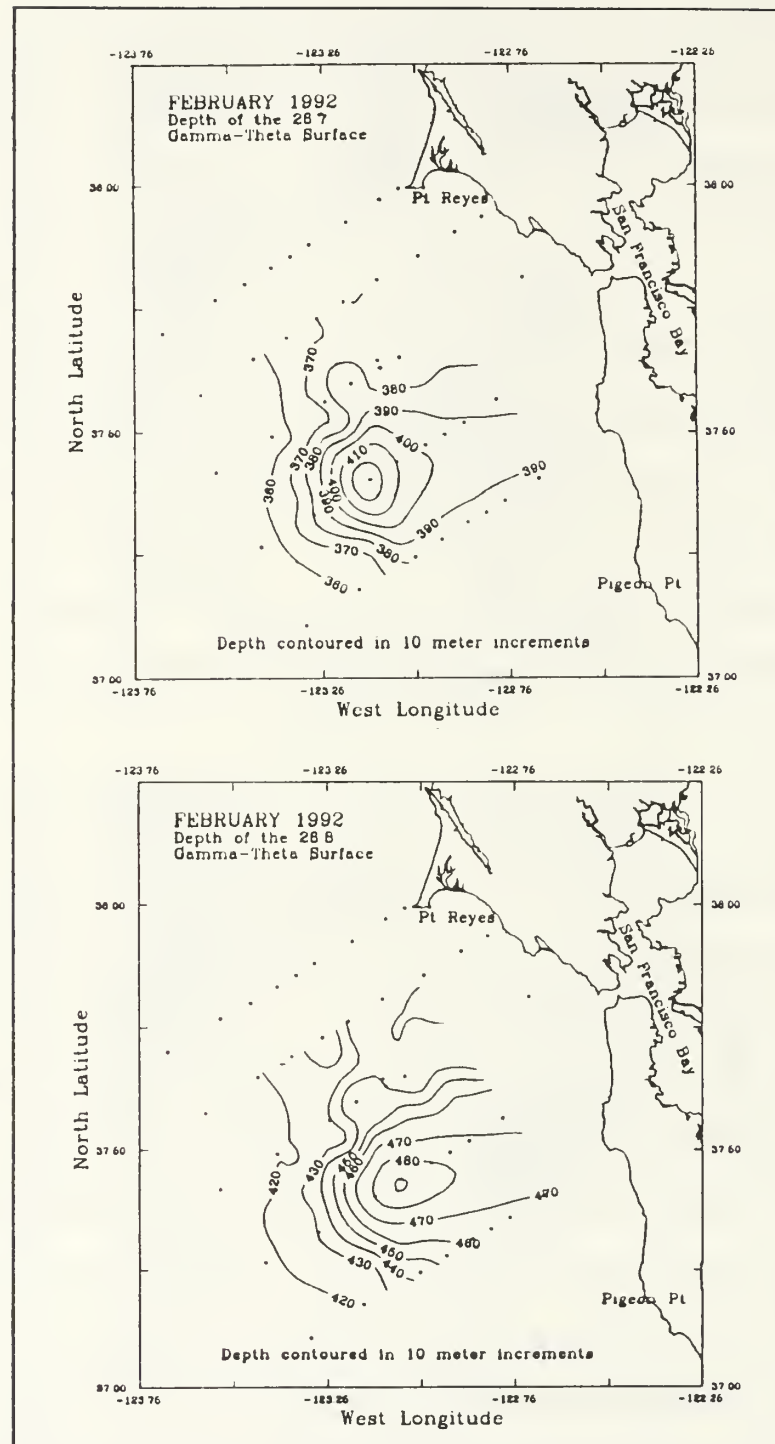


Figure 24.b Depth of $26.7 \gamma_\theta$ and $26.8 \gamma_\theta$ Surfaces. This figure shows the deep ocean eddy along the $26.7 \gamma_\theta$ and $26.8 \gamma_\theta$ surfaces in February, 1992. The plot of the shallower $26.7 \gamma_\theta$ surface during February 1992 is shown to illustrate the vertical structure of these eddies.

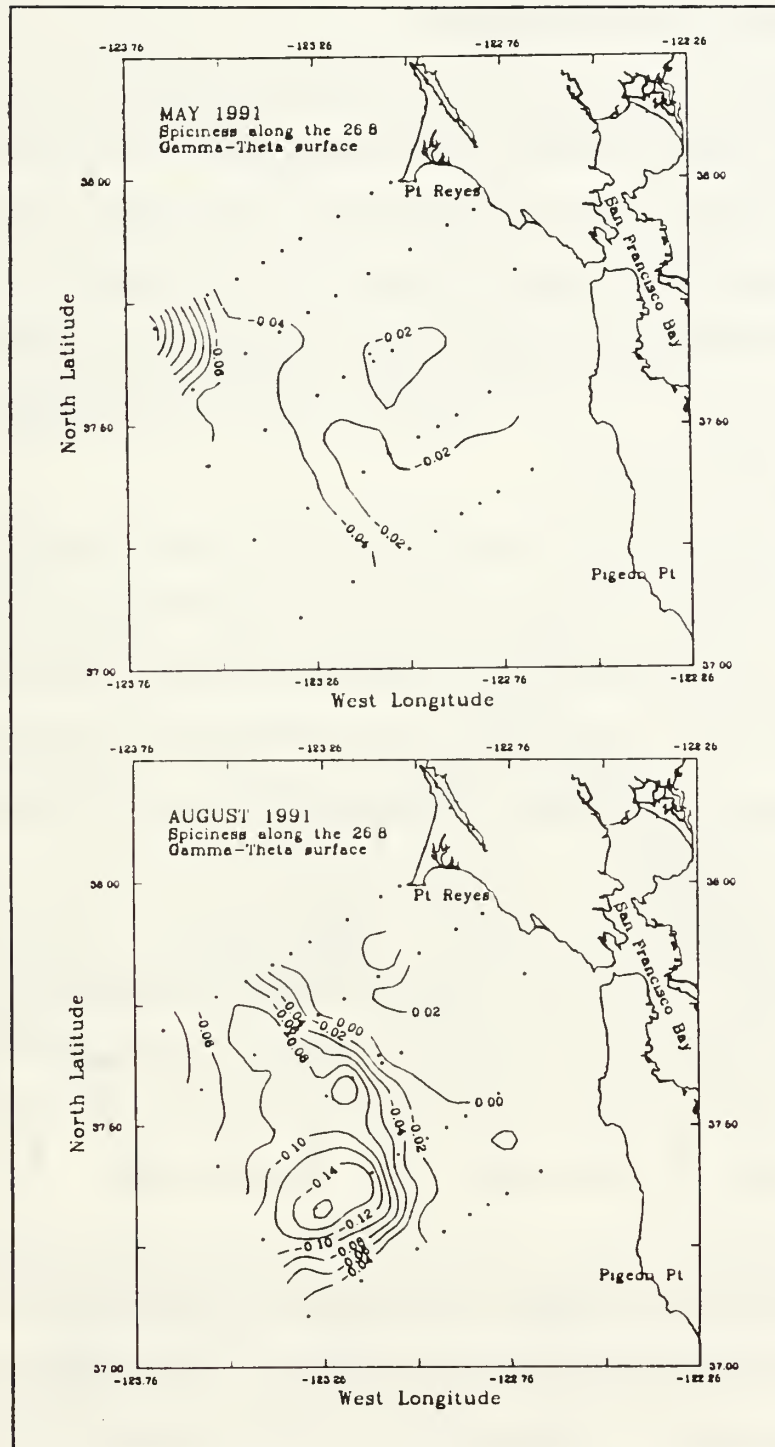


Figure 25.

Spiciness along the $26.8 \gamma_\theta$ Surface. This figure shows the intrusion of NPIW into the region, as indicated by the very low spiciness signature ($< -0.04 \pi$) in the offshore regime found in May (top) and August (bottom) along the $26.8 \gamma_\theta$ surface.

B. OTHER SUPPORTING DATA

The water mass analysis has shown that the anomalous conditions during February, 1992 were due primarily to thermocline/halocline depression, rather than by the invasion of non-local water masses. To determine if this depression was due to atmospheric or oceanic processes, we investigate the time of these events using coastal sea level data, current meter data, and maps of surface atmospheric pressure.

1. Sea Level Analysis

Monthly average sea level anomalies were taken from the Integrated Global Ocean Services System (IGOSS) Sea Level Program in the Pacific. (ISLP-Pac). These anomalies were calculated as deviations from the 1975-1986 mean annual cycle of sea level, and were corrected for the inverted barometer effect using atmospheric pressure fields provided by the National Meteorological Center (Figure 26).

The anomalies at Callao, Peru and the Gulf of Alaska both became positive in October 1991 and had a nearly identical rise, reaching a maximum in February, 1992. The stations along the California coast changed much later: at San Francisco and Crescent City, anomalies were still near zero in January, 1992 but jumped rapidly to greater than 10 cm by February, 1992.

Since Kelvin waves could not travel from Callao to Alaska without affecting the stations in between, an atmospheric teleconnection is suggested between the equatorial Pacific and the Aleutian low, which impacts the Gulf of Alaska. This process was investigated using surface atmospheric pressure charts from the north Pacific.

IGOSS MONTHLY MEAN SEA LEVEL ANOMALIES, 1991 - 1992

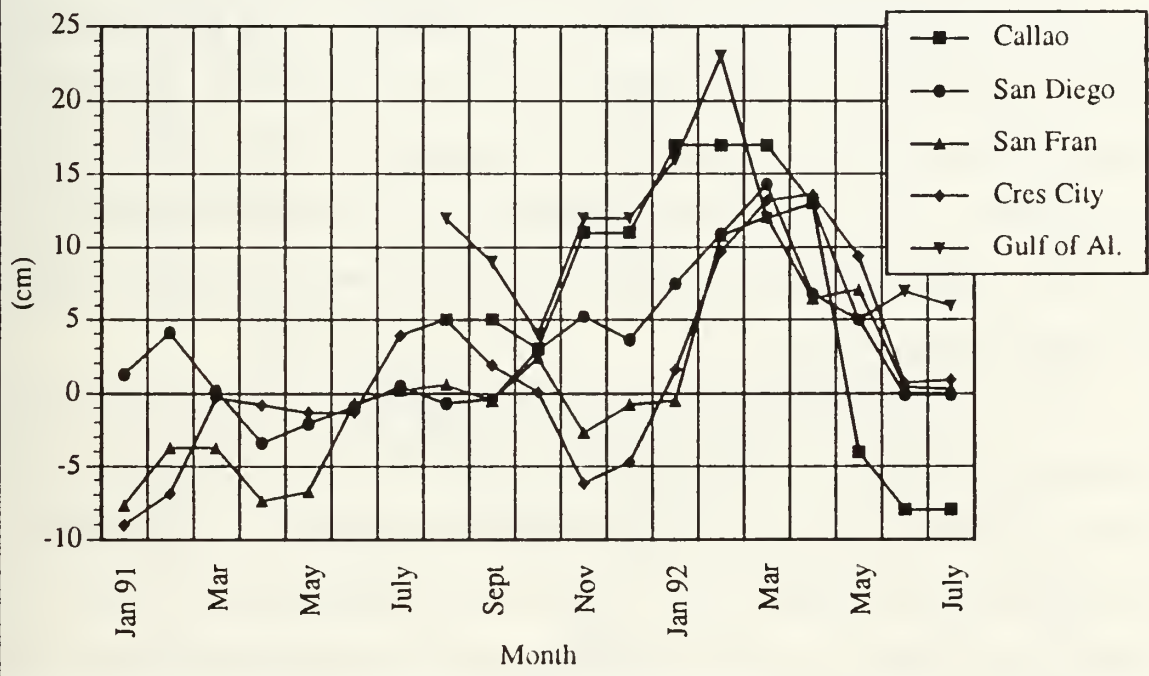


Figure 26. IGOSS Monthly Mean Sea Level Anomalies, 1991-1992. The graph shows that the stations at Callao (12°S) and the Gulf of Alaska (59.5°N) had nearly simultaneous rises in sea level, leading California data by two or three months.

2. Atmospheric Teleconnection

Emery and Hamilton (1985) identify three basic eastern Pacific atmospheric patterns: (1) the climatological mean; (2) an “intense” Aleutian low; and (3) weak North Pacific circulation causing a weak Aleutian low that is shifted to the west, associated with the reemergence of the North Pacific high from the southeast. They show the seasonal mean atmospheric patterns for the winter season from 1947 to 1982, and several have been chosen to illustrate the three basic patterns (Figure 27).

The climatological mean pattern is best typified by the winters of 1948 and 1979, the weak circulation pattern by 1972 and 1982, and the intensified Aleutian low pattern by 1958 and 1977 (*Emery and Hamilton, 1985*). The intensified Aleutian low is associated with anomalously strong southwesterly winds, which cause an onshore Ekman transport and downwelling along the coast. This causes positive coastal SST and sea level anomalies, and a deeper than usual pycnocline.

The conditions for 1991-1992 were compared with the Emery and Hamilton “mean states” using the monthly mean atmospheric sea level pressure (SLP) charts extracted from the Climate Diagnostics Bulletin (U.S. Department of Commerce, NOAA/NWS/NMC). The monthly mean atmospheric pattern for October 1991 (Figure 28, top) indicated a two-cell Aleutian system that was anomalously low in the central Pacific region. In November, the two-cell system migrated north, unified, spread and intensified (Figure 28, center). This intensified low was as much as 7 mb below the historical mean, based on the mean monthly patterns from August 1982 through July 1988. The North Pacific high appeared along the California coastal region and was centered north of the study area. By December, 1991, the North Pacific high had been forced to the

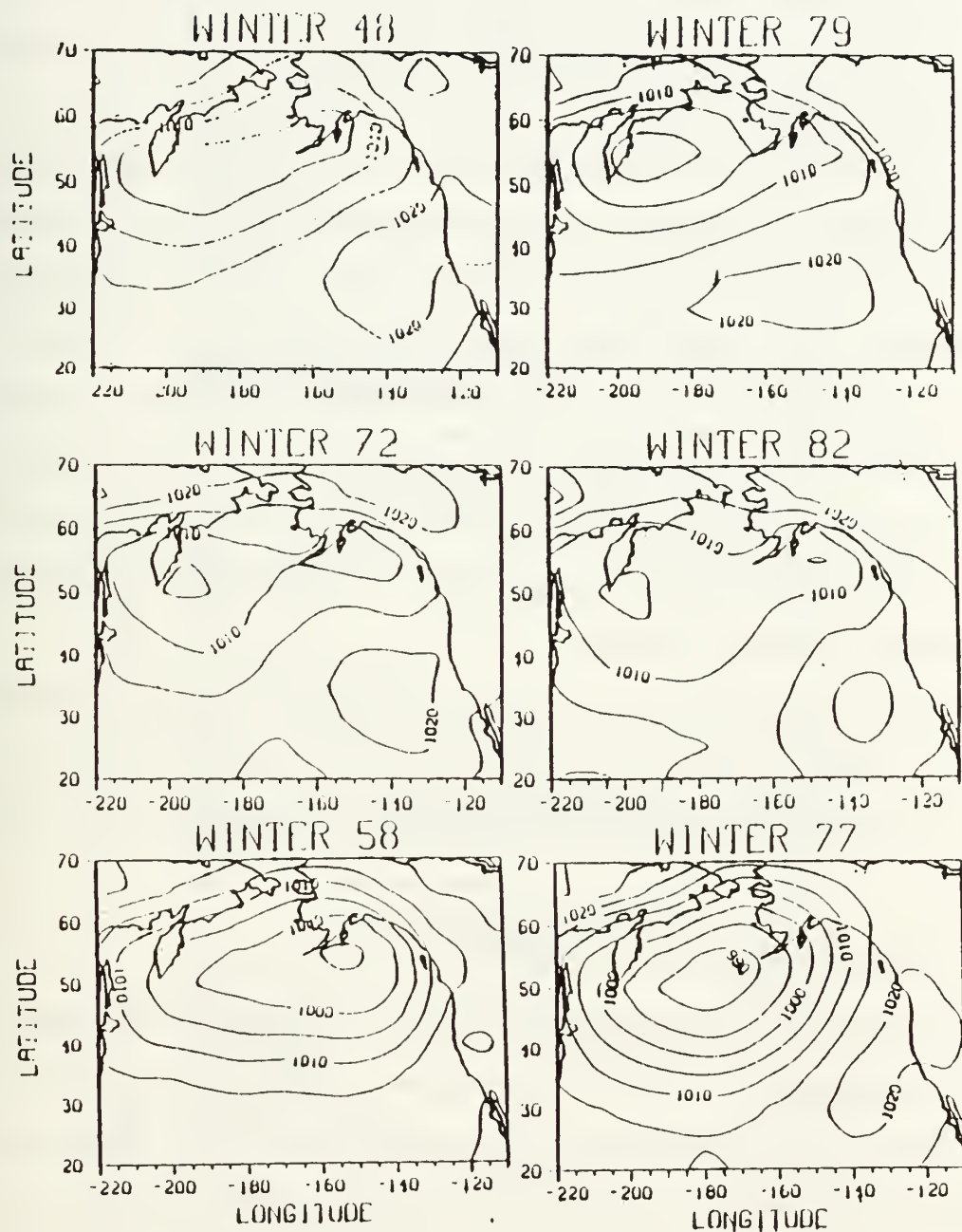


Figure 27. Primary Sea Level Pressure Patterns for the North Pacific. The top two figures (winters of 1948 and 1979) show the sea level atmospheric pressure pattern for a climatologically normal year, the middle two (winters of 1972 and 1982) show a “weak” circulation pattern, and the bottom two graphs (winters of 1958 and 1977) indicate the atmospheric pattern containing the intensified Aleutian low associated with ENSO (excerpted from *Emery and Hamilton, 1985*).

southwest, covering much of the tropical central Pacific basin (Figure 28, bottom). The Aleutian low continued to dominate the mid-latitudes and spread into the northwestern United States.

In January, 1992, the Aleutian low became more intense, but the winds off central California remained upwelling favorable due to a persistent small high located near 30°N, 124°W (Figure 29, top). In February, 1992, the Aleutian low again resembled the two-cell system observed in October, 1991 (Figure 29, center); however, the low intensification was stronger, and in the eastern cell, produced eastern Pacific anomalies 10 mb below the historical mean, based on the mean monthly patterns from August 1982 through July 1988 (Figure 29, bottom). This low engulfed the whole coast, causing onshore transport/downwelling conditions everywhere.

Based on this analysis, we conclude that the peak in sea level anomaly in February 1992 was likely forced by local onshore transport by the wind stress. Possible oceanic influence are investigated using the current meter data, which follows.

3. Current Meter Data

Current meter moorings were deployed in the Farallones region to collect an interannual time series of temperature and salinity data at a variety of depths (Table 4). This data was used to determine the inter-cruise characteristics of the region, the timing of the arrival of the El Niño signal, and the location of the strongest signal.

Time series of temperature and salinity were examined from the moorings in order to discern inter-cruise trends. Moorings **B** and **F** on the inner slope (Figure 2) were the only ones that showed the anomalous warming and freshening trends observed during February 1992. This agrees with the anomaly

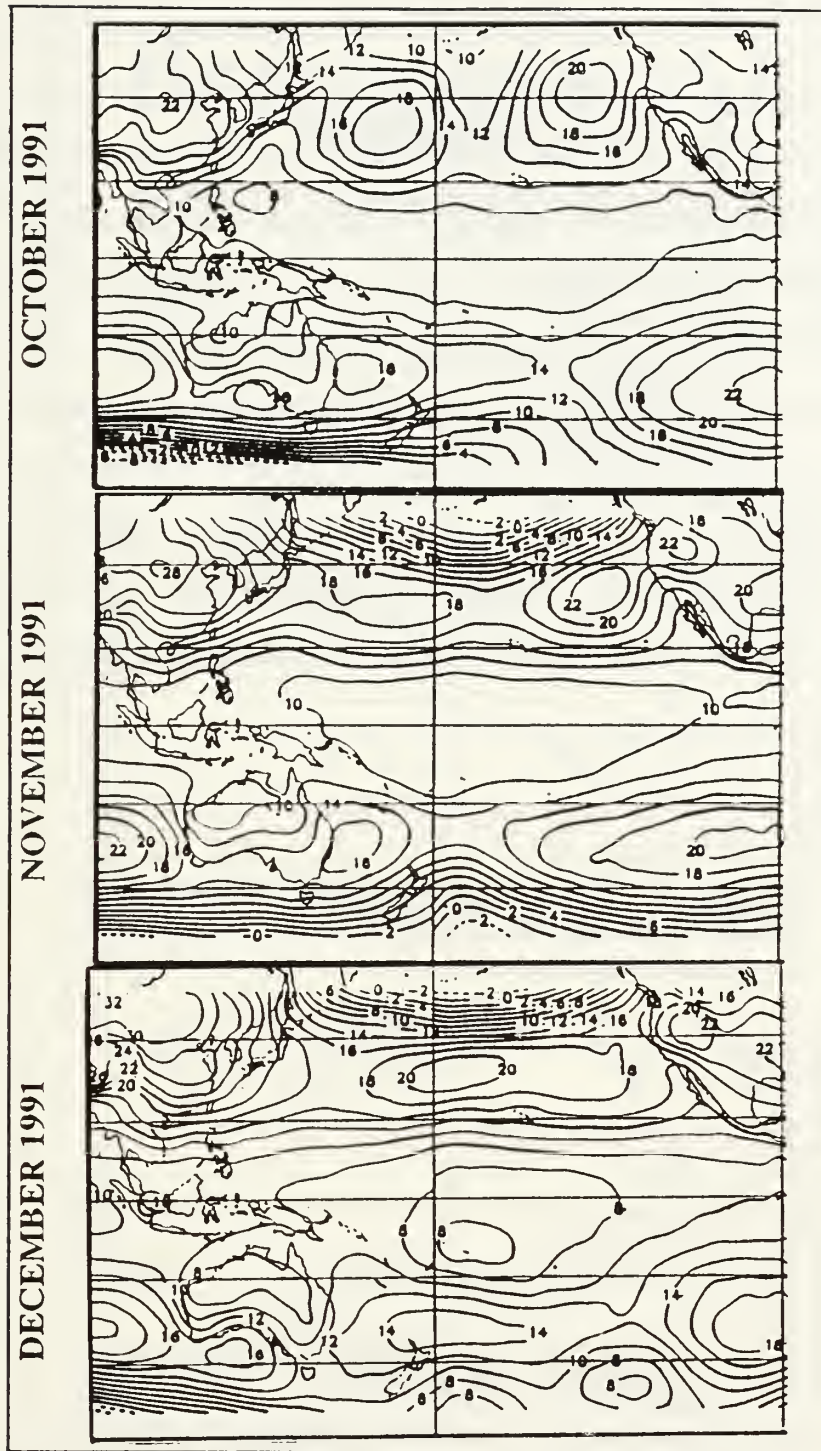


Figure 28. Sea Level Pressure, October-December, 1991. The upper panel is the October SLP showing a two-celled, weak Aleutian low. The middle panel shows November's broadening and strengthening low and the bottom panel indicates the migration of the North Pacific high.

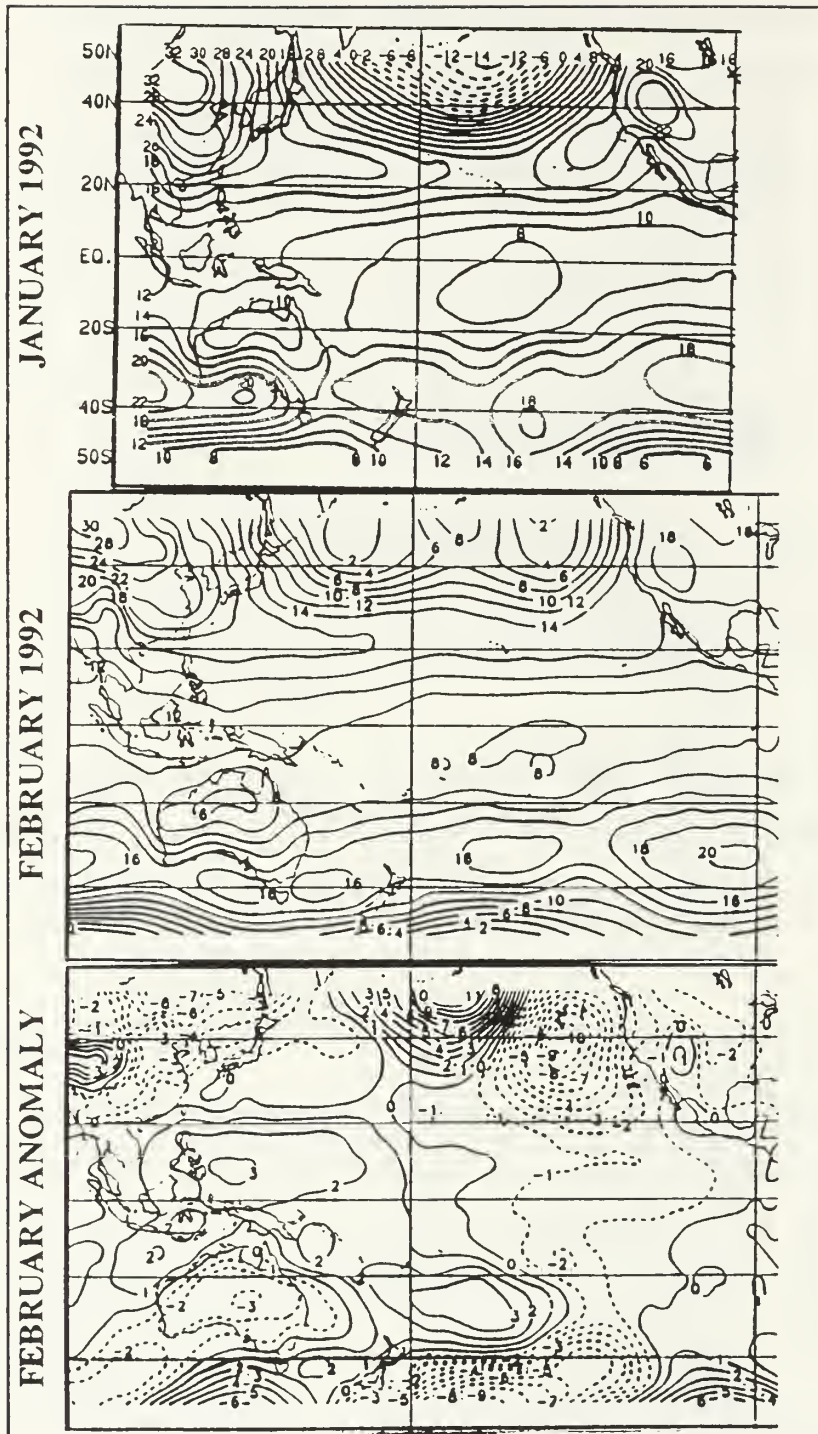


Figure 29. **Sea Level Pressure, January–February 1992.** The top panel clearly shows the broad, intense Aleutian low dominating the entire Pacific basin. The middle panel shows the reemergence of a two-cell Aleutian low, while the bottom panel shows the highly anomalous February, 1992 conditions.

plots that show the signal trapped close to shore. The time series of temperature at 390 m at mooring **B** and 223 m, 324 m, and 456 m at mooring **F** indicate an upward (warmer) trend beginning as early as January 1 at 456 m depth (Figure 30). The warming trend leads slightly at the deepest station suggesting that the El Niño signal was primarily a sub-surface manifestation (e.g., *Rienecker and Mooers, 1985; Cole and McLain, 1989; Huyer et al., 1991*). The timing between moorings **B** and **F** can not be distinguished due to mesoscale noise. The timing and structure of the salinity time series follows the same pattern as that of the temperature time series, showing a freshening trend in early January at 223 m depth (Figure 31). This early trend is not apparent in the SLP or coastal sea level data, and may indicate an oceanic teleconnection.

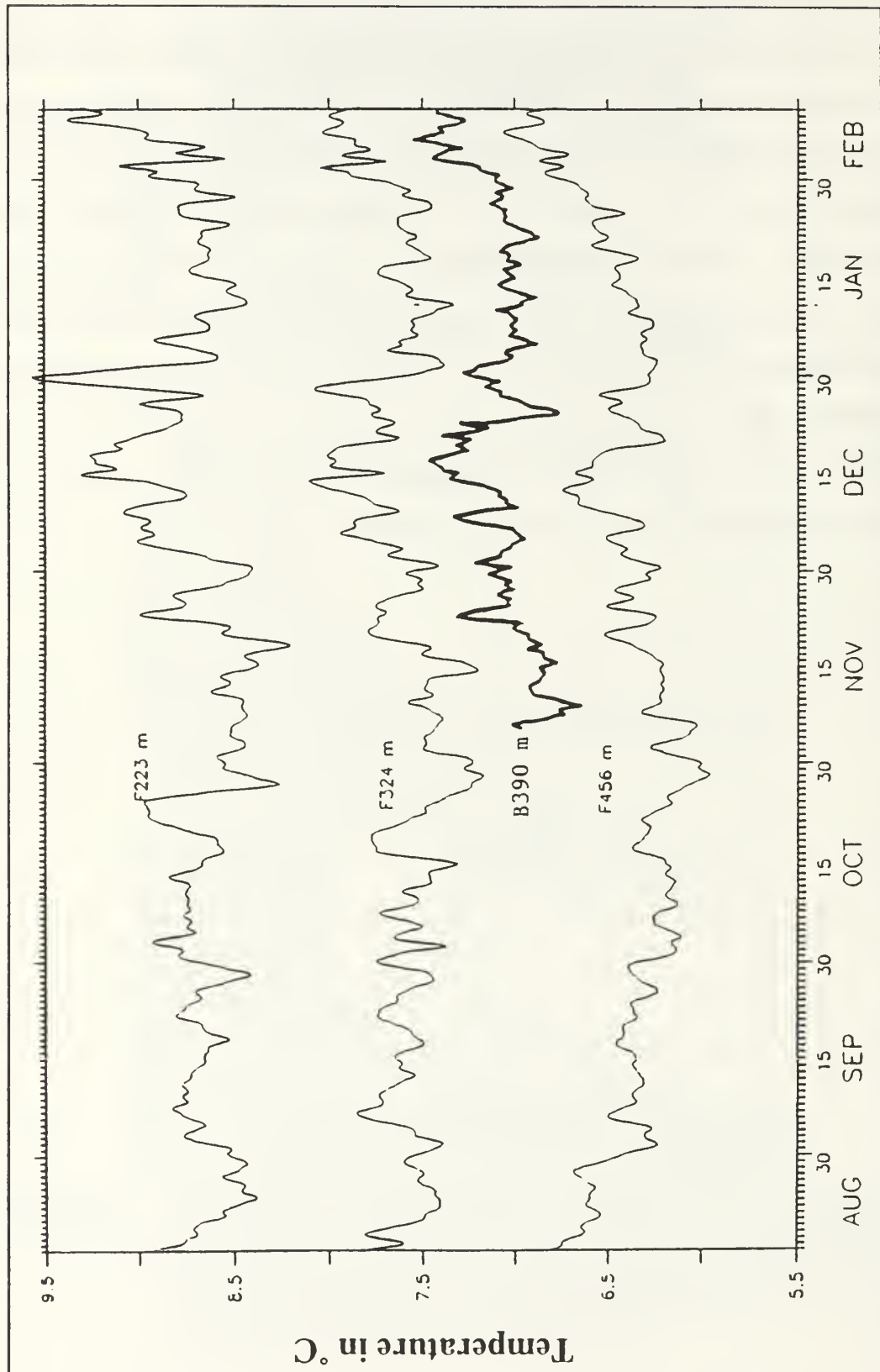


Figure 30. Time series of temperature from Farallones moorings B and F. There is a warming trend beginning in early January at both moorings, with the deeper signal leading slightly over the other 2 depths at mooring F.

Figure 30.

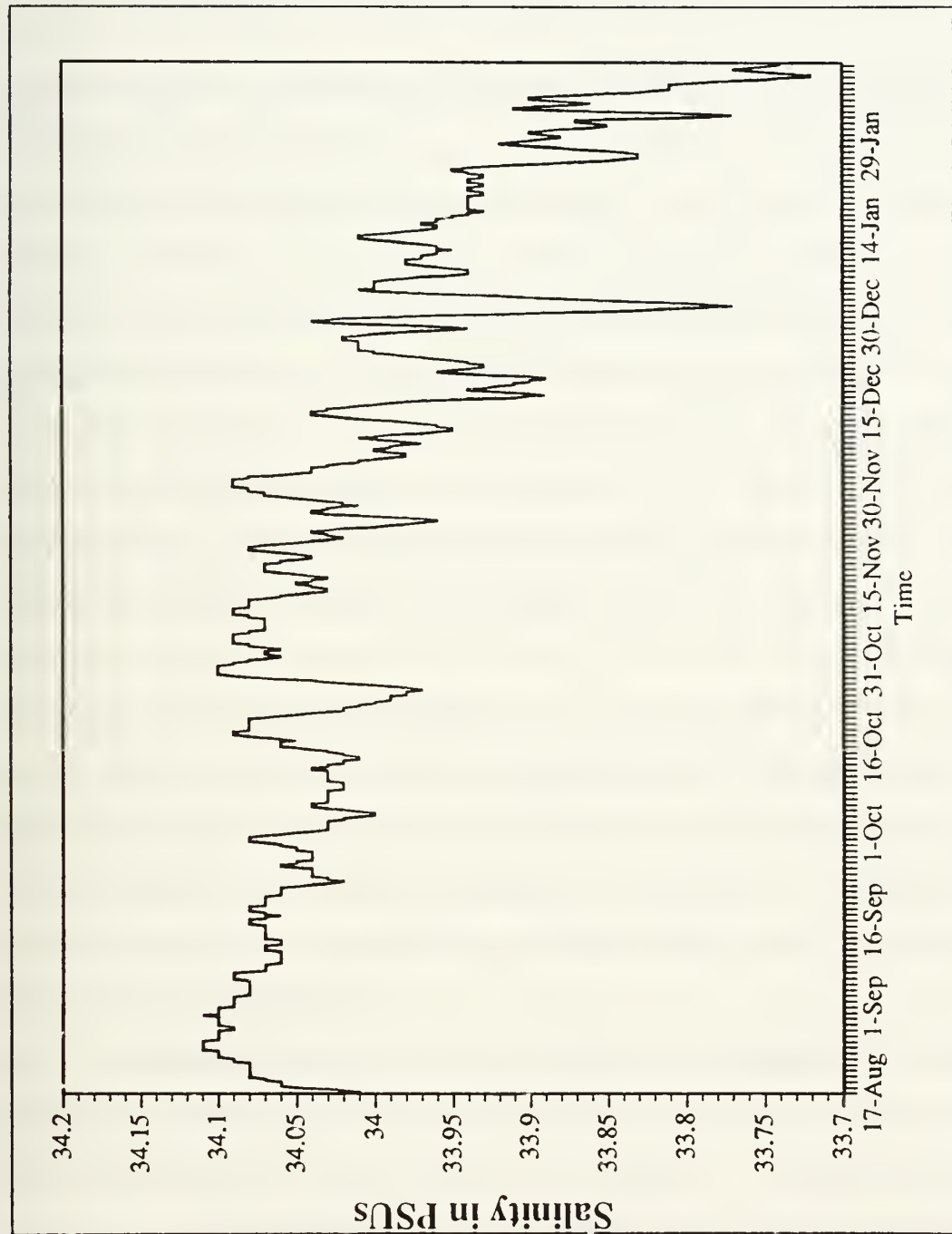


Figure 31. Time Series of Salinity from Farallones Mooring F. There is a freshening trend starting in early January, similar to the warming trend in Figure 30.

IV. COMPARISON WITH THE 1982-1983 EL NIÑO EVENT

A thorough account of the 1982-1983 El Niño for the region (approximately 35-40°N and offshore to 127°W) near the Farallon Islands was presented by *Rienecker and Mooers (1985)*. They showed that the largest anomalies were in the subsurface regime, thermocline depression was the cause of the positive temperature anomalies, and that PSAW intruded into the region sometime during the study. The greater intrusion of PSAW would be expected since their study region extended further north and offshore than our own. Further, there was anomalous intensification of the Aleutian low as described by *Emery and Hamilton, (1985)*, and they also acknowledge that the warming trend occurred prior to the atmospheric forcing, suggesting an oceanic compliment to the atmospheric forcing.

Rienecker and Mooers, however, ascribe the Kelvin wave signal to southern origin based on hindcast analysis of equatorial sea level variations conducted by *Busalacchi and Cane (1985)*. They further attribute an off- and on-shore migration of anomalies to shedding first and second mode Rossby waves, because the wave speeds can be approximated in a “gross” sense by the rate of anomaly migration. We do not observe this, possibly because of either the small size of the Farallones study region or that the phenomenon occurred later in 1992 than our February time frame. Due to the timing of this work, the temporal development of the entire 1991-1992 El Niño was not observed. Still greater anomalies and offshore “leakage” may have occurred later in the year. *Rienecker and Mooers* found significant sea level anomalies from southern California to the Gulf of Alaska, but characterized their properties as a near

simultaneous rise along the entire coast. This is the biggest difference from our study, where sea level anomalies originated simultaneously in both the north and south, and spread from both ends to the central California coast. The 1991-1992 El Niño had many similarities with the 1982-1983 El Niño, regardless of the proposed driving mechanisms.

Another study whose results approximate our own, but is south of the Farallones region (along CalCOFI line 90, 240°T starting at 33°25'N, 117°54.3'W), and extends further offshore (nearly 300 km versus our 78 km) is presented in *Simpson, 1984a* and *1984b*. Simpson's "simple model" supported atmospheric teleconnection through the expansion and intensification of the Aleutian low and the decrease in strength of the North Pacific high as the mechanism by which onshore transport and isopycnal depression occurred off southern California during the 1982-1983 event. He emphasized a resonated seasonal response during El Niño, versus an actual change in the hydrographic structure (an observation also supported by *Huyer and Smith, 1985*).

In *Simpson, 1984a*, an argument is made that the fresh anomalies found in the 1982-1983 data were *only* possible through the onshore transport of PSAW. While this signal is present, and may be quite strong in the far offshore domain, it does not sufficiently account for the anomalies that were found in the coastal region of the Farallones study.

Part of the impetus for *Simpson's* conclusion was the decrease or abatement of coastal upwelling conditions during the 1982-1983 El Niño event. The Farallones data for February, 1992 also indicate downwelling favorable conditions which contributed to the depression of the thermocline/halocline. Later however, once the thermocline/halocline is depressed, upwelling will bring

warmer and fresher water than usual to the surface, consistent with the El Niño signal, so the conditional requirement of upwelling abatement is a weak one.

Huyer and Smith (1985) conducted a study of similar scope as *Rienecker and Mooers (1985)*, but off of the Oregon coast (approximately 42°-49°N and offshore to 270 km). They too found the El Niño signal to be oceanically initiated, with atmospheric enhancement occurring 2-3 months later. The difference in timing is possibly due to their being further north (see timing of Crescent City sea level anomaly versus San Francisco in our Figure 26). They ascribe the oceanic data to coastal Kelvin waves and the atmospheric path to deepening and broadening of the Aleutian low.

Huyer and Smith also found the El Niño event to be an enhancement of the seasonal cycle, manifested in repetition of temperature maxima and persistence of poleward flow, high sea level and high temperature. Their data did not show any daily anomalies greater than the seasonal norm, the data had to be averaged over a month or more for any significant anomaly to be detected. They attributed the warm signal to the enhanced poleward flow of the warmer southern waters, and the salinity minimum to a combination of relaxed upwelling in the summer months, and increased rainfall and equatorward wind stress (downwelling favorable) in the fall and winter months.

In general, the Huyer and Smith results agree with our own. They found the initiation of the event to be in an oceanic pathway, and the atmospheric contribution to be significant. Their results did indicate a weaker El Niño signal off of Oregon in 1982-1983 than we found in the Farallones region in 1991-1992, however, this may be attributed to the “event scale weather” that dominated the Oregon coast during the 1982-1983 study period.

V. CONCLUSIONS AND RECOMMENDATIONS

A. THE EL NIÑO MECHANISMS SUPPORTED BY THIS DATA

After completion of the water mass analysis, and additional confirmation from other supporting data, the evidence suggests that vertical processes were the primary driving mechanism for the 1991-1992 El Niño event in the Farallon Islands region. Systematically, the five basic El Niño propagation theories were tested on this interannual, fine-scale gridded data set, with the following summary of results:

- (1) The single station anomalies showed a positive temperature anomaly, and corresponding negative salinity anomaly. This suggests that there was not simply an enhanced poleward advection of warmer water of equatorial origin, as this would produce a positive salinity anomaly.
- (2) The vertical sections indicated the strongest warm, fresh anomalies below the mixed layer. This suggests that an altered Northeast Pacific heat budget was not the driving factor in this ENSO event. Additional evidence can be found in the SLP charts, which do not indicate the high/low inversion necessary for the occurrence of this phenomenon.
- (3) The T-S analysis showed the absence of any large shifts in the shapes of the curves consistent with a massive intrusion of an alien watermass, especially between October/November 1991 and February, 1992. The small scale intrusions of PSAW along the $26.4 \gamma_0$ surface, and NPIW along the $26.8 \gamma_0$ surface are inconsistent with the warm, fresh anomalies associated with the El Niño and are of insufficient magnitude to cause the signals observed in the February 1992 data set. This refutes the idea that the anomalous onshore transport of different water

masses caused the warm fresh anomaly, at least close to shore. This may cause anomalies farther offshore (*Simpson 1984a, 1984b*).

(4) Thermocline/halocline depression via the coastally-trapped internal Kelvin wave may have caused the in-situ warming which began about 1 January, 1992, in the current meter records. If so, it was strongly coastally trapped and not observed at the other instruments. Further correlations between wind, current, and sea level will be necessary to test this hypothesis.

Thermocline/halocline depression via atmospheric teleconnection is presently the only demonstrated mechanism by which the 1991-1992 El Niño signal propagated into the Farallon Islands region. The theory is supported by the subsurface manifestation of the anomalies (Figures 8, 14, 30 and 31; Table 6), the vertical processes shown in the T-S curves (Figure 17) and the depth plots of the $26.4 \gamma_0$ surface (Figure 23). The southward propagation of SLP anomalies was detected in the SLP plots. The comparison of atmospheric patterns consistent with ENSO events (Figures 27 (bottom) and 28) with the 1991-1992 SLP maps showing that climatologically typical atmospheric conditions prevailed.

B. RECOMMENDATIONS

While the work presented here is complete in its water mass analysis, there are phenomena as of yet unexplained. The atmospheric teleconnection theory accounts for most of the anomalies in the data set, but does not explain the timing of the signal seen in current meter mooring F. The SLP charts support a February 1992 warming event, however the arrival of the temperature and salinity signal as early as 1 January, 1992 suggests that there may be an oceanic signal preceding the atmospheric signal. A more robust analysis of the sea level propagation needs to be done, including coherence and phase, to see if the phase speeds are consistent with coastally-trapped internal Kelvin wave theory.

The statistical analysis done in section III.A.1.a, Single Station Anomalies, is robust, but not as precise as possible. Our measure of significance was based solely on the standard deviation from the 20-year historical mean. A more precise statistical technique (*Wolf, 1962*) uses the variances of both the historical and Farallones data to test the hypothesis that the two means are equal or greater to each other, at a given confidence interval. The formula (*Wolf, 1962*) is

$$\bar{X} - \bar{Y} \geq 1.65 \sqrt{\frac{\sigma_X^2}{n} + \frac{\sigma_Y^2}{m}} \quad \text{Equation 1.}$$

where the “X” variables represent the Farallones data, the “Y” variables represent the historical data, and n and m are the number of data points that were used to calculate the two variances. The coefficient is weighted according to the desired confidence interval using the statistics for a normally distributed random variable. The factor 1.65 results in a 95% confidence interval. The results obtained here should be re-examined using this more precise technique to determine a quantitative measure of when the Farallones data were significantly different from the historical mean.

The passing of several major synoptic systems may have biased the atmospheric monthly mean SLP charts, especially in February, 1992 (personal communication, Dr. Tom Murphree, Department of Meteorology, U.S. Naval Postgraduate School, Monterey, CA). Detailed research may be required to determine if the February, 1992 SLP chart is biased in such a manner, and if the method proposed by *Emery and Hamilton (1985)* takes this possible biasing into account. It is our opinion, though, that since the SLP is averaged over the entire month, and that it is the same method used by *Emery and Hamilton*

(1985), the results are sufficiently conclusive to support thermocline/halocline depression via atmospheric teleconnection as one mechanism by which the 1991-1992 El Niño event propagated into the Farallon Islands region.

REFERENCES

Aceituno, P., 1992: El Niño, the Southern Oscillation, and ENSO: Confusing names for a complex ocean-atmosphere interaction, *Bull. Am. Met. Soc.*, **73**, No. 4, April 1992, pp. 483-485.

Allen, J.S., and R.D. Romea, 1980: On coastal trapped waves at low latitudes in a stratified ocean, *J. Fluid Mech.*, **98**, pp. 555-585.

Barnett, T.P., L. Dümenil, U. Schlese, E. Roeckner, M. Latif, 1992: The Asian snow cover-monsoon-ENSO connection, *Teleconnections linking worldwide climate anomalies*, M.H. Glantz, R.W. Katz and N. Nicholls, Eds., Cambridge Univ. Press., pp. 191-225.

Baumgartner, T.R., and N. Christensen, Jr., 1985: Coupling of the Gulf of California to large-scale interannual climatic variability, *J. Mar. Res.*, **43**, pp. 825-848.

Bernstein, R.L., 1982: Sea surface temperature estimation using the NOAA 6 satellite advanced very high resolution radiometer, *J. Geophys. Res.*, **87**, pp. 9455-9465.

Bray, N.A., and C.L. Greengrove, submitted 1992: Circulation over the shelf and slope off northern California, *J. Geophys. Res.*

Brink, K.H., 1982: A comparison of long coastal trapped wave theory with observations off Peru, *J. Phys. Oceanogr.*, **12**, pp. 897-913.

Brink, K.H., J.S. Allen, and R.L. Smith, 1978: A study of low frequency fluctuations near the Peru coast, *J. Phys. Oceanogr.*, **8**, pp. 1025-1041.

Bjerknes, J., 1966a: Survey of El Niño 1957-58 in its relation to tropical Pacific meteorology, *Inter. Am. Trop. Tuna Comm. Bull.*, **12**, pp. 1-62.

Bjerknes, J., 1966b: A possible response of the atmospheric Hadley cell to equatorial anomalies of ocean temperature, *Tellus*, **18**, pp. 820-829.

Bjerknes, J., 1969: Atmospheric teleconnections from the equatorial Pacific, *Mon. Weather Rev.*, **97**, pp. 163-172.

Busalacchi, A.J. and M.A. Cane, 1985: Hindcasts of sea level variations during the 1982-1983 El Niño, *J. Phys. Oceanogr.*, **15**, pp. 213-221.

Cane, M.A., 1983: Oceanic events during El Niño, *Science*, **222**, pp. 1189-1195.

Cane, M.A., 1986: El Niño, *Ann. Rev. Earth Planet. Sci.*, **14**, pp. 43-70.

Cane, M.A., and S.E. Zebiak, 1987: Prediction of El Niño events using a physical model, *Atmospheric and ocean variability*, H. Cattle, Ed. Royal Meteor. Soc. Press, pp. 53-182.

Cane, M.A., M. Munnich, and S.E. Zebiak, 1990: A study of self-excited oscillation of the tropical ocean-atmospheric system. Part I: Linear analysis, *J. Atmos. Sci.*, **47**, pp. 1562-1577.

Cannon, G.A., R.K. Reed, and P.E. Pullen, 1985: Comparison of El Niño events off the Pacific Northwest, in *El Niño North*, edited by W.S. Wooster and D.L. Fluharty, pp. 75-84.

Chelton, D.B., P.A. Bernal and J.A. McGowan, 1982: Large-scale interannual physical and biological interaction in the California Current, *J. Mar. Res.*, **40**, pp. 1095-1125.

Churgin, J. and S.J. Haliminski, 1974: Temperature, salinity, oxygen, and phosphate in waters off the United States, Volume III: Eastern North Pacific. Key to oceanographic records documentation no. 2, National Oceanographic Data Center, Washington, DC., 260 pp.

Clarke, A.J., 1983: The reflection of equatorial waves from oceanic boundaries, *J. Phys. Oceanogr.*, **13**, pp. 1193-1207.

Clarke, A.J. and S. VanGorder, 1992: On ENSO coastal currents and sea levels, submitted to *J. Phys. Oceanogr.*

Cole, DA and D.R. McLain, 1989: Interannual variability of temperature in the upper layer of the north Pacific eastern boundary region, 1971-1987, U.S. Department of Commerce, NOAA Technical Memorandum NMFS, NOAA-TM-NMFS-SWFC-125, 14 p.

Cornejo-Rodriguez, M.P., and D.B. Enfield, 1987: Propagation and forcing of high-frequency sea level variability along the west coast of South America, *J. Geophys. Res.*, **92**, pp. 14,323-14,346.

Cornillon, P.C., C. Gilman, L. Stramma, O. Brown, R. Evans, and J. Brown, 1987: Processing and analysis of large volumes of satellite-derived thermal infrared data, *J. Geophys. Res.*, **92**, pp. 12993-13002.

Eber, L.E., 1977: Contoured depth-time charts (0 to 200 m, 1950 to 1966) of temperature, salinity, oxygen and sigma-t at 23 CalCOFI stations in the California Current, *CalCOFI Atlas 25*, Calif. Coop. Oceanic Fish. Invest., Mar. Life Res. Program, Scripps Inst. Of Oceanogr., La Jolla, Calif, 9 pp. and 213 charts.

Enfield, D.B., 1989: El Niño, past and present, *Rev. of Geophys.*, **27**, pp. 159-187.

Enfield, D.B. and J.S. Allen, 1980: On the structure and dynamics of monthly mean sea level anomalies along the Pacific coast of North and South America, *J. Phys. Oceanogr.*, **10**, pp. 557-578.

Enfield, D.B., M.P. Cornejo-Rodriguez, R.L. Smith, and P.A. Newberger, 1987: The equatorial source of propagating variability along the Peru coast during the 1982-1983 El Niño, *J. Geophys. Res.*, **92**, pp. 14,335-14,346.

Fiedler, P.C., 1984: Satellite observations of the 1982-83 El Niño along the U.S. Pacific coast, *Science*, **224**, pp. 1251-1254.

Flament, P., 1986: Finestructure and subduction associated with upwelling filaments, Ph. D. dissertation, Univ. of Calif., San Diego.

Flohn, H., and H. Fleer, 1975: Climatic teleconnections with the equatorial Pacific and the role of ocean/atmosphere coupling, *Atmosphere*, **13**, pp. 98-109.

Godfrey, J., 1975: On ocean spindown I: A linear experiment, *J. Phys. Oceanogr.*, **5**, pp. 399-409.

Graham, N.E., and W.B. White, 1988: The El Niño cycle: A natural oscillator of the Pacific ocean-atmosphere system, *Science*, **240**, pp. 1293-1302.

Hickey, B.M., 1979: The California Current System - hypotheses and facts. *Prog. Oceanogr.*, **8**, pp. 191-279.

Hirst, A.C., 1986: Unstable and damped equatorial modes in simple coupled ocean-atmosphere models, *J. Atmos. Sci.*, **43**, pp. 606-630.

Hirst, A.C., 1988: Slow instabilities in tropical ocean basin-global atmosphere models, *J. Atmos. Sci.*, **45**, pp.830-852.

Hurlburt, H.E., J.C. Kindle, and J.J. O'Brien, 1976: A numerical simulation of the onset of El Niño, *J. Phys. Oceanogr.*, **6**, pp. 621-631.

Huyer, A., 1977: Seasonal variation in temperature, salinity, and density over the continental shelf off Oregon, *Limnol. Oceanogr.*, **22**, pp. 442-453.

Huyer, A., 1983: Coastal upwelling in the California Current system, *Prog. Oceanogr.*, **12**, pp. 259-284.

Huyer, A., 1984: Hydrographic observations along the CODE central line off northern California, 1981, *J. Phys. Oceanogr.*, **14**, pp.1647-1658.

Huyer, A., P.M. Kosro, J. Fleischbein, S. Ramp, T. Stanton, L. Washburn, F. Chavez, and T. Cowles, 1991: Currents and water masses of the Coastal Transition Zone off northern California, June to August 1988, *J. Geophys. Res.*, **96**, pp. 14,809-14,832.

Huyer, A., and R.L. Smith, 1985: The signature of El Niño off Oregon in 1982-83, *J. Geophys. Res.*, **90**, pp. 7133-7142.

Huyer, A., R.L. Smith, and E.J.C. Sobey, 1978: Seasonal differences in low-frequency current fluctuations over the Oregon continental shelf, *J. Geophys. Res.*, **83**, pp. 5077-5089.

Jessen, P.F., S.R. Ramp, C.A. Collins, N. Garfield, L.K. Rosenfeld, and F.B. Schwing, 1992a: Hydrographic and acoustic Doppler current profiler (ADCP) Data from the Farallones Shelf and Slope Study, 13-18 February 1991, *NPS-OC-92-003*, Naval Postgraduate Sch., Monterey, Calif., 165 pp.

Jessen, P.F., S.R. Ramp, C.A. Collins, N. Garfield, L.K. Rosenfeld, and F.B. Schwing, 1992b: Hydrographic and acoustic Doppler current profiler (ADCP) Data from the Farallones Shelf and Slope Study, 16-21 May 1991, *NPS-OC-92-004*, Naval Postgraduate Sch., Monterey, Calif., 168 pp.

Jessen, P.F., S.R. Ramp, C.A. Collins, N. Garfield, L.K. Rosenfeld, and F.B. Schwing, 1992c: Hydrographic and acoustic Doppler current profiler (ADCP) Data from the Farallones Shelf and Slope Study, 7-17 February 1992, *NPS-OC-92-005*, Naval Postgraduate Sch., Monterey, Calif., 136 pp.

Jessen, P.F., S.R. Ramp, C.A. Collins, N. Garfield, L.K. Rosenfeld, and F.B. Schwing, 1992d: Hydrographic and acoustic Doppler current profiler (ADCP) Data from the Farallones Shelf and Slope Study, 29 October - 3 November 1991, *NPS-OC-92-007*, Naval Postgraduate Sch., Monterey, Calif., 180 pp.

Julian, P.R., and R.M. Chervin, 1978: A study of the Southern Oscillation and Walker Circulation phenomenon, *Mon. Weather Rev.*, **106**, pp. 1433-1451.

Kosro, P.M., A. Huyer, S.R. Ramp, R.L. Smith, F.P. Chavez, T.J. Cowles, M.R. Abbott, P.T. Strub, R.T. Barber, P.F. Jessen, and L.F. Small, 1991: The structure of the transition zone between coastal waters and the open ocean off northern California, winter and spring 1987, *J. Geophys. Res.*, **96**, pp. 14,707-14,730.

Lighthill, M.J., 1969: Dynamic response of the Indian Ocean to onset of the southwest monsoon, *Phil. Trans. R. Soc. London*, **265**, pp. 45-92.

Lukas, R., S.P. Hayes, and K. Wyrtki, 1984: Equatorial sea level response during the 1982-1983 El Niño, *J. Geophys. Res.*, **89**, pp. 10,425-10,430.

Lynn, R.J., 1983: The 1982-83 warm episode in the California Current, *Geophys. Res. Lett.*, **10**, pp. 1093-1095.

Lynn, R.J., K.A. Bliss, and L.E. Eber, 1982: Vertical and horizontal distributions of seasonal mean temperature, salinity, sigma-t, stability, dynamic height, oxygen, and oxygen saturation in the California Current, 1958-1978, *CalCOFI Atlas 30*, 513 pp.

Lynn, R.J., and J.J. Simpson, 1987: The California Current System: The seasonal variability of its physical characteristics, *J. Geophys. Res.*, **92**, pp. 12,947-12,966.

Lynn, R.J., and J.J. Simpson, 1990: The flow of the undercurrent over the continental borderland off southern California, *J. Geophys. Res.*, **95**, pp. 12,995-13,008.

Magnell, R.A., C.D. Winant, N.A. Bray, C.L. Greengrove, J.F. Borchardt, J.M. Federiuk, C.E. Dorman, R.L. Bernstein, and J. Largier, 1991: Circulation on the northern California shelf and slope: Final report of the Northern California Coastal Circulation Study, *OCS Study MMS 91-0009*, May 1991, Prepared by EG&G Washington Analytical Services Center, Inc., for U.S. Department of the Interior, Minerals Management Service, Los Angeles, 543 pp.

McClain, C., 1985: Comparative performance of AVHRR-based multichannel sea surface temperatures, *J. Geophys. Res.*, **90**, pp. 11,587-11601.

McCreary, J.P., 1976: Eastern tropical ocean response to changing wind systems: with application to El Niño, *J. Phys. Oceanogr.*, **6**, pp. 632-645.

McCreary, J.P., 1984: Equatorial beams, *J. Mar. Res.*, **42**, pp. 395-430.

McDougall, T.J., 1987: Neutral surfaces, *J. Phys. Oceanogr.*, **17**, pp. 1950-1964.

Munk, W., 1981: Internal waves and small-scale processes, in *Evolution of Physical Oceanography*, edited by B.A. Warren and C. Wunsch, MIT Press, pp.264-291.

Namias, J., 1976: Some statistical and synoptic characteristics associated with El Niño, *J. Phys. Oceanogr.*, **6**, pp. 130-138.

Nelson, C.S., 1977: Wind stress and wind stress curl over the California Current. *Report No. NMFS SSRF-714*, Nat. Oceanic and Atmos. Admin., Monterey, Calif, 87 pp.

Nelson, C.S., and D.M. Husby, 1983: Climatology of surface heat fluxes over the California Current region, *NOAA Tech. Rep. NMFS SSRF-763*, 155 pp.

Noble, M., S.R. Ramp, and K. Kinoshita, 1992: Current patterns over the shelf and slope adjacent to the Gulf of the Farallones, Executive Summary, Prepared for the U.S. Environmental Protection Agency and the Western Division, Naval Facilities Engineering Command, 26 pp.

Philander, S.G.H., 1983: El Niño Southern Oscillation phenomena, *Nature*, **302**, pp. 295-301.

Philander, S.G.H., 1990: El Niño. La Nina, and the Southern Oscillation, Academic Press, Inc., 289 pp.

Pickard, G.L., and W.J. Emery, 1990: Descriptive Physical Oceanography, 5th Ed, Pergamon Press, 320 pp.

Quinn, W.H., 1974: Monitoring and predicting El Niño invasions, *J. Appl. Meteor.*, **13**, pp. 825-830.

Quinn, W.H., V.T. Neal, and S. Antunez de Mayolo, 1987: El Niño occurrences over the past four and a half centuries, *J. Geophys. Res.*, **92**, pp. 14,449-14,461.

Rago, T.A., S.R. Ramp, C.A. Collins, N. Garfield, L.K. Rosenfeld, and F.B. Schwing, 1992: Hydrographic and acoustic Doppler current profiler (ADCP) Data from the Farallones Shelf and Slope Study, 12-18 August 1991, *NPS-OC-92-006*, Naval Postgraduate Sch., Monterey, Calif., 183 pp.

Ramp, S.R., P.F. Jessen, K.H. Brink, P.P. Niiler, F.L. Daggett, and J.S. Best, 1991: The physical structure of cold filaments near Point Arena, California, during June 1987, *J. Geophys. Res.*, **96**, pp. 14,859-14,883.

Ramp, S.R., N. Garfield, C.A. Collins, L.K. Rosenfeld, and F.B. Schwing, 1992: Circulation Studies Over the Continental Shelf and Slope Near the Farallon Islands, CA, Executive Summary, Prepared for the U.S. Environmental Protection Agency and the Western Division, Naval Facilities Engineering Command, 40 pp.

Rasmusson, E.M., and J.M. Wallace, 1983: Meteorological aspects of the El Niño/Southern Oscillation, *Science*, **222**, pp. 1195-1202.

Reid, J.L., 1965: Intermediate waters of the Pacific Ocean, *Johns Hopkins Oceanogr. Stud.*, **2**, 85 pp.

Reid, J.L., 1972: The shallow salinity minima of the Pacific Ocean, *Deep-Sea Res.*, **20**, pp. 51-58.

Reid, J.L., and R.S. Arthur, 1975: Interpretation of maps of geopotential anomaly for the deep Pacific Ocean, *J. Mar. Res., suppl.*, pp. 37-53.

Reid, J.L., G.I. Roden, and J.G. Wyllie, 1958: Studies of the California Current System. CalCOFI Progress Report 1 July 1956 to 1 January 1958, *SIO Contribution, New Series* 998, 56 pp.

Rienecker, M.M., and C.N.K Mooers, 1986: The 1982-1983 El Niño Signal Off Northern California, *J. Geophys. Res.*, **91**, pp. 6597-6608.

Robinson, M.K., 1976: Atlas of North Pacific Ocean monthly mean temperatures and mean salinities of the surface layer, *Ref. Publ. 2*, Nav. Oceanogr. Off., Washington, D.C.

Roden, G.I., 1971: Aspects of the transition zone in the northeastern Pacific, *J. Geophys. Res.*, **76**, pp. 3462-3475.

Romea, R.D., and R.L. Smith, 1983: Further evidence or coastal trapped waves along the Peru coast, *J. Phys. Oceanogr.*, **13**, pp. 1341-1356.

Rómulo, J.S., 1991: Impact of ENSO events on the southeastern Pacific region with special reference to the interactions of fishing and climate variability, *Teleconnections linking worldwide climate anomalies*, M.H. Glantz, R.W. Katz and N. Nicholls, Eds., Cambridge Univ. Press., pp. 401-430.

Schopf, P.S., and M.J. Suarez, 1988: Vacillation in a coupled ocean-atmosphere model. *J. Atmos. Sci.*, **45**, pp. 549-566.

Simpson, J.J., 1983: Large-scale thermal anomalies in the California Current during the 1982-1983 El Niño, *Geophys. Res. Lett.*, **10**, pp. 937-940.

Simpson, J.J., 1984a: El Niño-induced transport in the California current during 1982-1983, *Geophys. Res. Lett.*, **11**, pp. 233-236.

Simpson, J.J., 1984b: A simple model of the 1982-83 Californian “El Niño”, *Geophys. Res. Lett.*, **11**, pp. 237-240.

Smith, R.L., 1978: Poleward propagating perturbations in currents and sea levels along the Peru coast, *J. Geophys. Res.*, **83**, pp. 379-391.

Smith, R.L., 1983: Peru coastal currents during El Niño: 1976 and 1982, *Science*, **221**, pp. 1397-1399.

Strub, P.T., J.S. Allen, A. Huyer, and R.L. Smith, 1987: Seasonal cycles of currents, temperatures, winds and sea level over the northeast Pacific continental shelf: 35°N to 48°N, *J. Geophys. Res.*, **92**, pp. 1507-1526.

Suarez, M.J., and P.S. Schopf, 1988: A delayed action oscillator for ENSO, *J. Atmos. Sci.*, **45**, pp. 3283-3287.

Sverdrup, H.V., and R.H. Fleming, 1941: The waters off the coast of southern California, March to July 1937, *SIO Contribution, New Series 136*, pp. 261-378.

Tracy, D. E., 1990: Source of cold water in Monterey Bay observed by AVHRR satellite imagery, Naval Postgraduate Sch., Monterey, Calif., Masters Thesis, 124 pp.

Tibby, R.B., 1941: The water masses off the west coast of North America, *J. Mar. Res.*, **IV**, pp. 112-121.

Tisch, T.D., S.R. Ramp, and C.A. Collins, 1992: Observations of the geostrophic current and water mass characteristics off Point Sur, California, from May 1988 through November 1989, *J. Geophys. Res.*, **97**, pp. 12,535-12,555.

Unesco, 1991: Processing of oceanographic station data, JPOTS Editorial Panel, Imprimerie des Presses Universitaires de France, Vendôme, 138 pp.

Walker, G.T., and E.W. Bliss, 1932: World Weather V, *Mem. Roy. Meteor. Soc.*, **4**, pp. 53-84.

Winant, C.D., R.C. Beardsley, and R.E. Davis, 1987: Moored wind, temperature, and current observations made during Coastal Ocean Dynamics Experiments 1 and 2 over the northern California continental shelf and upper slope, *J. Geophys. Res.*, **92**, pp. 1569-1604.

Wolf, F.L., 1962: Elements of Probability and Statistics, McGraw-Hill Book Company, Inc., pp. 225-226.

Wyrtki, K., 1975: El Niño: The dynamic response of equatorial Pacific ocean to atmospheric forcing, *J. Phys. Oceanogr.*, **5**, pp. 572-584.

Zebiak, S.E., and M.A. Cane, 1987: A model of El Niño/Southern Oscillation, *Mon. Weather Rev.*, **115**, pp. 2262-2278.

Zuta, S., D.B. Enfield, J. Voldvia, P. Lagos and C. Blondin, 1974: Physical aspects of the 1972-73 El Niño phenomenon, Paper resented at the IOC El Niño Workshop in December, 1974, Guayaquil, Ecuador.

INITIAL DISTRIBUTION LIST

	No. Copies
1. Defense Technical Information Center Cameron Station Alexandria, VA 22304-6145	2
2. Library, Code 52 Naval Postgraduate School Monterey, CA 93943-5000	2
3. Chairman (Code OC/Co) Department of Oceanography Naval Postgraduate School Monterey, CA 93943-5000	1
4. Chairman (Code MR/Hy) Department of Meteorology Naval Postgraduate School Monterey, CA 93943-5000	1
5. Professor Steven R. Ramp (Code OC/Ra) Department of Oceanography Naval Postgraduate School Monterey, CA 93943-5000	1
6. Mr. Paul F. Jessen (Code OC/Js) Department of Oceanography Naval Postgraduate School Monterey, CA 93943-5000	1
7. LT Kevin A.S. Hays, USN SWOSCOLCOM Student, Department Head School Class 128 446 Cushing Road Newport, RI 02841-1209	1
8. Commanding Officer Fleet Numerical Oceanography Center Monterey, CA 93943-5005	1

9. Chairman	1
Oceanography Department	
U.S. Naval Academy	
Annapolis, MD 21402	
10. Office of Naval Research (Code 420)	1
Naval Ocean Research and Development Activity	
800 N. Quincy Street	
Arlington, VA 22217	
11. Library	1
Scripps Institute of Oceanography	
P.O. Box 2367	
La Jolla, CA 92037	
12. Chief, Ocean Services Division	1
National Oceanic and Atmospheric Administration	
8060 Thirteenth Street	
Silver Springs, MD 20910	
13. U.S. Environmental Protection Agency, Region IX	1
75 Hawthorne Street	
San Francisco, CA 94105	
ATTN: Mr. Alan Ota	

DUDLEY KNOX LIBRARY
NAVAL POSTGRADUATE SCHOOL
MONTEREY CA 93943-5101

GAYLORD S



DUDLEY KNOX LIBRARY



3 2768 00018970 8